



**UiT** The Arctic University of Norway

The Faculty of Science and Technology  
Department of Geoscience

**Sedimentology of Late Precambrian storm-influenced pro-deltaic successions: Varanger, eastern Finnmark**

Julia Skorgen

GEO-3900 Master thesis in Geology

September 2020







## Abstract

This study investigates the sedimentology of the Klubbnasen and Andersby formations of the Late Precambrian (Neoproterozoic) succession in Varanger, eastern Finnmark. Additionally, the lower parts of the Fugleberget and Paddeby formations overlying the Klubbnasen and Andersby formations, respectively, were superficially investigated in order to provide stratigraphic context. The investigated formations are part of the Vadsø Group, which have previously been interpreted to represent a syn-rift succession of Late Riphean age. The present study is based on extensive field work along the northern coastline of the Varangerfjorden and document storm-bed (i.e. tempestite) variability within the Klubbnasen and Andersby formations, and interpret their depositional environments and sequence stratigraphic development. Ten lithofacies were identified based on outcrop investigations, which further are grouped into four lithofacies associations reflecting outer shelf deposits (FA1), storm-influenced prodelta deposits (FA2), storm-influenced delta front deposits (FA3) and braided river deposits (FA4; only occurring in the Fugleberget and Paddeby formations). The numerous tempestite beds of Klubbnasen and Andersby formations were mainly governed by wave-enhanced turbidity currents and storm waves producing a variety of storm-bed architectures (e.g. wave-modified turbidite). Deposition of a typical tempestite (e.g. wave-modified turbidite) was typically preceded by erosion of strong, but decelerating, offshore-directed turbidity currents, which were followed by a gradually more oscillatory-dominated flow governed by storm waves. The beds are characterized by high aggradation rates where the bed-architecture was controlled by the temporal and spatial evolution of the two transporting agents. Seafloor topography may also have affected the deposition. The abundance of soft-sediment deformation structures, including the presence of a laterally extensive slump deposit, suggest a trigger mechanism related to seismic activity. The cyclic stacking trend of that the Klubbnasen-Fugleberget and the Andersby-Paddeby formations and the sharp, erosive boundaries within these stratigraphic couplets, may suggest deposition within a seismically active rift-basin where the basin fill evolution was largely governed by hanging wall-subsidence and limited sediment supply (due to small catchment area). Periods of increasing subsidence rates may have led to the formation of marine flooding surfaces (as observed in the Klubbnasen and Andersby formations), while sudden uplifts of the footwall resulted in episodes of extensive erosion of the underlying deltaic units and the formation subaerial unconformities (as observed at the bases of the Fugleberget and Paddeby formations). Tectonic uplift and exposure of larger areas eventually promoted the generation of extensive braided river systems (as represented by the cross-bedded sandstone of the Fugleberget and Paddeby formations).



## Acknowledgements

First, I would like to thank my supervisor Sten-Andreas Grundvåg for great supervision during the process of writing my thesis. Your feedback and guidance have been greatly appreciated. Additionally, I would like to thank the Department of Geoscience for financial support.

I further would like to thank my field assistance and office buddy Egil for helpful discussions and memorable times during the fieldwork in Finnmark and at the office. Thank you also for proofreading parts of my thesis.

I would also like to thank Birgitte and Ragnhild for good support and memorable times during the years at the university. A special thanks to Ragnhild for taking the time to proofread my thesis.

Finally, I would like to thank family and friends, for support and encouragement throughout the writing process. A special thanks goes to my parents for always believing in me and encouraging me throughout my studies.

Parts of this research is funded by ARCEX and the Research Council of Norway (grant number 228107).

Julia Skorgen

Tromsø, September 2020



## Contents

Abstract .....	I
Acknowledgements .....	III
1. Introduction .....	1
1.1 Background and motivation .....	1
2. Geological setting .....	4
2.1 Introduction .....	4
2.1.1 The Timan-Varanger belt.....	5
2.2 Structural framework .....	8
2.2.1 Rodinia.....	8
2.2.2 Baltica during the assemblage and break-up of Rodinia .....	9
2.2.3 The Trollfjorden-Komagelv Fault Zone and the Sredni-Rybachy Fault Zone .....	10
2.2.4 The Varangerfjorden fault zone .....	13
2.3 Lithostratigraphy of the Tana-Varangerfjorden Region (TVR).....	15
2.3.1 The Vadsø Group .....	17
2.3.2 The Klubbnasen and Andersby formations .....	18
2.3.3 The Tanafjorden Group .....	20
2.3.4 The Vestertana Group .....	20
3. Methods .....	21
3.1 Fieldwork.....	21
3.2 Post-fieldwork .....	21
4. Results .....	22
4.1 Lithofacies .....	22
4.1.1 Lithofacies 1: Laminated mudstone and siltstone.....	22
4.1.2 Lithofacies 2: Interbedded sandstone/siltstone heterolithics.....	23
4.1.3 Lithofacies 3: Hummocky cross-stratified/deformed siltstone (silty sandstone) .....	26
4.1.4 Lithofacies 4: Massive sandstone .....	28
4.1.5 Lithofacies 5: Planar laminated sandstone.....	29
4.1.6 Lithofacies 6: Hummocky cross-stratified sandstone (isotropic vs anisotropic) .....	30
4.1.7 Lithofacies 7: Swaley cross-stratified sandstone .....	34
4.1.8 Lithofacies 8: Combined-flow rippled sandstone .....	36
4.1.9 Lithofacies 9: Cross-bedded sandstone .....	38
4.1.10 Lithofacies 10: Planar-bedded sandstone .....	39
4.2 Facies associations .....	43

4.2.1 Facies association 1: Offshore .....	43
4.2.2 Facies association 2: Storm-influenced prodelta deposits .....	45
4.2.3 Facies association 3: Storm-influenced delta front .....	51
4.2.4 Facies association 4: Braided river deposits .....	56
4.3 Stratigraphic development of the Klubbnasen and Andersby formations .....	59
4.4 Soft-sediment deformation structures (SSDS) .....	63
4.4.1 Load structures .....	63
4.4.2 Convolute and contorted lamination/bedding (deformed lamination) .....	67
4.4.3 Sandstone dykes .....	70
4.4.4 Syneresis cracks .....	72
4.4.6 Syn-sedimentary faults .....	78
4.4.5 Large-scale deformation - the Vadsø locality .....	80
5. Discussion .....	88
5.1 Origin of the event beds of the Klubbnasen and Andersby formations .....	88
5.2 Storm-bed variability across the shelf .....	93
5.3 Formative mechanisms and possible triggers of the SSDS .....	95
5.4 Stratigraphic development of the Klubbnasen and Andersby formations .....	101
5.5. Depositional environment .....	104
6. Conclusion .....	107
7. References .....	109







# 1. Introduction

## 1.1 Background and motivation

Coastal storms are one of the major agents in redistributing and depositing sediments on the shelf area, and since the 1960s and 1970s storm deposits have received considerable attention (e.g. Ball et al., 1967; Hayes, 1967; Perkins and Enos, 1968; Harms, 1975; Hamblin et al., 1979; Bourgeois, 1980; Duke, 1991; Myrow et al., 2002; Pattison, 2005; Traykovski et al., 2007; Ide et al., 2011; Quin, 2011; Morsilli and Pomar, 2012; Basilici et al., 2012; Myrow, 2005; Xiong et al., 2018). Numerous studies have been conducted on both ancient shelf successions and on modern continental shelves to get a better understanding of the processes governing sediment transport and deposition in these environments. Earlier studies have shown that these successions typically consist of sandstone beds interbedded with mudstone, where the sandstone beds represent deposition during single storm events and the mudstone beds represent deposition during fair-weather conditions (Dott Jr and Bourgeois, 1982; Duke, 1985; Brenchley et al., 1993; Krassay, 1994; Ide et al., 2011; Bowman and Johnson, 2014). Many storm beds (i.e. tempestites) display a distinctive sedimentary structure called hummocky cross-stratification (HCS; e.g. Harms, 1975; Xiong et al., 2018). The origin of HCS are still under discussion, but there is a general agreement that these structures are generated by the aggradation and migration of 3D bedforms that form by a combination of several hydrodynamic processes, including surface storm waves and various unidirectional bottom currents (Duke, 1991; Morsilli and Pomar, 2012). Recent studies have also established that storm induced underflows and internal waves in the water column could play important roles in the development of HCS (Quin, 2011; Basilici et al., 2012). HCS commonly occur in tempestite beds together with other specific sedimentary structures such as scour marks, gutter casts, wave ripple cross-lamination and planar lamination (Morsilli and Pomar, 2012; Myrow, 2005). Tempestite beds have several similarities with turbidite beds (i.e. the classical Bouma sequence Bouma, 1962), notably when the storm-generated facies successions are deposited by combination of oscillatory and unidirectional flows under waning energy conditions. Consequently, tempestite beds are normally graded, as well as displaying similar sedimentary structures typical of turbidite beds (Myrow, 2005; Myrow et al., 2002). Thus, distinguishing these deposits could potentially be problematic and have led to several discussions (e.g. Mutti et al., 2003; Basilici et al., 2012).

Both tempestite and turbidite beds commonly occur in pro-deltaic environments where the former usually accumulate between storm and fair-weather bases and the latter below the storm wave base (Pattison, 2005; Basilici et al., 2012; Dufois et al., 2014). Pro-delta deposits are usually therefore a result of both episodes of gravity flows down the delta slope as well as reworking of sediments by storm waves and storm-induced currents (Traykovski et al., 2007). Numerous pro-deltaic successions have been investigated in the last few decades, both ancient and modern, where the main focus have been to establish the processes of deposition (e.g. Pattison, 2005; Bhattacharya and MacEachern, 2009; Basilici et al., 2012; Dufois et al., 2014). However, in the modern, it is difficult to do accurate measurements during and immediately after storms, thus investigating their resultant deposits is important to understand storm processes and flow dynamics.

This case study investigates two Late Precambrian storm-influenced pro-deltaic successions, the Andersby and Klubbnasen formations of the Vadsø Group in eastern Finnmark, northern Norway. The Andersby and Klubbnasen formations are both heterolithic siltstone-dominated units, which earlier have been described to be part of regressive deltaic systems that developed during a rift episode in the Late Riphean (Banks et al., 1974; Røe, 2003). Apart from being briefly mentioned in a few papers on the general lithostratigraphy of the area, the Andersby and Klubbnasen formations are poorly described in terms of sedimentary facies and sequence stratigraphic architecture, as such a detailed understanding of the depositional processes and depositional environment are lacking. This is despite the two formation being excellently exposed along the southern coastline of the Varanger Peninsula (Fig. 1c). Thus, the main objective of this thesis is to document storm-bed variability and the depositional architecture of the two interpreted pro-deltaic units and establish a more detailed understanding of the depositional environment under which the formations accumulated, focusing particularly on storm-emplaced facies.

Thick cross-bedded sandstone units of the Paddeby and Fugleberget formations overlie the Klubbnasen and Andersby formations, respectively (Banks et al., 1974). Previous studies indicate that these cross-bedded sandstone successions are of fluvial origin and was deposited in extensive braid-plain settings (Banks et al., 1974; Røe, 2003). However, there is

limited knowledge about the relationship to the underlying pro-deltaic units of this study. A second aim of this study will thus be to document and interpret the relationship between the pro-deltaic and fluvial units in regard to their sequence stratigraphic development. The syn-rift character of the investigated pro-deltaic units is evident by the extensive soft-sediment deformation and add yet another dimension to this study, as most other ancient pro-deltaic successions described in the literature mostly represent foreland or passive margin systems. A third objective is therefore to investigate the influence of tectonic activity on deposition and the evolution of the pro-delta successions of the Andersby and Klubbnasen formations.

## 2. Geological setting

### 2.1 Introduction

The Late Precambrian sedimentary succession in the Tanafjorden and Varangerfjorden region, eastern Finnmark, northern Norway (Figs 2A & 2B), have previously received considerable attention through the years with several papers describing the structural and stratigraphic development of the area (e.g. Banks et al. 1974, Hobday 1974, Sidlecka et al. 1995). This includes the succession exposed on the southwestern side of the Varanger Peninsula, south of the Trollfjord-Komagelv Fault Zone, a regional lineament that have had a major control on the stratigraphic development of the area (Johnson et al., 1978a; Røe, 2003). During deposition of the Precambrian succession in the Varanger area, the supercontinent Rodinia was splitting up into several segments, one of them being Baltica, which comprises the present Fennoscandian Shield (Nystuen et al., 2008). Baltica was at this time located on the southern hemisphere where the Varanger Peninsula was a part of a northeastern passive margin with eastward progradation of deltas out into an extensional peripheral basin (Zhang et al., 2015). The resulting deposits are today exposed in several outcrops along the west—east trending coastline in the Varanger area (Fig. 2C). As well as being autochthonous, the successions have only experienced low grade metamorphism and relatively little tectonic deformation (Roberts and Siedlecka, 2002).

In total, the succession is c. 4000 m thick and comprises the upper Riphean Vadsø and Tanafjord groups as well as the Vendian to lowermost Cambrian Vestertana Group (Johnson, 1978). They are deposited on top of the crystalline basement and have suffered only minor tectonic deformation (Banks et al., 1974). The groups generally consist of various fluvio-deltaic and shallow-marine shelf deposits (Røe, 2003). The depositional and stratigraphic setting of the three groups are generally well understood, but some parts have received little attention, such as the Andersby and Klubbnasen formations of the Vadsø Group, which are the focus of this study. These heterolithic siltstone-dominated formations have earlier been described to be part of regressive deltaic systems that developed during the main rift episode in the Late Riphean (Banks et al., 1974; Røe, 2003). Apart from only briefly being mentioned in a few papers on the general lithostratigraphy of the area, the Andersby and Klubbnasen formations are poorly described and the understanding of the depositional processes and environment are lacking.

The Neoproterozoic Era comprises the Tonian (1,000-850 Ma), Cryogenian (850-630 Ma) and Ediacaran (630-542) periods (Gradstein et al. (2004). Although, in Russian and Nordic geological literature, the older Russian terms Riphean and Vendian are widely used. For convenience, these terms will also be used in this thesis. Riphean corresponds to the Mesoproterozoic, Tonian and Cryogenian periods, while the Vendian corresponds to the Ediacaran period as shown in Figure 1 (Nystuen et al., 2008; Roberts and Siedlecka, 2012).

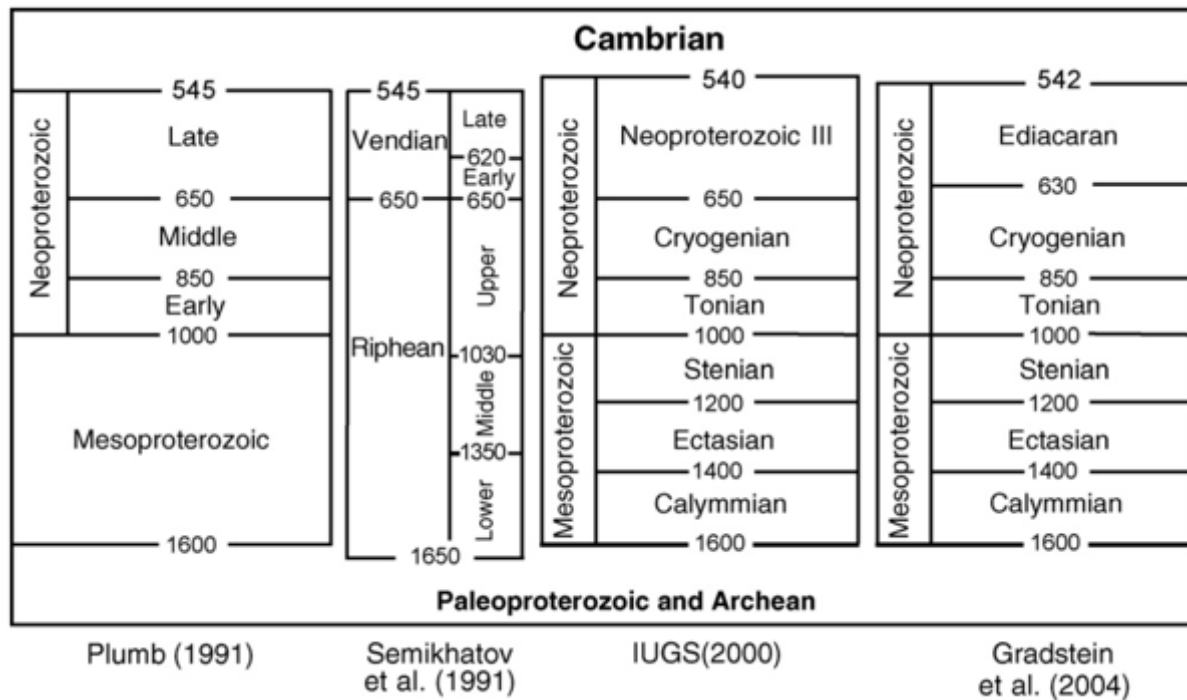


Figure 1. Comparison between the different timescales. Figure from Pease et al. (2008).

### 2.1.1 The Timan-Varanger belt

Along the margin of northern Europe, on the Norwegian and Russian coast, remnants of a sedimentary succession of mainly Neoproterozoic age, can be traced for c. 1800 km along the so-called Timan-Varanger belt (Figs 2A, 4A & 4B). These NW—SE trending successions are deposited in a pericontinental to basinal setting and have only experienced low-grade metamorphism (Roberts and Siedlecka, 2002; Roberts and Olovyanishnikov, 2004; Nystuen et al., 2008). Towards the southeast, the Timan-Varanger belt changes orientation from NW—SE into a N—S trend nearly parallel with the central and southern Urals (Fig. 4A) (Roberts and Siedlecka, 2002).

The deposition is considered to have occurred during the break-up of Rodinia when Baltica experienced crustal extension and rifting, eventually leading to the formation of passive margins (Roberts and Siedlecka, 2002). Today the successions can be followed from the Timan Range in the east to the Varanger Peninsula in the west, including the Rybachi and Sredni Peninsulas and the Kildin Island (Fig. 4A) (Roberts, 1996). During the last century, there have been conducted several studies on these excellently exposed Late Precambrian successions. Already in the late 1800s, several outcrops were investigated; among these were the famous Bigganjargga tillite (e.g. Reusch, 1891; Holtedahl, 1918; Bjørlykke, 1967; Edwards, 1972). Later, sedimentary, structural and petrographic studies, as well as isotopic dating and paleomagnetic investigations led to several important advances in the knowledge of the Precambrian successions (e.g. Holtedahl, 1918; Siedlecka and Siedlecki, 1967; Banks et al., 1974; Hobday, 1974; Levell and Roberts, 1977; Johnson et al., 1978b; Karpuz et al., 1995b; Olovyanishnikov et al., 1997; Roberts and Siedlecka, 2002; Røe, 2003; Zhang et al., 2015).

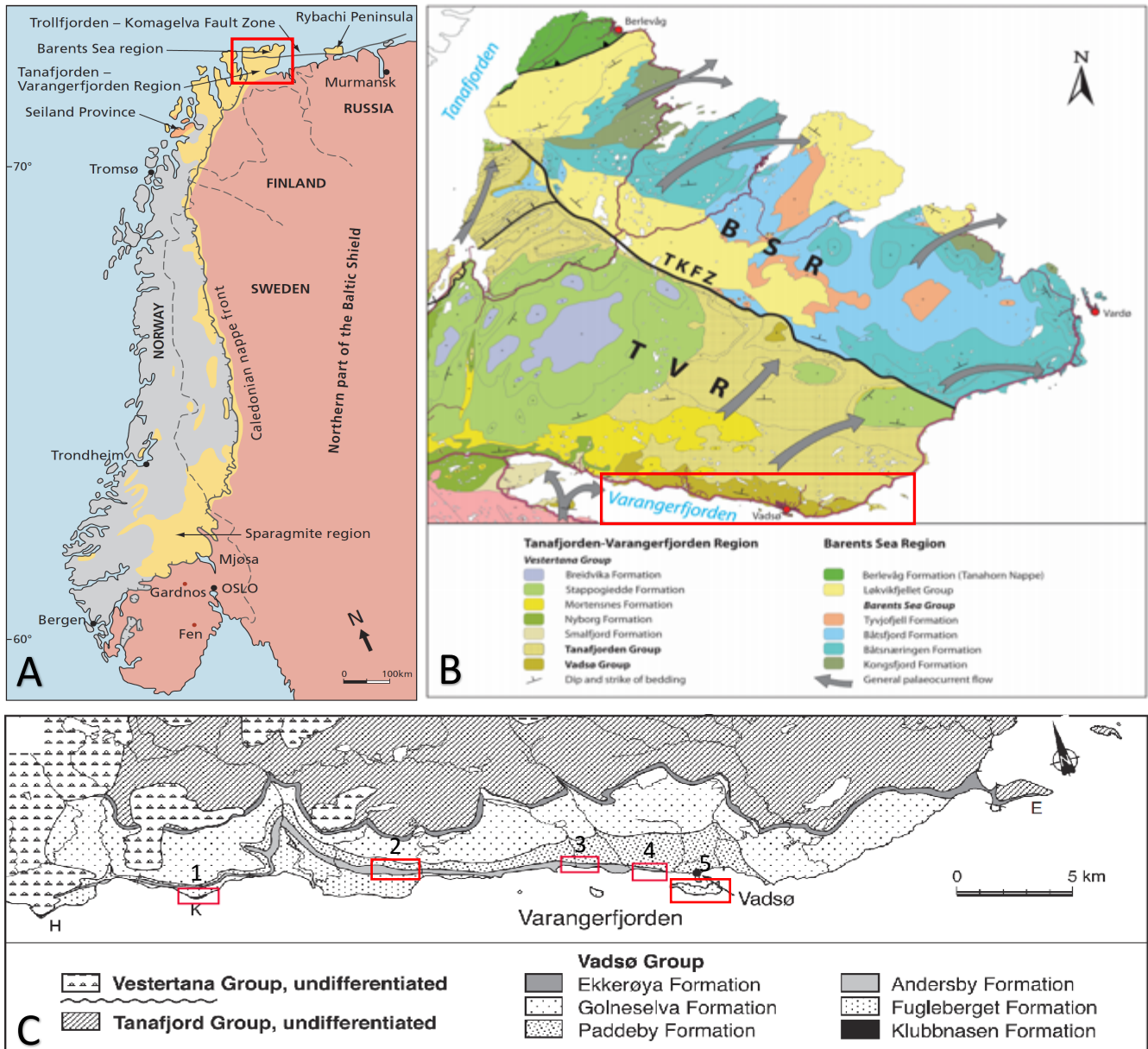


Figure 2. A) Map of Northwestern part of Baltica. The Neoproterozoic rocks (yellow) are positioned along the Caledonian thrust front (grey). Red square marks the Varanger Peninsula. Modified from Nystuen et al. (2008). B) Geological map of the Varanger Peninsula. Arrows displaying general paleocurrent flow. BSR- Barent Sea Region and TVR-Tana-Varangerfjorden Region. Red square marks the study area. Figure modified from Roberts and Siedlecka (2012). C) Geological map of southernmost part of Varanger Peninsula showing the distribution of the Vadsø Group. The red squares represent the investigated localities in this study. Investigated localities: 1. Klubbnasen, 2. Paddeby, 3. Bergelva, 4. Vadsø coastal section, 5. Vadsøya. Figure modified from Røe (2003).

## 2.2 Structural framework

### 2.2.1 Rodinia

Towards the end of the Precambrian, in the Late Mesoproterozoic time, most of Earth's continental fragments were assembled into one supercontinent called Rodinia (Fig. 3A) (Bogdanova et al., 2009; Cawood and Pisarevsky, 2017; Merdith et al., 2017). During the formation of Rodinia, several plates collided into the central plate of Laurentia, forming numerous orogenic belts along the collision zones (e.g. Grenville, Sveconorwegian, Valhalla and Sunsas belts) (Cawood et al., 2007). In the Early Neoproterozoic (around 800 Ma), Rodinia started to break apart after being assembled for 150 million years (Li et al., 2008).

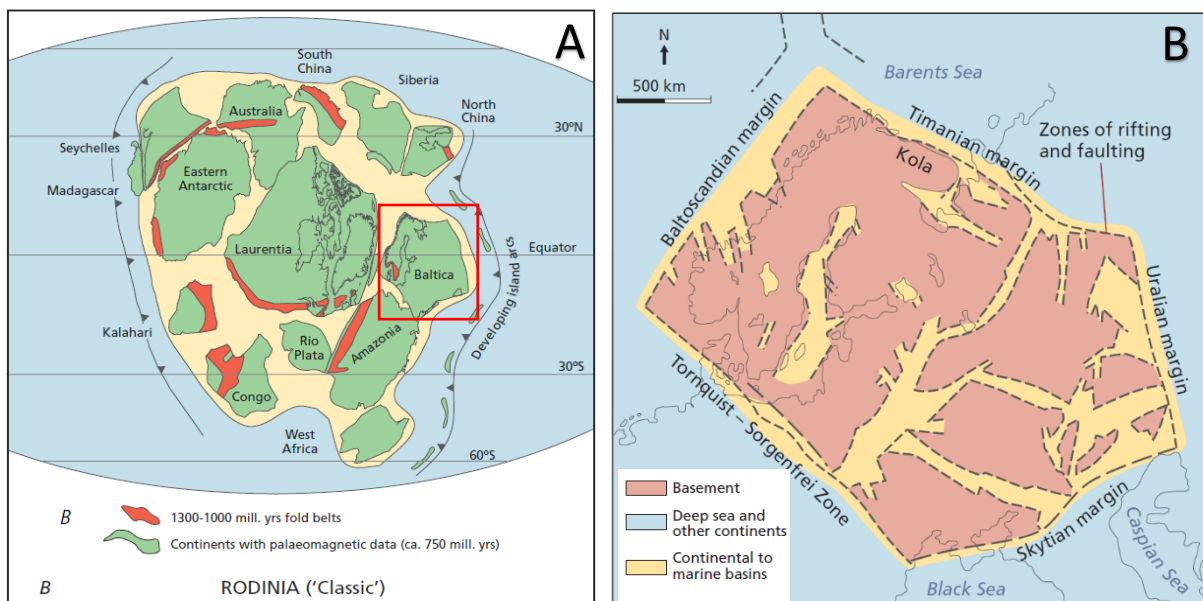


Figure 3. 3A) Figure showing the distribution of the continents during the assembly of Rodinia. Modified from Nystuen et al. (2008). 3B) Map of Baltica during the separation from Rodini where the Timanian margin represents the northeastern passive margin of Baltica. (Nystuen et al. (2008)).

The break up itself occurred in a discontinuous manner with widespread continental rifting presumably initiated by a mantle superplume (Bogdanova et al., 2009). As well as several rift zones, the break up led to the formation of numerous dyke swarms and large igneous provinces (LIPs). The end of the Rodinia supercontinent is marked with the opening of the Iapetus Ocean between Laurentia and Baltica, which took place between 650 and 550 Ma (Bogdanova et al., 2009).



### 2.2.2 Baltica during the assemblage and break-up of Rodinia

Baltica (Fig. 3B), which is the Precambrian part of northeastern Europe, consists of three different terranes named Volgo-Uralia, Sarmatia and Fennoscandia (Johansson, 2009). These segments presumably collided in Paleoproterozoic time (around 2.1-1.7 Ga) and primarily consists of an Archean core (Pease et al., 2008; Bogdanova et al., 2016). Baltica became a part of the Rodinia assembly when the plate collided with Laurentia and Amazonia. The collision led to the Sveconorwegian Orogeny, which is assumed to be a small segment of the global Greenville belt (Bingen et al., 2005). Throughout the Rodinia assembly, Baltica was located on the southern hemisphere, mostly likely attached to the northeastern margin of Laurentia and with the Amazonian plate in southeast (Fig. 3A) (Bogdanova et al., 2016). The orientation of the Baltic shield during the assembly have previously been under discussion. Some researcher have proposed that Baltica was inverted from currently orientation throughout the assembly (Torsvik et al., 1996; Torsvik and Cocks, 2005). This theory was later proven to be wrong based on paleomagnetic measurements (Cawood and Pisarevsky, 2006) and today there is a general agreement that northwestern Baltica was located adjacent to northeastern Laurentia as shown in Figure 3A (Cawood and Pisarevsky, 2006; Cawood et al., 2007; Li et al., 2008; Nystuen et al., 2008; Johansson, 2009; Merdith et al., 2017).

During the break-up of Rodinia, Baltica experienced intracatonic extension, rifting and formation of small and restricted rift basins. The succession of this study was presumably deposited in one of these active rifts-basins (Siedlecka and Siedlecki, 1967; Røe and Hermansen, 1993; Røe, 2003). In Neoproterozoic time, the margin of these basins turned into pericontinental passive shelves along the northeastern margin of Baltica (Fig. 3B), promoting the development of large depositional systems ranging from fluvial to deep marine (Siedlecka and Siedlecki, 1967; Johnson et al., 1978a; Olovyanishnikov et al., 1998; Røe, 2003). Some of the resulting deposits can today be found in the eastern part of Finnmark and northwestern Russia (Fig. 4A). Baltica also started to drift apart from Laurentia, eventually leading to the opening of the Iapetus Ocean in the Early Cambrian (Johansson, 2009). The separation resulted in Baltica being an independent continent with its passive margins receiving and accommodating large amounts of sediments (Fig. 3B) (Nystuen et al., 2008).

During the early Ordovician, subduction-zones formed on both side of the Iapetus Ocean, eventually leading to an oblique collision between Laurentia and Baltica. During the collision, the margin of Baltica was subducted beneath Laurentia creating the Caledonian orogeny, which today extends over a distance of c. 2000 km along the entire western margin of Scandinavia (Roberts, 2003; Gee et al., 2008), including eastern Finnmark (Rice, 2014). The collision was followed by an orogenic collapse with widespread extension and sedimentation in the Devonian (Torsvik and Cocks, 2005).

### 2.2.3 The Trollfjorden-Komagelva Fault Zone and the Sredni-Rybachy Fault Zone

A major NW—SE trending fault zone, which can be followed from the southwestern Barents Sea to the Kanin-Timan region in the east, separates the percontinental and basinal regimes in Finnmark and northwestern Russia (Figs 4A, 4B & 4C) (Karpuz et al., 1994; Roberts, 1996; Røe, 2003). The Trollfjorden-Komagelva fault zone (TFKZ), which represents the western part of the regional fault zone (Fig. 2B), divides the Varanger Peninsula in two geological regimes, the Tana-Varanger Region (TVR) and the Barents Sea Region (BSR) (Fig. 2B) (Siedlecka and Siedlecki, 1967; Sturt et al., 1975; Johnson et al., 1978b; Karpuz et al., 1995a; Roberts, 1996; Roberts and Siedlecka, 2002; Siedlecka et al., 2004).

The Trollfjorden-Komagelva fault zone is approximately 75 km long and between 1 and 5 km in width where its main lineaments are generally topographic and have braided or anastomosing structural pattern (Fig. 2B) (Herrevold et al., 2009). The fault zone is considered to have originated in Archean time and have since been active in different periods (Herrevold et al., 2009). During this time, the fault zone have played a major role on the geology in the area, including strike-slip reactivation during the Caledonian Orogeny where it tectonically translated the entire Barent Sea Region along the fault zone to its present position (Ramberg et al., 2008).

In the Late Mesoproterozoic to Neoproterozoic time however, the TFKZ presumably acted as a normal fault (Siedlecka and Siedlecki, 1967; Karpuz et al., 1993; Herrevold et al., 2009). The area within and immediately adjacent to the TFKZ have been exposed to both brittle and ductile deformation (e.g. metamorphism, folding, duplexes and flower structures), where the degree and orientation of the deformation vary across the Peninsula (Røe, 2003; Herrevold et al., 2009). The deformation most likely originates from both the Caledonian (500-430 Ma) (Gee et al., 2008) and the Timanian orogens (600-550 Ma) (Fig. 4c) (Roberts

and Olovyanishnikov, 2004). In the western area, where the Caledonian thrust front is located, folds and cleavages have a NE-SW to ENE-WSW trend where the Neoproterozoic successions pass into the Caledonian Parautochthon and subsequently into the Lower Allochthon (Gaissa Nappe complex) (Sturt et al., 1975; Roberts, 1996). The age of the deformation is believed to be Late Silurian-Early Devonian (Roberts, 1996; Roberts and Siedlecka, 2002). The Caledonian deformation terminates towards the east, where the Peninsula becomes more affected by the Timanian orogeny (Roberts, 1995; Roberts and Olovyanishnikov, 2004; Herrevold et al., 2009). The Timanian orogeny, which is of Late Vendian to Early Cambrian age (Roberts, 1996), formed during inversion of the fault zone, which earlier had acted as an extensional regime with passive margins in northeastern Baltica. The Timanian deformation trends dominates the northeastern part of the Varanger Peninsula in the basinal domain, north of the TKFZ (Fig. 4C). Compared to the northern side of the TKFZ, the southeastern side (the pericontinental regime) have less abundant deformation structures (Olovyanishnikov et al., 1998; Roberts and Olovyanishnikov, 2004) (Roberts and Olovyanishnikov, 2004; Olovyanishnikov et al., 1998).

The TKFZ continues eastward into Russia along the coast of Kola where it has been termed the Sredni-Rybachy Fault Zone (SRFZ) (Figs 4B & 4C). The SRFZ crosses both the Sredni and Rybachy peninsulas where the successions on the Sredni Peninsula represent the pericontinental regime and the Rybachy represents the basinal regime (Roberts, 1996). Also, in this area, the structural deformation changes significantly across the fault zone (Roberts, 1996; Roberts and Siedlecka, 2002). The fault zone continues further east to southeast, where it possibly correspond to the Central Timan Fault in the Timan region (Fig. 4A) (Røe, 2003).

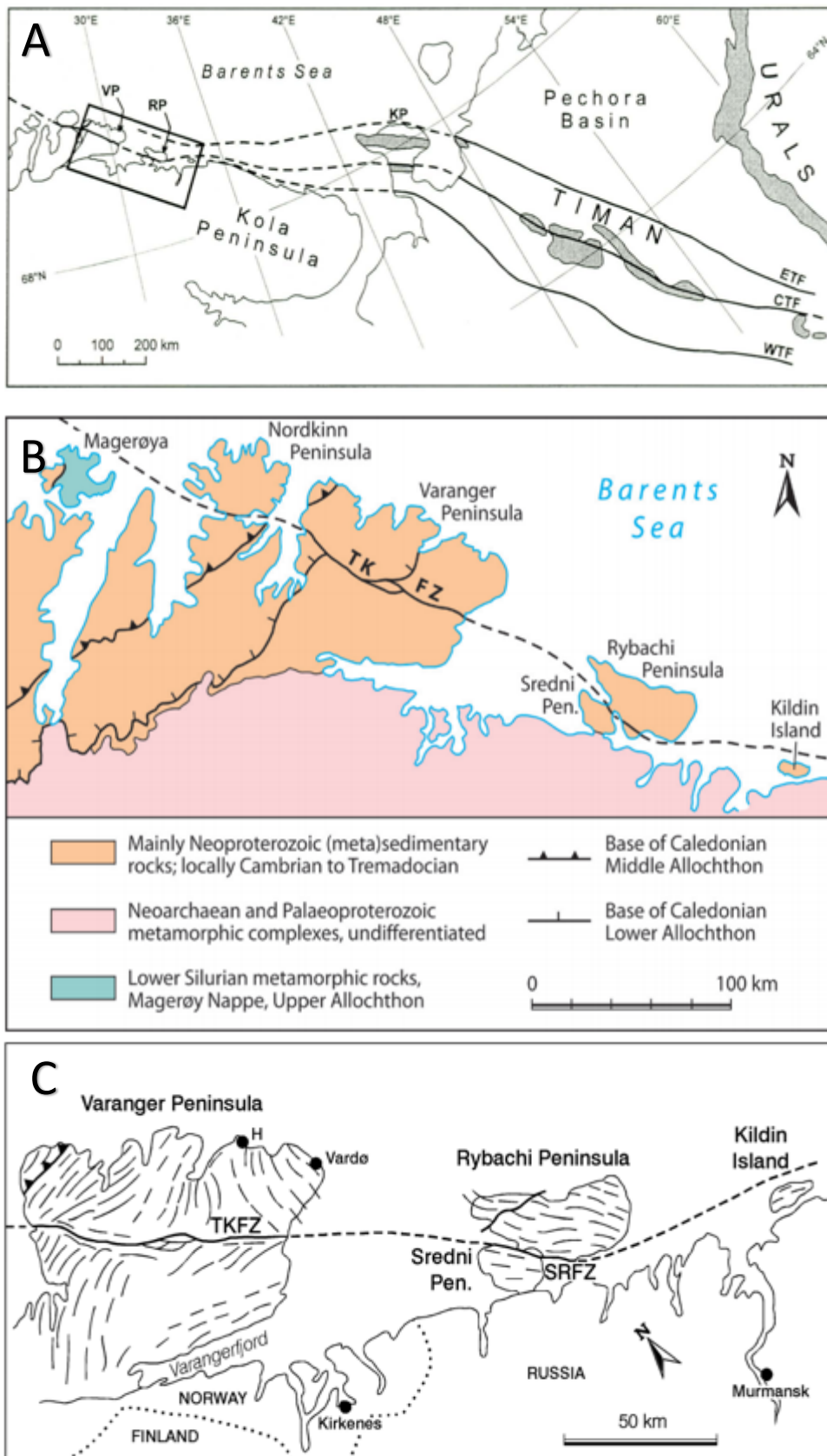
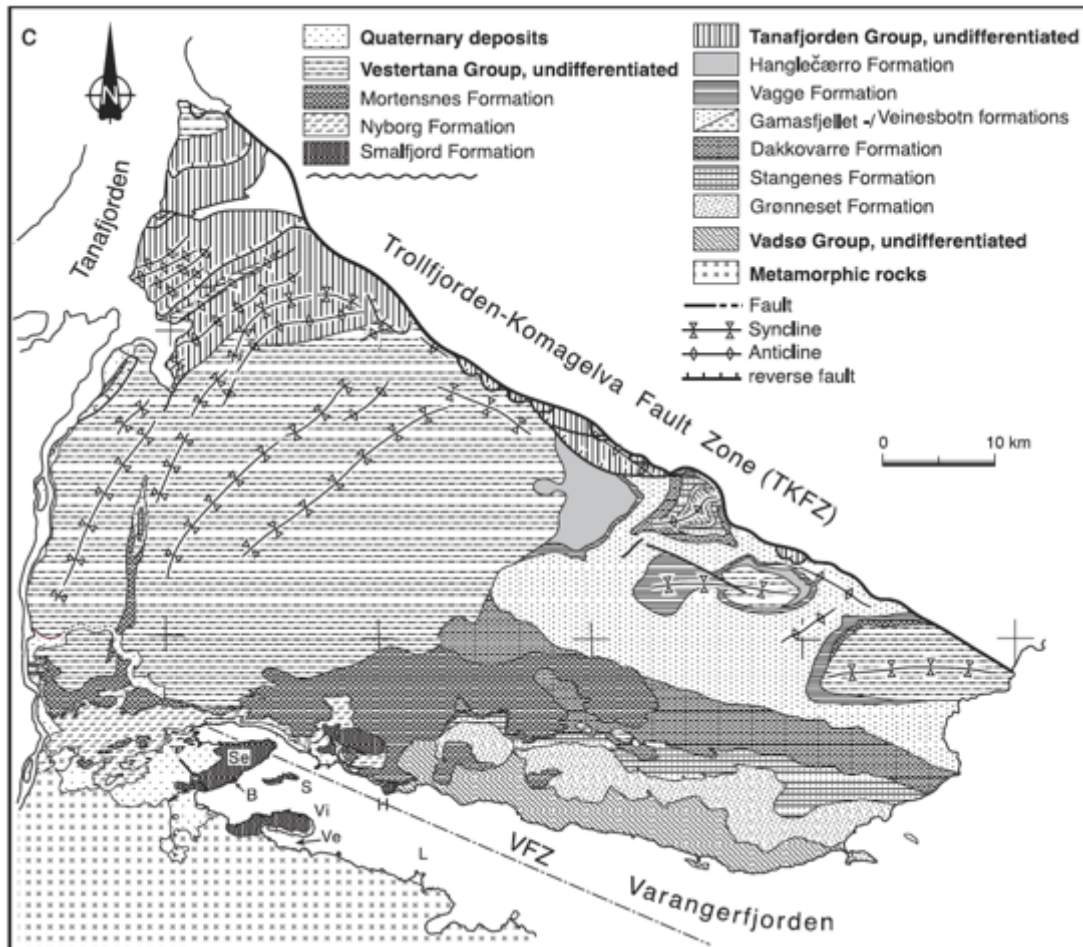


Figure 4. 4A) Location map showing the eastern Finnmark, Kola Peninsula, Timanians and northern Ural (Roberts (1996)). 4B) Map showing the Varanger peninsula, Rybachi and Sredni peninsulas and Kildin Island. The Neoproterozoic and Cambrian successions are in orange. Figure from Roberts and Siedlecka (2012). 4C) Map of the Varanger Peninsula, Rybachi and Sredni Peninsulas and Kildin Island showing the structural trends (axial surface traces of folds and Strike). Figure from Olovyanishnikov et al., 1998.

### 2.2.4 The Varangerfjorden fault zone

Røe (2003) have previously proposed the presence of a NW—SE trending fault zone in Varangerfjorden (Fig. 5). The theory is based on a revised stratigraphic correlation between the most likely younger (Late Riphean) Veinsbotn Formation, south of the Varangerfjorden, and the Riphean successions (the Vadsø and Tanafjorden groups), north of the Varangerfjorden.



Figur 5. Map of the Tana-Varanger region with the proposed Varangerfjorden fault zone (VFZ) in Varangerfjorden. Figure from Røe (2003)

The Veinsbotn Formation, which is deposited on top of the crystalline basement in the southern part of Varangerfjorden, was earlier suggested to be part of the lowermost formation of the Riphean succession. However, new evidence based on lithology and paleocurrents implies that the Veinsbotn Formation is possibly part of a younger succession, namely the Tanafjorden Group (Fig. 8). Thus, to explain the position of the Veinsbotn Formation, a fault zone (The Varangerfjorden fault zone, VFZ) separating the younger

formation with the older successions was proposed (Figs 5 & 6). The VFZ most likely experienced two episodes of extensional fault activity. First in the Late Riphean, during sedimentation of the lower part of the Riphean successions (the Vadsø Group and lowermost Tanafjorden Group). The active period was followed by a sea-level rise where post-rift sediments (the upper Tanafjorden Group) were deposited onlapping on the basal margin (crystalline basement) (Figure 6A). The Veinsbotn Formation was most likely deposited during this post-rift period. Later, a reactivation of the VFZ resulted in fault-block rotation and footwall erosion, which led to the low-angle unconformity between the Veinsbotn Formation and the Lower Riphean succession (Fig 6B & C) (Røe, 2003).

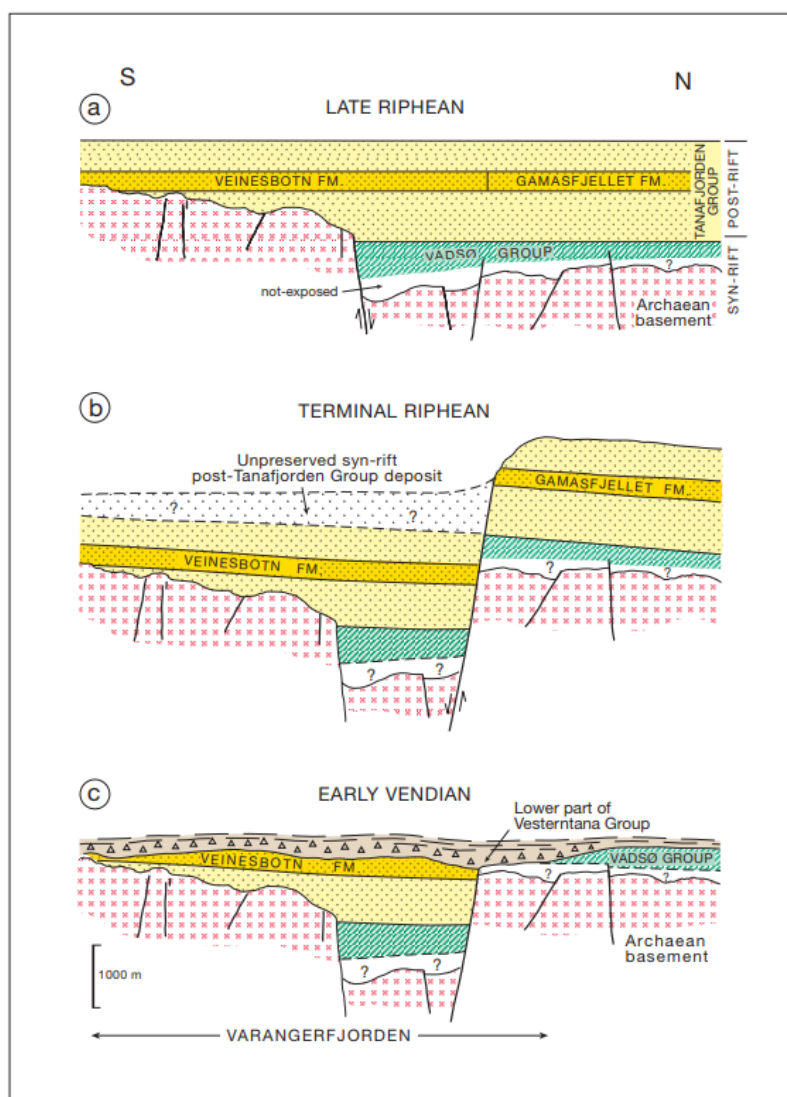


Fig. 6. Figure showing hypothetical cross section of the Varangerfjorden with the Varangerfjorden fault zone. 6A) First phase, syn-rift sedimentation followed by post-rift sedimentation, which on-lap the basin. 6B) Second Phase where part of the Veinsbotn Fm is downfaulted. 6C) Vendian erosion and deposition of the Vestertana Group. Figure from Røe (2003).



The VFZ is only hypothetically considered, as Vendian and Quaternary deposits conceal the modern fjord and there are no seismic reflection profiles available from the inner part of Varangerfjorden. In 2011, multibeam bathymetric data and reflection-seismic data were collected from the outer Varangerfjorden. This data did not reveal the presence of a NE—SE trending lineament in the outer fjord, which led these authors to dispute the presence of a fault zone in the Varangerfjorden (Roberts et al., 2011).

### 2.3 Lithostratigraphy of the Tana-Varangerfjorden Region (TVR)

The TVR comprises the Upper Riphean Vadsø and Tanafjorden groups and the Vendian to Lower Cambrian Vestertana Group (Fig.7). The succession is in total c. 4000 m thick and mainly consist of various fluvio-deltaic and shallow-marine shelf deposits, including Vendian tillites (Johnson et al., 1978b; Røe, 2003). Several hiatuses characterize the succession; among these are the unconformity between the Tanafjorden Group and the Vestertana Group. The break represents a significant episode involving tectonic tilting and erosion where most of the southern Riphean deposits were removed due to extensive erosion (Røe, 2003). Two regional hiatuses related to uplift and glacial erosion also occur in the succession (Nystuen et al., 2008).

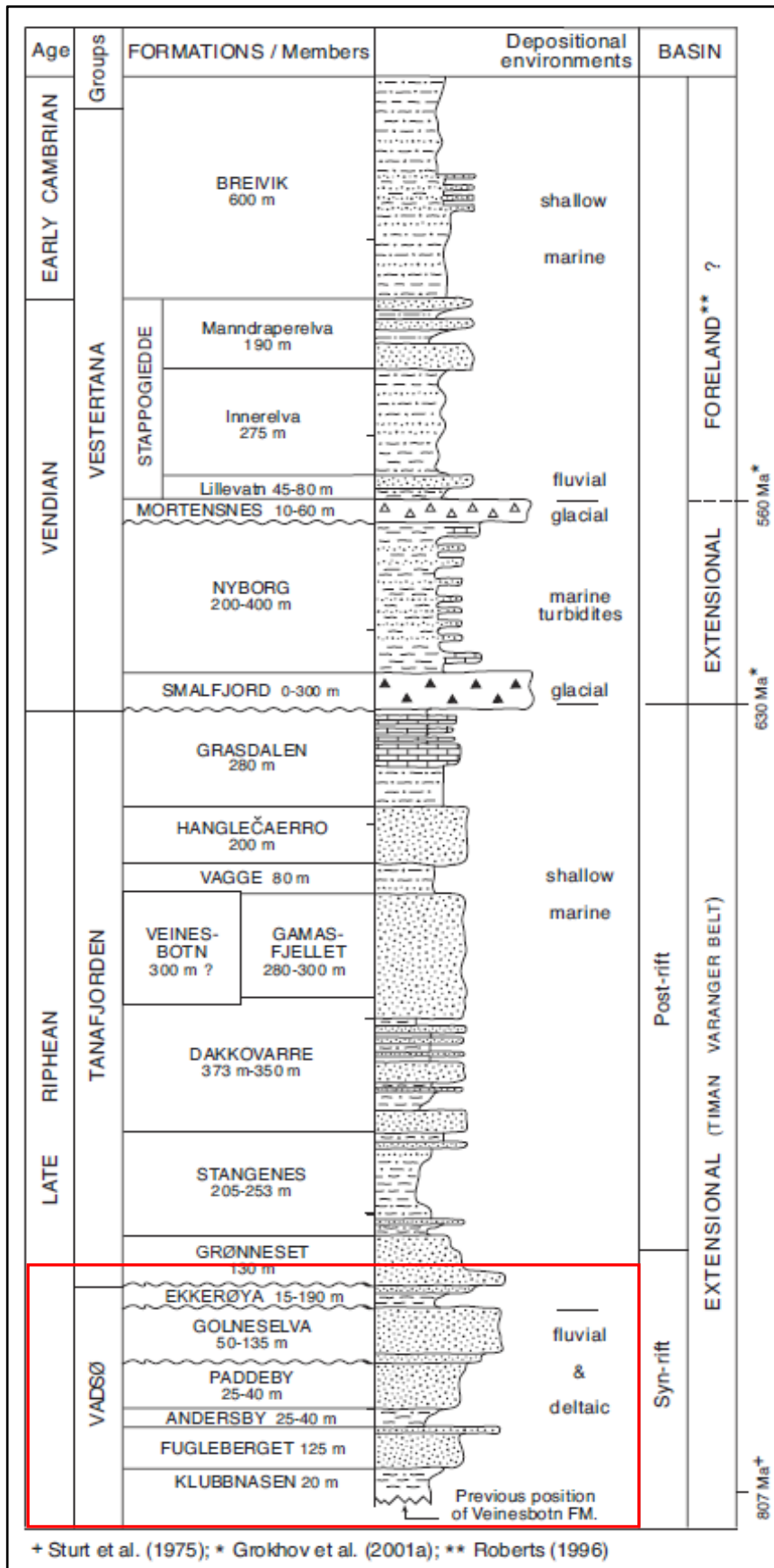


Fig. 7. Lithostratigraphy of the Vadsø Group, the Tanfjorden Group and the Vestertana Group. Red square highlights the Vadsø Group, which the Andersby and Klubbnasen formations belong to. Figure from Røe (2003).



### 2.3.1 The Vadsø Group

The Vadsø Group consists of a 290-660 m thick (Banks et al., 1974) mainly siliclastic fluvio-deltaic succession (Fig. 8). The group is considered to have been deposited in a syn-rift setting during the first phase of fault activity in the VFZ (Røe, 2003). The succession includes six formations, which can be divided into three lower-order tectonostratigraphic units separated by regional unconformities (Fig. 8). The lower of these tectonostratigraphic units consists of the Klubbnasen, Fugleberget, Andersby and Paddeby formations. Both the Klubbnasen and Andersby formations of the present study consist of heterolithic siltstone units interbedded with sandstone beds. The sandstone beds commonly display sole marks, parallel lamination and cross-lamination and the beds become thicker and more abundant towards the upper part of the formations (Banks et al., 1974). The Klubbnasen and Andersby formations are both considered to be deposited in regressive deltaic environments, whereby the deltas apparently prograded eastward (Røe, 2003). The Fugleberget (overlies Klubbnasen Formation; e.g. Røe, 1987; Røe and Hermansen, 1993) and Paddeby (overlies Andersby Formation; Røe and Hermansen, 1993) both consist of thick cross-bedded fluvial sandstones suggesting deposition in braided river systems where the direction of transport being approximately to the east (Banks et al., 1974; Røe, 2003). Together with the Andersby and Klubbnasen formations, respectively, these units form two vertically stacked coarsening-upward successions, indicating recurrent regressive conditions and deltaic shoreline accretion (Røe, 2003).

The second tectonostratigraphic unit of the Vadsø Group comprises the Golneselva Formation, which is characterized by two different depositional environments. The lower part consists of wave-rippled sandstones deposited in an estuarine environment, while coarse-grained, fluvial sandstones characterize the upper part of the unit. The paleocurrent direction is mainly to the northwest, indicating a change in transport direction compared to the lowermost tectonostratigraphic unit, which displays mostly eastward-directed paleocurrents (Banks et al., 1974; Røe, 2003). The Ekkerøya Formation represents the upper and youngest tectonostratigraphic unit of the Vadsø Group and is characterized by a coarsening-upward shelf to shoreline succession containing storm-dominated structures like hummocky cross-stratification and pervasive soft sediment deformation structures (Johnson, 1975; Johnson, 1978; Røe, 2003).

### 2.3.2 The Klubbnasen and Andersby formations

The Klubbnasen Formation, which is the lowermost unit in the Vadsø Group (Røe, 2003), is approximately 50 m thick and mainly consists of heterolithic siltstone. The upper part is exposed ca. 3 km west of Vestre Jakobselv at Klubbnasen (Fig. 2C), while the middle unit is hidden beneath the fjord. The basal part of the formation is exposed on Skjåholmen, an island southwest of Klubbnasen (Banks et al., 1974). Due to its stratigraphic completeness, only the Klubbnasen locality has been investigated in this thesis. Both Hobday (1974) and Banks et al. (1974) have given a general description of the formation where it is described to be consisting of an upward-coarsening succession of siltstone interbedded with fine-grained sandstone containing different sole marks and deformation structures. The lithostratigraphic boundary to the overlying fluvial Fugleberget Formation is regarded to be transitional and is in the previous literature defined by the first occurrence of a flat-bedded sandstone bed (Banks et al., 1974). The Fugleberget Formation was also investigated at the Vadsøya locality, in addition to the Klubbnasen locality (Fig. 2C). A Rb-Sr dating has also been conducted on the Klubbnasen Formation where the unit yielded an age of 810 +/- 90 Ma corresponding to the Late Riphean rift phase (Fig. 1) (Pringle, 1972; Bylund, 1994).

The Andersby Formation, which overlies the Fugleberget Formation, is approximately 25 – 40 m thick (Fig 8). The unit is exposed along the shoreline between Vadsø and Per-Larsavik, which lies west of Vestre Jakobselv (Fig. 2C). At the Vadsø location, the formation is ca. 40 m thick, while at Per-Larsavik the unit is only 25 m thick (Banks et al., 1974). In this thesis, the Vadsø location where investigated together with the Bergelva and Paddeby locations (Fig 2C). As well as consisting of siltstone beds interbedded with sandstone beds, the Andersby Formation displays many sedimentary characteristics similar to the Klubbnasen Formation, including sole marks and soft sediment deformation structures (Banks et al., 1974; Røe, 2003). The boundary between the overlying Paddeby Formation and the Andersby Formation have previously been described to be transitional and is lithostratigraphically defined on the occurrence of the first sandstone unit thicker than 1 m (Banks et al., 1974). Similar to the Klubbnasen Formation, the Andersby Formation is also considered to be deposited in a syn-rift environment during the Late Riphean (Røe, 2003).

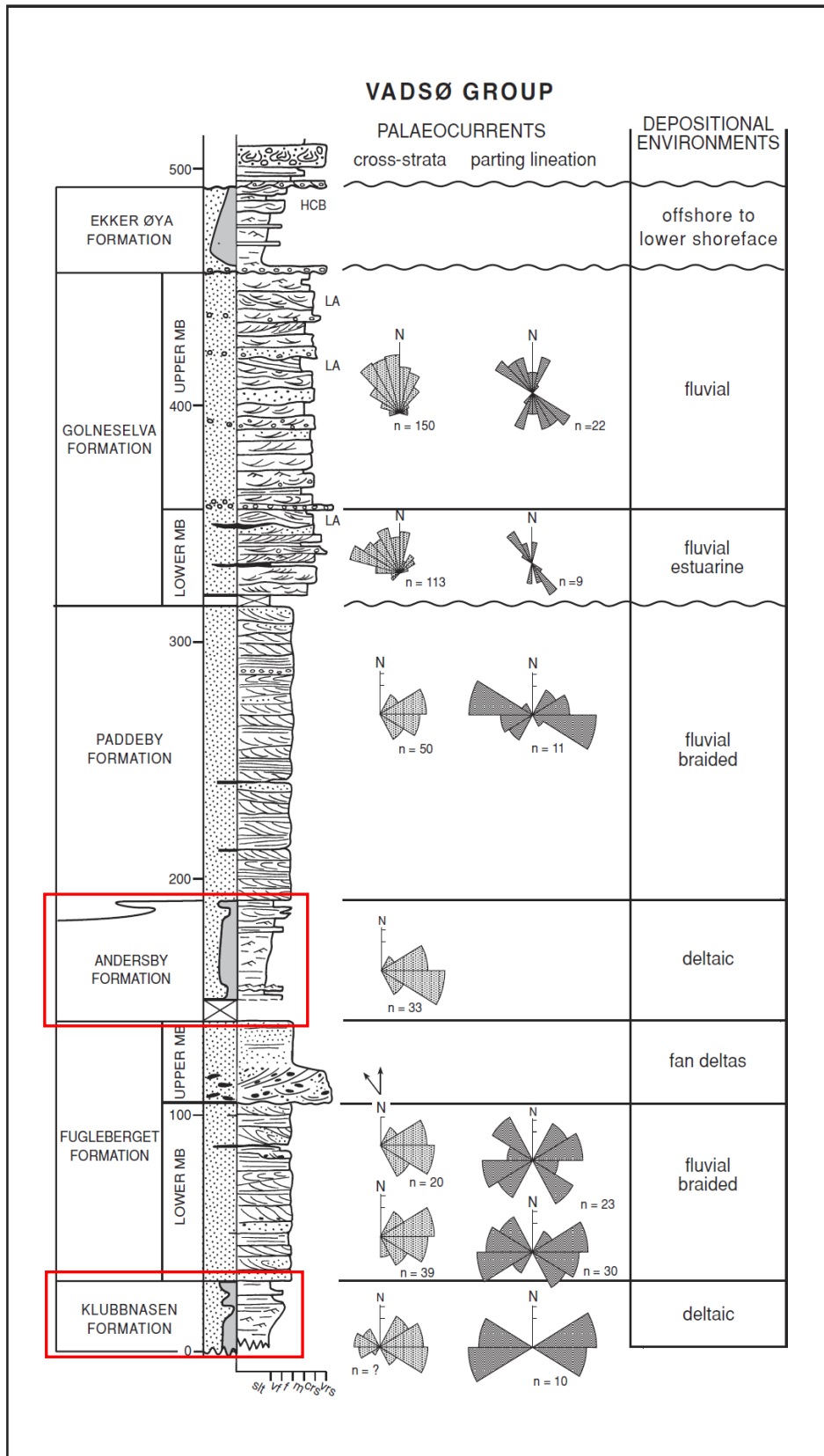


Fig. 8. Lithostratigraphy, paleocurrent data and depositional environments of the Vadsø Group. The focus of this study, the Klubbnasen and Andersby formations, are marked with red squares. Figure modified from Røe (2003).

### 2.3.3 The Tanafjorden Group

The Tanafjorden Group forms a 1448 to 1665 m thick succession consisting primarily of sandstones and siltstones (Fig. 8). The upper part of the succession includes a mixture of carbonate and muddy- siliciclastic sediments. During deposition of the group, the area experienced several shoreline shifts, which were related to transgressive and regressive episodes (Siedlecka and Roberts, 1992; Røe, 2003). According to Røe (2003), the upper part of the group is considered to be deposited in a post-rift environment, while the lower part characterizes a syn-rift environment (Fig. 8).

### 2.3.4 The Vestertana Group

Two tillite-bearing formations, respectively the Smalfjord and the Mortensnes formations, including the famous Bigganjargga (e.g. Bjørlykke, 1967), characterize the Vestertana Group (Fig. 8). Nearshore and shelf deposits overlie the tillite-bearing formations, while interglacial deep-water, turbiditic deposits separate the two formations. The group includes two hiatuses, both located beneath the tillites, indicating a regional glacial erosion (Røe, 2003; Nystuen et al., 2008).

## 3. Methods

### 3.1 Fieldwork

The data collected for this thesis was obtained from fieldwork during a 10-day period in September 2018 and 4 days in June 2019. Conventional sedimentological investigations were conducted at five locations; Klubbnasen, Bergelva, Vadsø coastal section, Paddeby and Vadsøya (Fig. 2C). The collected data set primary consists of sedimentological logs.

Sedimentary properties and features such as lithology, sorting, bed thickness, bed geometry, boundaries, primary and secondary sedimentary structures, paleocurrent directions (from flute casts and current ripple cross-lamination) and grain size variations were described and measured during the logging. At the Klubbnasen locality, a nearly continuous log of the whole unit was obtained as the bedding was dipping towards west (by some few degrees) and thus giving excellent access to the whole formation (The Klubbnasen Formation, Fig.8). At the Bergelva and Vadsø localities, the logging were limited by the steepness and relief of the coastal cliffs, which range from c. 3 to 8 m in height and thus only display parts of the unit (Andersby Formation, Fig. 8). By logging several vertical sections along the outcrops, a detailed description of the lateral variations of the Andersby Formation was established. In addition, a correlation panel of the c. 900 m lateral W—E oriented section at Vadsø was constructed, focusing particularly on the lateral development of soft sediment deformation structures within the Andersby Formation. To obtain the data sets, a hand lens, meter stick, geological hammer, geological compass and grain size identification sheet were used. A Panasonic DMC-GX1 camera with a 14 mm lens and a Panasonic DMX-GH4 with 14-56 mm lens were also used to take photos.

### 3.2 Post-fieldwork

Post-fieldwork included digitalizing logs and lateral profiles in the software CorelDRAW version 19.0.0.328 (2017). In addition, figure compilation and photo analysis were also conducted in this software. Several of the overview photos were also stitched into panoramas using the software Hugin Panorama photo stitcher 2018.0.0. The complete data set mentioned above is presented in the following chapters.

## 4. Results

### 4.1 Lithofacies

Eight lithofacies (Table 1) have been recognized in the Klubbnasen and Andersby formations based on grain size distribution and sedimentary structures, as well as bed geometry.

Additionally, two lithofacies are identified in the lower part of the Fugleberget and Paddeby formations. The ten lithofacies are described and interpreted below and summarized in Table 1.

#### 4.1.1 Lithofacies 1: Laminated mudstone and siltstone

##### *Description:*

Lithofacies 1 consists tabular units of mudstone and siltstone with small proportions of very fine-grained sandstone (Figs 9A and 9B). It is characterized by dark grey/green to red parallel lamination, where each lamina is rarely thicker than 0.5 cm. The lamination is mostly planar (Fig. 9A), but may also display a more undulating character. Symmetrical, straight crested ripples, which frequently displays bifurcation occur in places (Fig. 9G). Small, discontinuous sandstone lenses of very fine-grained sandstone, 0.5-2 cm thick, are observed in the upper part of the facies, commonly producing a pinch- and swell bed geometry (Fig. 9B). Internally, they have slightly asymmetrical rounded crests with low-angle foresets. They are typically located in the upper part of the facies, but may also be randomly distributed in the whole facies. At the Vadsø locality (Fig 2C) the siltstone appears to be mostly homogeneous and shows little diversity in grain size distribution (Fig. 9A), especially in the lower part of the succession. In contrast, facies 1 at the Bergelva and Klubbnasen localities (Fig. 2) exhibit a more heterolithic character with more abundant sand lenses (Fig. 9B). The facies typically defines the base of an upward-coarsening succession and usually underlies lithofacies 2 or lithofacies 3.

##### *Interpretation:*

The parallel lamination in facies 1 is most likely deposited in a low-energy depositional environment as hemipelagic fall-out during periods of fair-weather suspension settling. The deposition has occasionally been interrupted by episodes of stronger currents leading to the formation of small sandstone lenses. The symmetrical, straight-crested ripples indicate wave activity, while the slightly asymmetrical rounded foresets found in the sandstone lenses

characterize combined-flow ripples, which will be further elaborated in the description and interpretation of lithofacies 7 (Harms, 1969; Dumas et al., 2005; Lamb et al., 2008; Basilici et al., 2012). Considering the mudstone and siltstone dominated nature of this facies, as well as sandstone only being present as small, subordinate lenses, the deposition most likely took place in water depths below mean storm-wave base with limited influence from storms (Krassay, 1994; Midtgaard, 1996; Einsele, 2000; Baniak et al., 2014).

#### 4.1.2 Lithofacies 2: Interbedded sandstone/siltstone heterolithic

##### *Description:*

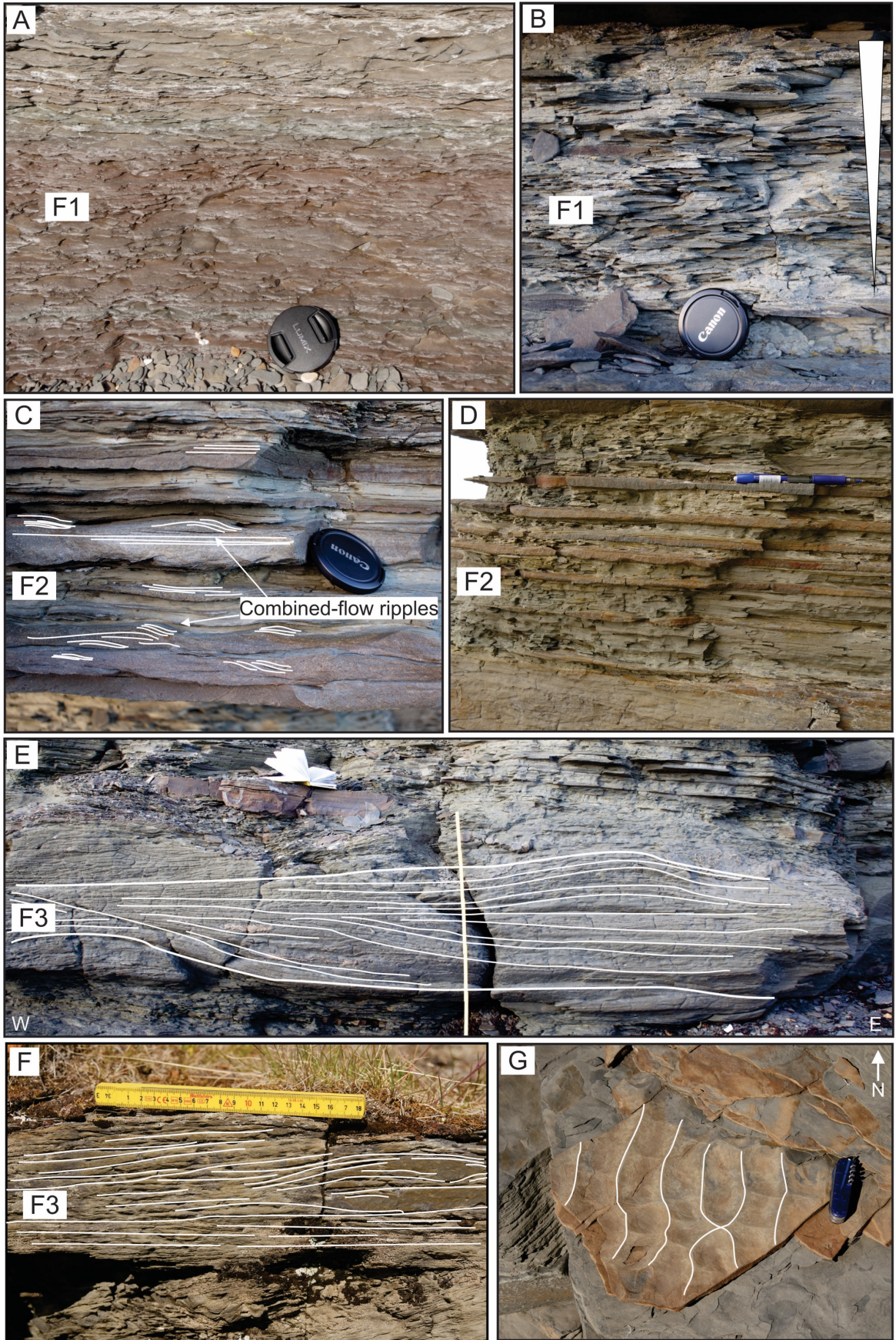
Lithofacies 2 is characterized by tabular units of alternating thin-bedded red to brown sandstone beds and dark to light grey siltstone lamination (Figs 9C and 9D). It shares many similarities to lithofacies 1, but is characterized by a higher abundance of sandstone interbeds, and is one of the most abundant facies within the investigated successions. It is present throughout the formations and is frequently found on top of lithofacies 1, as well as in lateral extensive units in between thicker sandstone beds. The thin sandstone beds in lithofacies 2 are normally graded, consist of very fine-to-fine-grained sandstone and typically exhibit a pinch-and-swell bed geometry (Fig. 9D). The individual beds rarely exceed a thickness above 4 centimetres and the average bed is approximately 1-2 centimetres thick. Structures characterizing the sandstone beds are slightly asymmetrical round-crested ripples (Fig. 9C) similar to those observed in facies 1, as well as planar- to undulating lamination occurring in the bed divisions below the ripples. Although some of the beds may display a more massive appearance (Fig. 9D). Each siltstone interbed differs considerably in thickness, but they are normally between 2 and 10 centimetres thick.

##### *Interpretation:*

Lithofacies 2, which is found in both the Andersby and Klubbnasen formations, represents a general low-energy depositional environment. The laminated siltstone is most likely deposited during fair-weather conditions as hemipelagic fall-out, while each thin-bedded, lenticular sandstone bed likely represent single storm events in more distal, deep water settings (Alfaro et al., 2002; Basilici et al., 2012; Brenchley et al., 1993; Dumas et al., 2005; Arnott, 1993). The rippled sandstone beds also display similarities with thin bedded turbidites elsewhere and could therefore represent deposition by dilute, low-density

turbidity currents (Lamb et al., 2008). However, due to the presents of rounded, slightly asymmetrical ripples, these beds are likely deposited by oscillatory-dominated flow with a relatively weak unidirectional component and therefore more likely deposited by combined flows during waning storms that reached considerable depths or a combination between (Arnott and Southard, 1990; Basilici et al., 2012). Lithofacies 2 is therefore interpreted as distal storm beds deposited above the average storm-wave base in water depths where only major storms affected the seafloor. The siltstone lamination represents background deposition during fair-weather periods.







Figur 9. Representative photos of lithofacies 1 to 3. 9A) Lithofacies 1, laminated mudstone. Lens cap for scale (5 cm) 9B) Lithofacies 1, laminated siltstone with small sandstone lenses (white triangle indicates coarsening upward). Lens cap for scale (5 cm). 9C) Lithofacies 2, interbedded siltstone and sandstone where the sandstone display combined-flow ripple lamination. 9D) Lithofacies 2, interbedded siltstone and sandstone Pen for scale (13 cm). 9E) Lithofacies 3, sandy siltstone bed with HCS obtaining a pinch-and-swell geometry. Meter stick for scale (1 m). 9F) Lithofacies 3, unit of a typical HCS-bearing sandy siltstone bed with planar lamination in the lower part. Ruler for scale (20 cm). 9G) Wave ripples on bedding surface (sandstone). Pocket knife for scale (8 cm)

#### 4.1.3 Lithofacies 3: Hummocky cross-stratified/deformed siltstone (silty sandstone)

##### *Description:*

Lithofacies 3 consists of dark to light grey siltstone with considerable proportion of very fine-grained sandstone (Fig. 9E and 9F). The lithofacies is observed in the lower part of the successions at both the Klubbnasen (Klubbnasen Formation) and Bergelva (Andersby Formation) localities, while it is more uncommon in the Vadsø locality. The siltstone beds are usually normally graded (from very fine-grained sandstone to siltstone), commonly 50-100 centimetres thick, sometimes reaching thicknesses up to 2 meters. They normally extend laterally for several hundred meters typically displaying a weak pinch-and-swell bed geometry (Fig. 9F). The upper boundary is usually gradational, commonly grading upwards into siltstone-dominated sediments (lithofacies 1 and 2), while the lower boundary is typically sharp and erosive. Internally, lithofacies 3 is predominated by large-scale hummocky cross-stratification (HCS) and occasionally planar to low-angle undulating laminations (Figs 9E and 9F). The HCS usually display an isotropic (i.e. no preferred orientation of dipping stratification) appearance and is characterized by the presence of several second-order truncations internally (*Sensu* Dott Jr and Bourgeois, 1982). The sedimentary structures are frequently heavily disturbed by soft-sediment deformation structures (e.g. ball-and-pillow structures; Figs 24C and 24D) and only remnants of the primary structures can be observed several places.

##### *Interpretation:*

Lithofacies 3 is dominated by the distinctive structure HCS, which is a prominent evidence of deposition by storm-dominated flows (Harms, 1975). Based on the isotropic character of the HCS, deposition most likely took place under an oscillatory dominated flow by vertical aggradation during storm events. The second order truncations within the HCS indicate several erosional events representing fluctuation in the storm-produced flow or multiple

storm events (Duke, 1991; Cheel and Leckie, 2009; Morsilli and Pomar, 2012), while the normally graded character of the beds is attributed to overall waning storm conditions.

The planar to low-angle undulating lamination (Fig. 9F), which occasionally underlies the HCS, is believed to be a product of deposition under high-energy oscillatory dominated combined-flow conditions (e.g. Arnott, 1993) and will be further discussed in lithofacies 5.

The presence of sharp base indicate erosion during peak storm activity. Lithofacies 3 is thus interpreted to be formed by waning storms close to storm-wave base where only very-fine sand and silt were available.

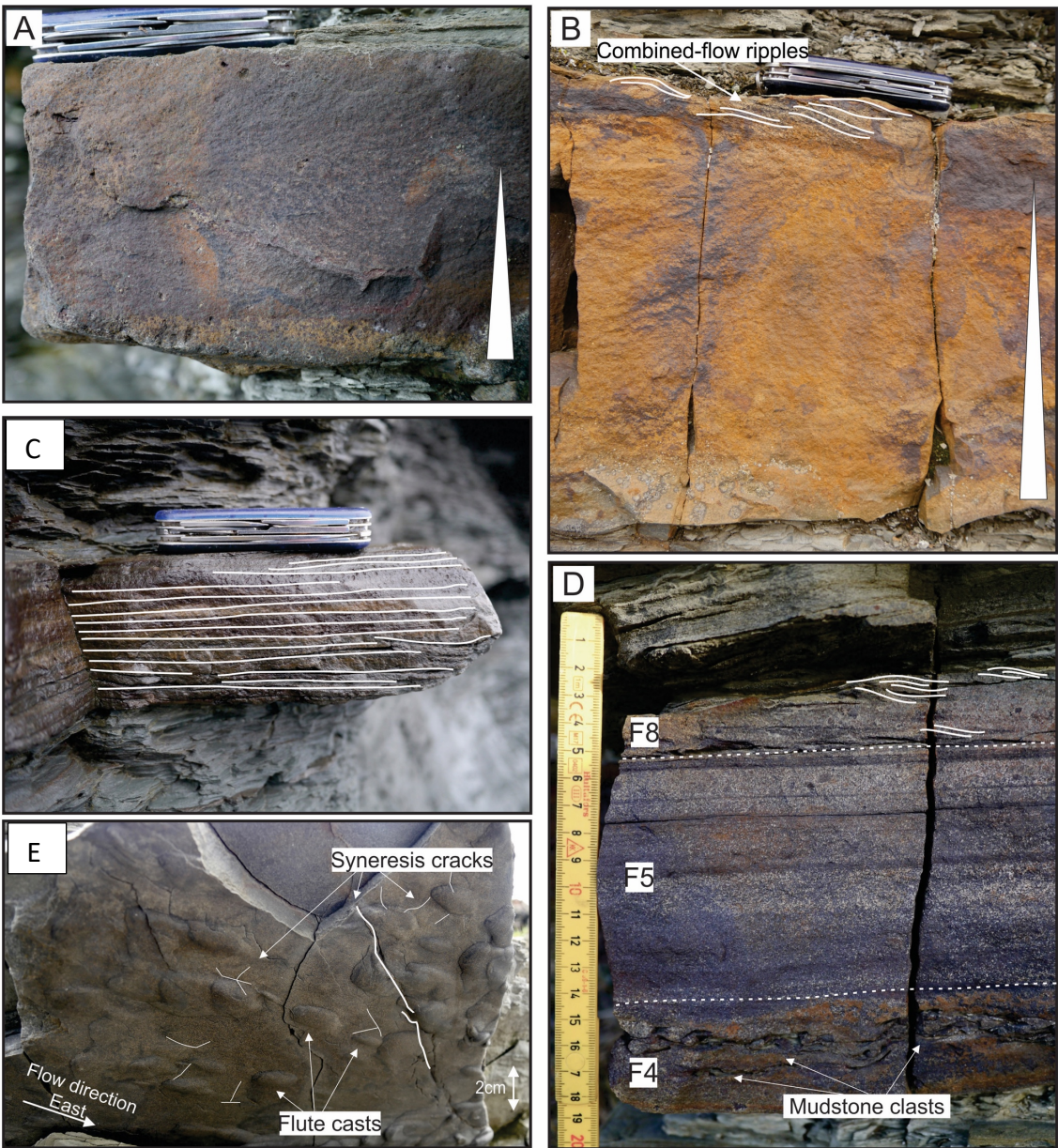


Figure 10. Representative photos of lithofacies 4 and 5. 10A) Massive sandstone displaying normal grading (marked by white triangle; lithofacies 4). 10B) Typical massive sandstone bed capped with combined-flow ripple lamination (lithofacies 8). 10C) Sandstone displaying planar lamination (lithofacies 5). 10D) Typical event bed with a lower massive base with mudstone clasts, overlain by planar lamination which are capped with combined-flow ripple lamination. 10E) Sandstone base with both flute casts and syneresis cracks. Flow direction towards east. Pocket knife for scale (8 cm).

#### 4.1.4 Lithofacies 4: Massive sandstone

##### *Description:*

Lithofacies 4 typically occurs in the lower part of sandstone beds (e.g. event beds) that otherwise is characterized by wave-generated/traction structures, although it may also completely dominate some beds (Figs 10A and 10B). It consists of massive (structureless), commonly weak normally graded, very fine-to-fine-grained sandstone, which may contain small horizontally aligned rip-up mudstone clasts towards the base (Fig. 10D). The thickness of this facies varies from a few centimetres to approximately 15 centimetres, usually displaying a sharp lower boundary with abundant and well-developed sole marks such as flute casts, longitudinal scours and gutter casts. The flute casts are by far the most abundant sole marks in this lithofacies and ranges in length from 2 to 10 centimetres (Fig. 10E), depending on the bed thickness. Paleocurrent data from the measured flute casts shows a predominantly orientation toward east. The upper part of the facies may display very weak planar lamination, often marking a diffuse transition from lithofacies 4 to lithofacies 5/lithofacies 6.

##### *Interpretation:*

The lack of sedimentary structures in lithofacies 4 indicates deposition under upper-flow regime conditions with high aggradation rates. Under these conditions, rapid fallout suppresses the tractive transport of grains therefore inhibit the formation of lamina causing a structureless deposit. This was demonstrated during a flume experiment conducted by Arnott and Hand in 1989 where different bedforms were produced under different flow rates and sediment input. Lithofacies 4 also contain different sole marks, including flute casts, indicating the presence of a highly erosive unidirectional, turbulent flow before deposition commenced (Beukes, 1996; Lamb et al., 2008). The mudstone clast present at the base of lithofacies 4 is interpreted to be ripped up during the early erosive stage of the flow and transported for a short distance before being incorporated into the sandstone. The depositional features given above is typically recognized in turbidites (Arnott and Hand, 1989; Mutti et al., 2003; Basilici et al., 2012). Accordingly, lithofacies 4 may be interpreted to



represent the  $T_a$  interval in a typical Bouma sequence (Bouma, 1962). However, the occurrence of structures reflecting an oscillatory flow (see lithofacies 6 and 7) overlying lithofacies 4 implies the presence of wave action at these depths.

Based on these observations, lithofacies 4 is probably deposited by a waning high-velocity flow governed by initial erosion and later abundant sediment fall-out. The flow is interpreted to be unidirectional with the possibility of a small oscillatory component being present.

#### 4.1.5 Lithofacies 5: Planar laminated sandstone

##### *Description:*

This lithofacies generally represents the lower or middle part of individual sandstone beds (e.g. event beds, characterized by a structureless lower division, i.e. lithofacies 4), and exhibits planar laminated fine to very-fine grained sandstone (Figs 10C and 10D). The thickness of each laminae is usually less than 0.5 cm and commonly not graded, although some beds as a whole display weak normal grading. The planar laminated sandstone commonly transfers upwards into low-angle, weakly undulating lamination, which may be divided into lamina-set separated by low-angle truncation surfaces. The laminae show vertical aggradation and may extend laterally throughout the bed length, although it may occasionally pinch out. This facies may also contain small horizontally aligned mudstone clasts in the lower division, which are a few millimetres across similar to those found in lithofacies 4. The facies is typically overlain by HCS sandstone (lithofacies 6), but may also be capped by combined-flow ripples (lithofacies 7, Fig. 10D). The lower boundary is usually sharp or erosional, occasionally displaying different scour marks like flute casts and small gutter casts (Fig. 10E).

##### *Interpretation:*

The planar lamination of lithofacies 5 is believed to represent deposition under upper flow regime conditions where any former structures would be erased (Dumas et al., 2005). Rapidly migrating bed-load sheets might have caused the thin lamination found present. Although, it may also be formed under fluctuations in current velocity or sediment load in conditions where bed load sheets are suppressed (Arnott and Hand, 1989; Duke, 1991; Myrow et al., 2002). The undulating, low angle lamination observed in this facies, displays several similarities to the quasi-planar lamination described by Arnott (1993). These

structures were produced in an flume experiment in a upper plane bed phase under combined flow conditions with a small unidirectional component (Arnott and Southard, 1990). The various sole marks and rip up mudstone clasts occasionally observed on the base of the lithofacies (Fig. 10E), indicate erosion by the initial strong unidirectional turbulent flow, which were later deposited. According to these observations, lithofacies was deposited by a waning high-energy flow that reached upper flow regime conditions. Similar features are commonly observed in both storm beds as well as the Bouma sequence ( $T_b$  interval), while the quasi-planar lamination is generally linked to storm-generated currents.

#### 4.1.6 Lithofacies 6: Hummocky cross-stratified sandstone (isotropic vs anisotropic)

##### *Description:*

Hummocky cross-stratified sandstone (Fig. 11) is the most prominent feature of the Andersby and Klubbnasen formations, constituting an important bed division of a typical vertical facies succession. Both in the Andersby and Klubbnasen formations, the HCS ranges considerably in both scale and internal stratification geometry. The HCS beds commonly consist of very fine to fine-grained sandstone, red- to yellowish brown, typically normally graded comprising 5 to 30 centimetres thick beds (Figs 11A and 11B). Each lamina is normally 0.2 to 1 centimetre thick, forming undulating parallel lamina sets, which occasionally separated by surface truncations. The HCS frequently contain rip-up mudstone clasts towards their base, often displayed together with both loading structures and frequently flute casts (Fig. 10E).

In the Andersby Formation, the HCS beds extend laterally for several hundred meters commonly displaying a pinch and swell architecture with a meter scale wavelength (Fig. 11D and E). The beds are usually found in association with other typical tempestite structures such as combined flow ripples and quasi-planar/planar lamination. The HCS units are dominantly isotropic (Fig. 11B), but locally displays a preferred dip-orientation towards west. As well as being typically non-amalgamated and isolated (Fig. 11D), the beds frequently grade into soft-sediment deformation structures when traced laterally (Fig. 18). The base is sharp, normally flat to weakly undulating with the occurrence of flute casts and rare load casts, particular in thicker beds with quasi- to planar lamination (lithofacies 5) present (Fig.

11C, Log B5). The upper boundary of a typical HCS unit is usually capped by combined flow-ripples and occasionally climbing-ripple lamination (lithofacies 8, Figs 13A, 13F and 15E).

The HCS units in the Klubbnasen Formation commonly obtain low-angle undulating (low angle sigmoidal foresets) lamination with a preferred dip orientation towards east (Fig. 12A, 12B and 12C). These anisotropic HCS beds are typically amalgamated and sharp-based displaying second order truncation surfaces between the beds sets (10 cm thick). The HCS units often exhibit a tabular bed geometry, while the bed sets usually are discontinuous with a pinch and swell geometry of generally small lateral extent (Figs 12A and Fig. 12B). Several bed sets are observed to split into multiple thinner beds by second order truncations when followed laterally. Thin siltstone layers (> 2 cm) frequently follows these second order truncations surfaces and thus separating the HCS beds into isolated units (Fig. 12B).

Horizontally aligned rip-up mud clasts are commonly observed in the lower part of each bed set (Fig. 12E), although several places only the imprints occur due to recent weathering.

#### *Interpretation:*

Hummocky cross-stratification is a well-known sedimentary structure from the literature, typically interpreted to represent storm-influenced deposition (Harms, 1975; Dott Jr and Bourgeois, 1982; Myrow and Southard, 1996; Dumas and Arnott, 2006). It is commonly agreed that HCS is formed by aggradation and migration of 3D bedforms deposited by purely oscillatory flows or oscillatory-dominated combined-flows (Dott Jr and Bourgeois, 1982; Arnott and Southard, 1990; Duke, 1991; Hill et al., 2003; Morsilli and Pomar, 2012). In both the Andersby and Klubbnasen formations, a variety of HCS structures are observed, reflecting differences in both flow properties, as well as sediment availability and proximity to the sediment source.

The predominance of isolated HCS beds with erosive bases observed in the Andersby Formation indicate that the deposition was preceded by strong, erosive unidirectional and turbulent currents towards east forming eastward flute casts (Myrow and Southard, 1996; Lamb et al., 2008). The initial erosive stage was followed by deposition of sand and further reworking by intense oscillatory sheet flows leading to the formation of HCS. Based on the isotropic to weakly anisotropic character of the beds, the deposition most likely took place during a waning oscillatory flow with presence of only a weak unidirectional component

(Morsilli and Pomar, 2012). According to Dumas and Arnott (2006) isotropic HCS is typically found above, but near storm-wave base in distal settings where the input of sand is mostly limited to storm events. These types of HCS beds are commonly observed in association with quasi- to planar lamination (lithofacies 5) as well as combined flow ripples typical tempestite bed.

In contrast, the Klubbnasen Formation mainly consists of amalgamated and anisotropic HCS with the presence of abundant rip-up mudstone clast towards their base. The predominantly anisotropic nature of the HCS indicates that the formation took place under a combined flow with a sufficient unidirectional component (Nøttvedt and Kreisa, 1987; Arnott and Southard, 1990; Dumas and Arnott, 2006; Grundvåg et al., 2020; Jelby et al., 2020). These conditions led to deposition on the lee side of the HCS and thereby generating dune-like bedforms migrating eastward. According to Dumas and Arnott (2006) anisotropic HCS similar to those observed in the Klubbnasen Formation form in proximal settings above storm-wave base where the unidirectional component is strong enough to generate lamination with a preferred orientation. The present rip-up mudstone clasts in the lower parts of each bed-set likely indicate the presence of an erosive current before being transported and later deposited together with the sand. As well as being anisotropic, several of the HCS of the Klubbnasen Formation also display amalgamation. The amalgamated beds consist of multiple stacked bed sets divided by second order truncations and occasionally thin discontinuous siltstone layers (lenses). This implies that the sand deposited was frequently exposed to erosion and reworking together with periodically deposition of fair-weather siltstone (Leckie and Walker, 1982; Cheel and Leckie, 1992). The lateral variation in several of the HCS units, transferring from amalgamated to isolated HCS, suggests that several of the HCS units are the product of amalgamation of single storm events (Brenchley et al., 1993). The amalgamated and anisotropic HCS is thus interpreted to be formed above storm-wave base in proximal settings where frequent storms led to erosion and reworking of sand.



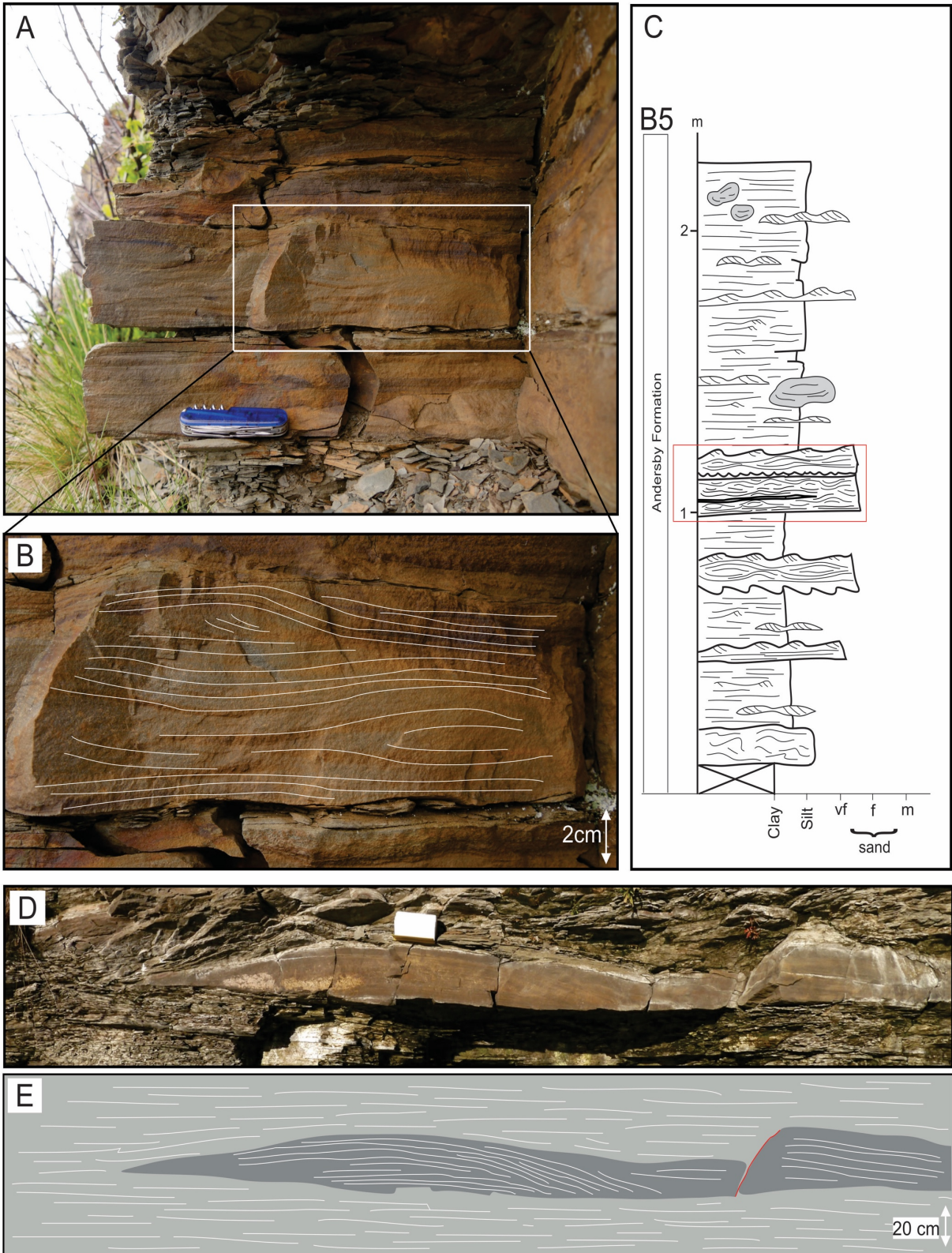


Figure 11. Lithofacies 6. 11A) Amalgamated sandstone beds of HCS and planar lamination. Pocket knife for scale (8 cm). 11B) Closer view of isotropic HCS bed. Notice the occurrence of combined-flow ripple lamination in the upper left part. 11C) Detailed log from the Bergelva locality (panel 1) Amalgamated HCS beds is marked with red square. 11D) Pinch-and architecture of isotropic HCS bed. Red line represents a small fault. Note book for scale (18 cm). 11E) An interpretative sketch of the HCS bed shown in 11D.

#### 4.1.7 Lithofacies 7: Swaley cross-stratified sandstone

##### *Description:*

Lithofacies 7 comprises units of fine to medium grained light yellow to light grey sandstone beds displaying swaley cross-stratification (SCS, sensu Leckie and Walker, 1982). The units are 0.20 to 0.70 meter thick commonly amalgamated containing bed sets (10-20 cm thick) of low-angle trough cross-stratification (concave-upward sets) with erosional shallow scours cutting into the underlying strata (Figs 12B and 12D). The swaley troughs commonly obtain an asymmetrical profile where the lamina has a preferred dip-direction eastward. Thin siltstone beds and lenses may be interbedded between certain bed sets (Fig. 12B). Each bed set displays sharp bases coupled with frequent mudstone clasts (Fig. 12E). The upper surface is commonly flat to undulated with a sharp transition to the overlying siltstone. Lithofacies 7 is only observed at the Klubbnasen locality in the middle to upper part of the formation, normally in association with anisotropic HCS (Fig.12A, B, C and D)

##### *Interpretation:*

SCS is commonly found in association with HCS and is interpreted to be genetically related and deposited by storm-dominated processes above fair-weather wave base (Leckie and Walker, 1982; Dumas and Arnott, 2006). The low-angle swales characterizing SCS indicate low aggradation rates, which is a product of higher sediment rates closer to shore (Dumas and Arnott, 2006). The laminae with preferred dip direction eastward imply the presence of a weak unidirectional current leading to offshore-directed bed form migration (Nøttvedt and Kreisa, 1987). In the Klubbnasen Formation, SCS is usually observed overlying or interbedded with anisotropic HCS, which indicates deposition in shallower water. The presence of only thin siltstone beds and lenses in between the SCS suggest frequent reworking and removing of fair-weather deposits by storms. Accordingly, lithofacies 7 is interpreted to be deposited in proximal settings where frequent storm events occurred obtaining a sufficient unidirectional current resulting in the formation of lamina with a preferred dip-direction offshore.



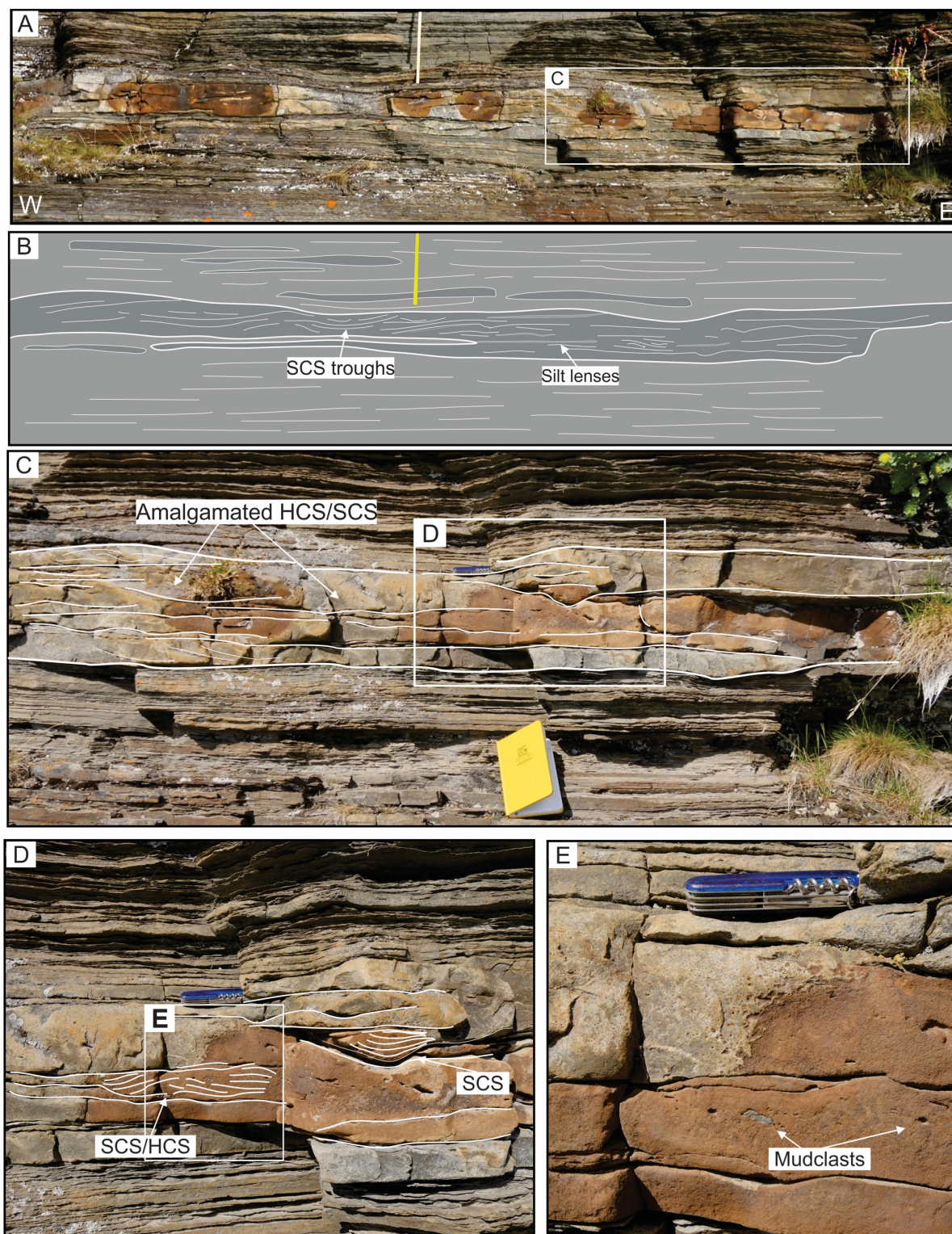


Figure 12. Lithofacies 6 and 7. 12A) Overview of amalgamated beds of both HCS and SCS. 12B) Interpretative sketch of 12A. Notice the thin silt lenses and the occurrence of Swaley troughs. 12C) Amalgamated and gently east-dipping HCS/SCS: 12D) Close-up view amalgamated SCS and SCS. Notice the occurrence swaley-trough marked with arrow. 12E) Mudstone clasts in the amalgamated sandstone. Pocket knife for scale (8 cm).

#### 4.1.8 Lithofacies 8: Combined-flow rippled sandstone

##### *Description:*

Lithofacies 8 consists of very fine to fine-grained sandstone normally displaying low angle cross-lamination with slightly asymmetrical to symmetrical rounded crests (Figs 10B, 10D, 13A and 13B). The foresets are usually sigmoidal with a convex-up shape, although tangential foresets also occur (Figs 13B and 13F). They are usually less than 3 centimetres thick (13F) and rarely contain more than two sets of ripples. However, a variation of this lithofacies consists of low-angle climbing ripple cross-lamination usually displaying weakly asymmetrical rounded crests (Fig. 13C, 13D and 13 E). Their thickness ranges from a couple centimetres to approximately 15 centimetres, but are usually between 2 to 10 centimetres. Lithofacies 8 typically overlies either HCS (lithofacies 6) or plane parallel lamination (lithofacies 5)(Fig. 10B and 10D), but may occasionally overlie massive sandstone (lithofacies 4), especially in the thinner beds. Where the bed planes are visible, they exhibit both 2D and 3D ripple forms, often gradually changing between the two endmembers.

##### *Interpretation:*

Lithofacies 8, composed of asymmetrical and rounded crested ripples, displays typical characteristics of combined-flow ripples (Arnott and Southard, 1990; Yokokawa et al., 1995). Based on the weak asymmetrical to symmetrical character of the ripples, the flow was most likely oscillatory dominated waning flow with only a weak unidirectional component present (Harms, 1969; Myrow and Southard, 1991; Yokokawa et al., 1995; Myrow et al., 2002; Lamb et al., 2008; Yamaguchi and Sekiguchi, 2010; Basilici et al., 2012) . The sigmoidal form of the majority of the foresets indicates that wave-generated vortices in the troughs of the ripples were present during their formation and thus diminishing stoss side erosion (Yokokawa et al., 1995). The climbing-ripple cross-lamination present in parts of the formations are indicative of deposition by a decelerating combined-flow with high sediment input favouring both aggradation and bed form migration (Myrow et al., 2002). Both combined-flow ripples as well as climbing-ripple cross-lamination similar to those observed are recognized in other ancient tempestite and turbidite deposits, representing parts of a so called wave-modified turbidite (e.g. Myrow et al., 2002).



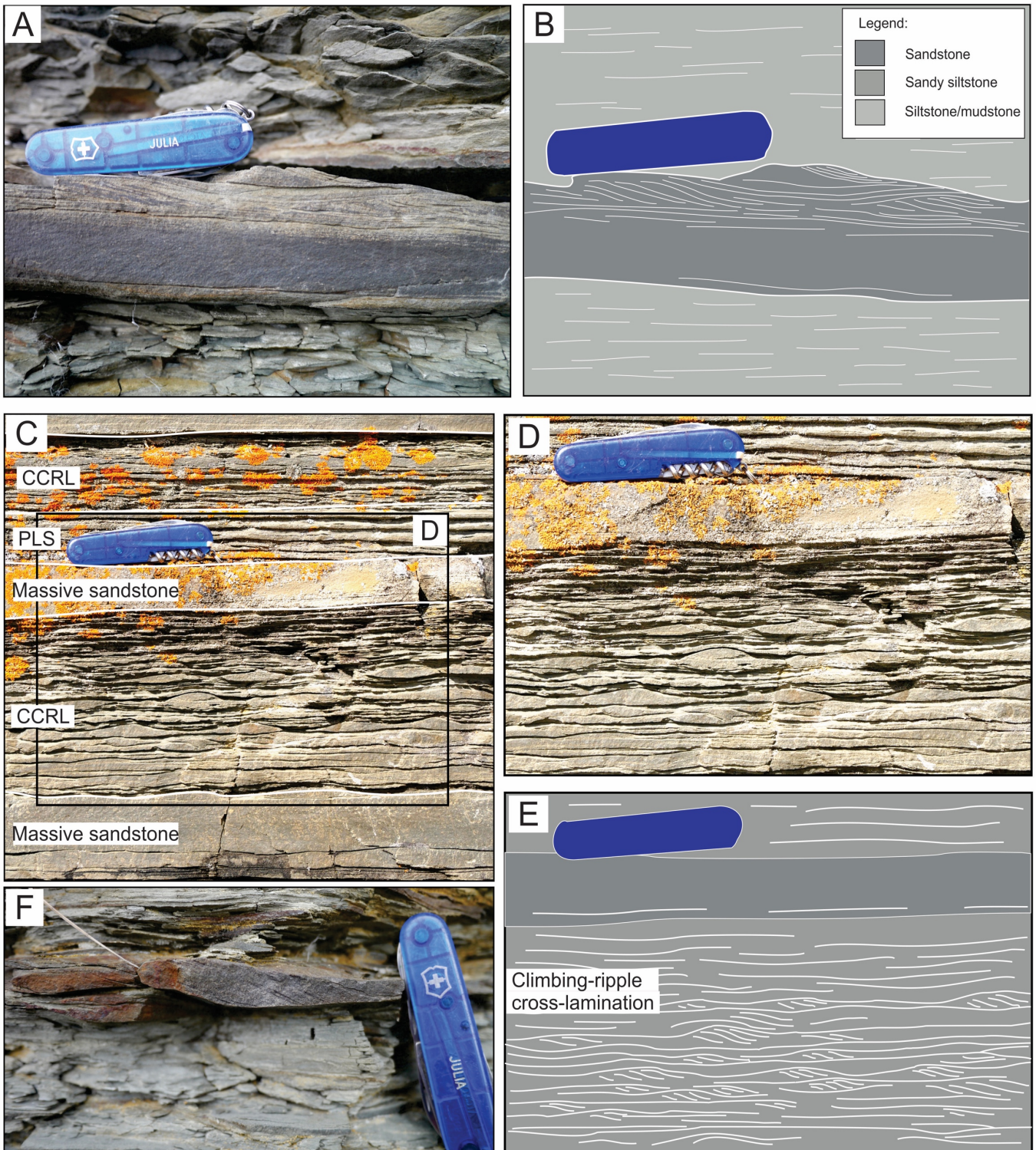


Figure 13. Lithofacies 8. 13A) Thin sandstone bed containing combined-flow ripples. The lower part display massive stratification. 13B) Interpretative sketch of Fig. 13A. Notice the foresets (some sigmoidal) with a convex-up shape. 13C) Photo displaying combined-flow rippled lamination (CCRL), which overlies and underlies massive stratified sandstone beds (lithofacies 4). The upper unit of CCLR is overlying planar laminated sandstone (PLS, lithofacies 5). 13D) Close-up view of the CCRL in Fig. 13C. 13E) Interpretative sketch of Fig. 13D) Distinctive sandstone lens displaying combined-flow ripple lamination. Notice the pinch-and-swell architecture of the lens. Pocket knife for scale (8 cm).

#### 4.1.9 Lithofacies 9: Cross-bedded sandstone

##### *Description:*

Lithofacies 9 is characterized by light brown to light yellow, fine to medium-grained sandstone exhibiting both planar and trough cross-stratification dipping towards east (Fig. 14). It is mainly found in the middle to upper part of the Klubbnasen Formation in distinct, sharp-based bed sets (Fig. 14A), as well as being a dominant feature in the overlying Fugleberget Formation (Fig. 14C). The beds are often stacked where each set range in size from 10 to 50 centimetres with one to two centimetres thick cross-strata (Fig. 14A, B and C). In the Klubbnasen Formation, the cross-bedded sandstones typically display tabular to tangential convex-upward foresets where the dip angle typically decreases towards the toe set (Fig. 14F). The beds are frequently horizontal and tabular, although vertical changes in both bed architecture and inclination occur. Through cross-bedding (Fig. 14B and 14C) is less common, but do occasionally occur in association with planar-cross bedding and planar-bedded sandstone (lithofacies 10). The beds, which rarely exceed 20 centimetres in thickness, frequently contain rip-up mudstone clasts towards their base. Where the bedding surface are visible, they frequently display rib-and-furrow structures (Fig. 14D). In the lowermost part of the Fugleberget Formation, which is situated on top of the Klubbnasen Formation, both planar and through cross-bedding are observed (Fig.14C). They are typically thicker (20-50 cm thick) than the cross-bedded sandstone found in the Klubbnasen and is commonly overlain by planar-bedded sandstone and occasionally weakly laminated siltstone.

##### *Interpretation:*

Lithofacies 9 displays typical structures associated with migration and stacking of both 2D (tabular/tangential cross-bedding) and 3D (trough-bedding) dunes. Dune migration are usually generated in a steady, uniform unidirectional traction current where sand grains are transported and deposited as bedload on the lee side (Bridge et al., 1986). Based on this, lithofacies 9 is interpreted as having been formed by unidirectional traction currents in an intermediate flow regime where the supply of sand is adequate to promote dune formation.

#### 4.1.10 Lithofacies 10: Planar-bedded sandstone

##### *Description:*

Lithofacies 10 is relatively rare and only observed in a few beds in the middle part of the Klubbnasen Formation (Fig. 14B) as well as in the lowermost part of the overlying Fugleberget Formation (Fig. 14C). The facies consists of fine to medium-grained sandstone exhibiting centimetre thick plane parallel stratification where the bed surfaces typically display parting lineation oriented in an east-west trend (Fig. 14E). In the Klubbnasen Formation the planar-bedded sandstone usually exhibits 10 and 20 centimetres thick bed-sets interbedded with lithofacies 9, occasionally containing rip-up mudstone clasts towards their base. The planar-bedded sandstones found in the lower part of the Fugleberget Formation generally consist of thicker beds (0,4 to 2 meters) typically overlying through-cross bedding (lithofacies 9; Fig. 14C).

##### *Interpretation:*

Based on the presence of parting lineations in lithofacies 10, the planar-bedded sandstone most likely record deposition under upper-flow regime conditions. In these settings the formation of ripples and dunes are inhibited, and the planar beds are formed during traction transport of sand grains along the bed. The parting lineations are formed by microvortices sorting the sand grains into parallel, elongated ridges (Fielding, 2006; Cheel, 1991). Based on its stratigraphic position, the presence of unidirectional -dominated structures above and below, and the lack of wave-generated structures, lithofacies 10 is considered to be deposited by a unidirectional current. The planar-bedded sandstones within the Klubbnasen Formation are thus interpreted to be formed in upper-plane bed conditions by unidirectional currents in nearshore settings where the sand supply is sufficient (Allen, 1984; Cheel, 1990). While the beds of the Fugleberget Formation are formed under the same hydrodynamic conditions, but in a fluvial setting.



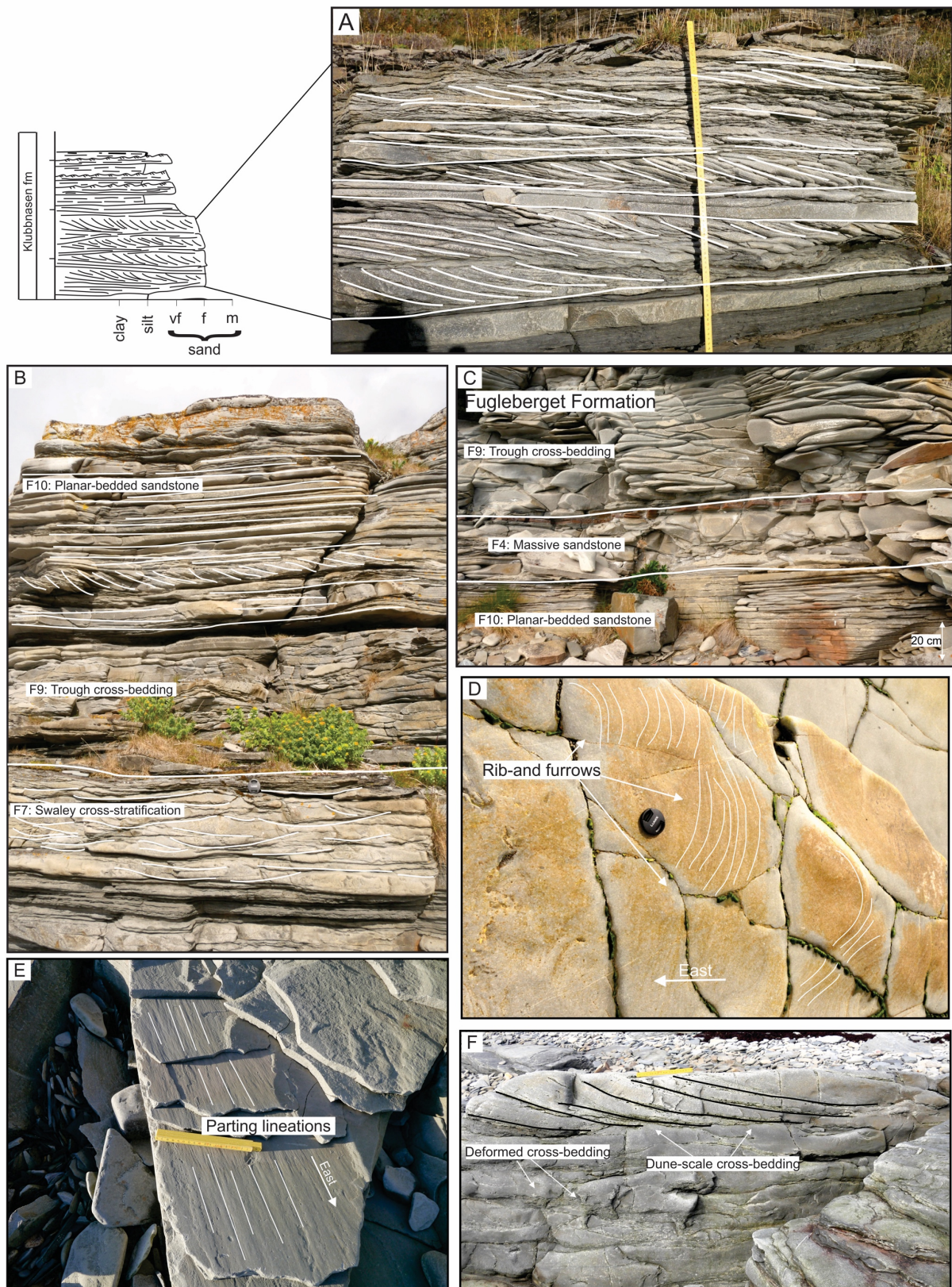
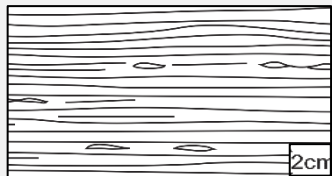


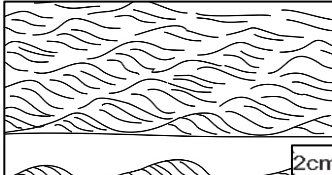
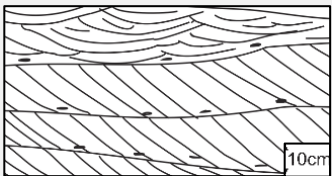
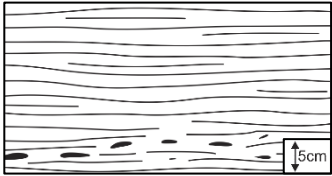


Figure 14 Lithofacies 9 and 10. 14A) Cross-bedded sandstone of the Klubbnasen Formation with representative log. Meter stick for scale (1 m). 14B) Overview of a typical sequence of SCS (lithofacies 7), trough cross-bedding (lithofacies 9) and planar laminated sandstone (lithofacies 10). Klubbnasen locality. 14C) Typical structures of the Fugleberget Formation. 14D) Bedding surface displaying rib-and-furrows. Lense cap for scale (5 cm). 14E) Bedding surface displaying parting lineation. Ruler for scale (20 cm) 14F) Sandstone bed with dune-scale cross-bedding. Notice the decrease in dip-angle towards the toe. Ruler for scale (20 cm).



Table 1. Summary of lithofacies.

LITHOFACIES	DESCRIPTION	INTERPRETATION	FACIES SKETCH
<p><b>1</b> Laminated siltstone and mudstone</p>	<p>Tabular units of laminated siltstone and mudstone with scattered cm-scale sandstone lenses, some displaying wave ripple or combined-flow ripple cross-lamination. Sand-filled syneresis cracks occur frequently in some horizons. Thickness: 0.1 to 2 m</p>	<p>Hemipelagic fallout sporadically interrupted by minor deposition of sand from weak oscillatory flows and oscillatory combined-flows. Deposition took mostly place below storm wave base (SWB). Syneresis cracks may be caused by fluctuating palaeosalinity stress or de-watering triggered by wave-induced stress or seismic shocking.</p>	
<p><b>2</b> Interbedded sandstone/siltstone</p>	<p>Interbedded very-fine grained sandstone and siltstone units. The sandstone beds are lenticular commonly containing planar lamination and combined-flow ripple cross-lamination or less commonly wave ripple cross-lamination. Ball-and-pillow structures occur locally. Thickness: 0.1 to 1 m</p>	<p>Hemipelagic fallout frequently interrupted by deposition of sand from dominantly combined-flows governed by storms and turbidity currents above SWB.</p>	
<p><b>3</b> Hummocky cross-stratified siltstone</p>	<p>Isotropic hummocky cross-stratified (HCS) and low-angle laminated sandy siltstone with a weak pinch-and-swell bed geometry and abundant dewatering and ball-and-pillow structures. Internal second-order truncations (<i>sensu</i> Dott &amp; Bourgeois, 1982) occur sporadically. Thickness: 0.2 to 2 m</p>	<p>Erosion and deposition by storm generated high to medium speed oscillatory combined-flows with relatively high aggradation rates. Internally truncations represents reworking by several storm events and/or fluctuation in the storm-produced flow.</p>	
<p><b>4</b> Massive sandstone</p>	<p>Tabular, non-graded to normally graded structureless very-fine to fine grained sandstone beds with erosional bases containing frequent flute casts. Thickness: 2 to 15 cm</p>	<p>Erosion by strong unidirectional to unidirectional dominated turbulent currents preceded by deposition from waning flow with high aggradation rates where the tractive transport is suppressed.</p>	
<p><b>5</b> Planar laminated sandstone</p>	<p>Planar and quasi-planar laminated (<i>sensu</i> Arnott, 1993) very-fine to fine grained sandstone occasionally containing mudstone clasts and flute casts. Thickness: 2 to 30 cm</p>	<p>Erosion by strong unidirectional to unidirectional dominated currents followed by deposition from high waning unidirectional to combined-flows with high aggradation rates. Any potential bedform would be erased, resulting in flat beds.</p>	

6	Hummocky cross-stratified sandstone	<p>Isotropic to anisotropic HCS very-fine to fine grained sandstone beds containing frequent mudstone clasts and occasionally flute casts at their base. The isotropic hummocky cross-stratified sandstone usually display distinct pinch-and-swell geometry. Soft-sediment deformation structures are common. The HCS are frequently capped with combined-flow ripple.</p> <p>Thickness: 5 to 30 cm</p>	<p>Formed by aggradation and migration of 3D bedforms deposited by strong to intermediate waning oscillatory to oscillatory dominated currents. Deposition may be preceded by strong, erosive unidirectional currents.</p>	
7	Swaley cross-stratified sandstone	<p>Swaley cross-stratified (SCS, <i>sensu</i> Leckie &amp; Walker, 1982) fine to medium grained sandstone beds containing abundant mudstone clasts and soft sediment deformation structures. The beds are commonly amalgamated with erosive low-angle stratification.</p> <p>Thickness: 5 to 30 cm</p>	<p>Generated by storm induced currents commonly above fair-weather base (overlying HCS) with a lower aggradation rates due to higher sediment transport rates closer to shore.</p>	
8	Combined-flow rippled sandstone	<p>Low-angle cross-laminated very-fine to fine grained sandstone with asymmetrical rounded crests and sigmoidal, convex-up foresets. Sets of climbing-ripples occur locally.</p> <p>Thickness: 1 to 15 cm</p>	<p>Formed by waning oscillatory dominated combined-flows with wave-generated vortices in the foresets. Decelerating combined-flow with high sediment input favouring aggradation and bed form migration results in the formation of climbing-ripple cross-lamination.</p>	
9	Cross-bedded sandstone	<p>Both planar (tabular/tangential) and trough cross-bedded fine to medium grained sandstone. Soft-sediment deformation structures (e.g. convolute bedding, de-watering structures) and rip up mudstone clasts occur frequently.</p> <p>Set thickness: 10 to 50 cm</p>	<p>Generated by steady and uniform unidirectional currents in an intermediate flow regime. Sand grains deposited as bedload on the lee side of migrating two-dimensional and three-dimensional.</p>	
10	Planar-bedded sandstone	<p>Planar-bedded medium grained sandstone with parting lineations (on bed surfaces) and rip up mudstone clasts.</p> <p>Thickness: 0.4 to 2 m</p>	<p>Formed by unidirectional currents in upper-flow regime conditions.</p>	

## 4.2 Facies associations

Based on the lithofacies analysis (summary Table 1), four facies associations are recognized within the investigated formations at the five different locations. These are described and interpreted below. The different facies associations are presented and interpreted in terms of depositional environment, from distal to proximal settings. The Klubbnasen and Bergelva localities only contain FA1 and FA2 (Figs 18 and 19), while all FAs occur in the Klubbnasen locality (Fig. 21).

### 4.2.1 Facies association 1: Offshore

#### *Description:*

Facies association 1 (FA1) mainly consists of parallel laminated mudstone and siltstone (lithofacies 1) as well as rare interbedded sandstone, both lenses and thin beds (lithofacies 2). The association is recognized in the lowermost part of both the Klubbnasen (Fig. 21) and Andersby formations (Fig. 18) making up respectively two upward-coarsening units. In both the Bergelva and Vadsø locations, FA1 rarely exceeds a thickness of 1.5 metres, while at the Klubbnasen location, it may obtain a thickness of up to three metres. The facies association contains few well-developed sedimentary structures with the exception of planar lamination (Fig. 9A) and rare combined-flow- (Fig. 9C) and wave ripples in sandstone lenses and beds (<2 cm, Fig. 9G). However, the majority of the sandstones appear to be structureless or display very weak developed planar lamination. The sandstones are commonly restricted to the upper part of the facies association, especially at the Vadsø location where FA1 is dominated by highly homogenous laminated mudstone and siltstone throughout the lower and middle part of the facies association (Fig. 9A). Rare isolated ball-and-pillow structures are recognized in the middle to upper part at all three localities. They are commonly <15 centimetres in diameter and occasionally display well preserved internal structures with a concave-upward stratification towards their margin (Fig. 24). FA1 obtains a gradational transition to the overlying FA2 where the sandstone beds gradually increase in both number and thickness upwards (Fig. 21).

*Interpretation:*

Based on the predominance of laminated siltstone, FA1 is interpreted to be deposited in an outer shelf setting below main storm-wave base. The laminated siltstone represents prolonged periods of fair-weather deposition (Brenchley et al., 1986), while the presence combined-flow ripple and wave ripples in coarser lenses and thin beds as well as massive beds mark a significant increase in energy associated with either distally waning storm events (Myrow, 1992; Einsele, 2000) or dilute, low-density turbidity currents (Bouma, 1962; Myrow et al., 2008). Distinguishing these processes may be problematic as their distal deposits display several similarities both in architecture and sedimentary structures. Although, several of these beds, both structureless and rippled, may represent a combination of both storm- and turbidity currents, respectively wave-modified turbidites (Mutti et al., 1996; Myrow et al., 2002; Lamb et al., 2008). Similar deposits are observed in several ancient offshore environments (e.g. Lamb et al., 2008). The ball-and-pillow structures commonly found in the upper part of the facies association indicate the existence of a reversed density gradient (sandstone overlying siltstone) accompanied with a trigger mechanism (Rossetti, 1999). FA1 is consequently considered to represent an outer shelf depositional environment where only rare storm events and turbidity currents affected the sea floor.

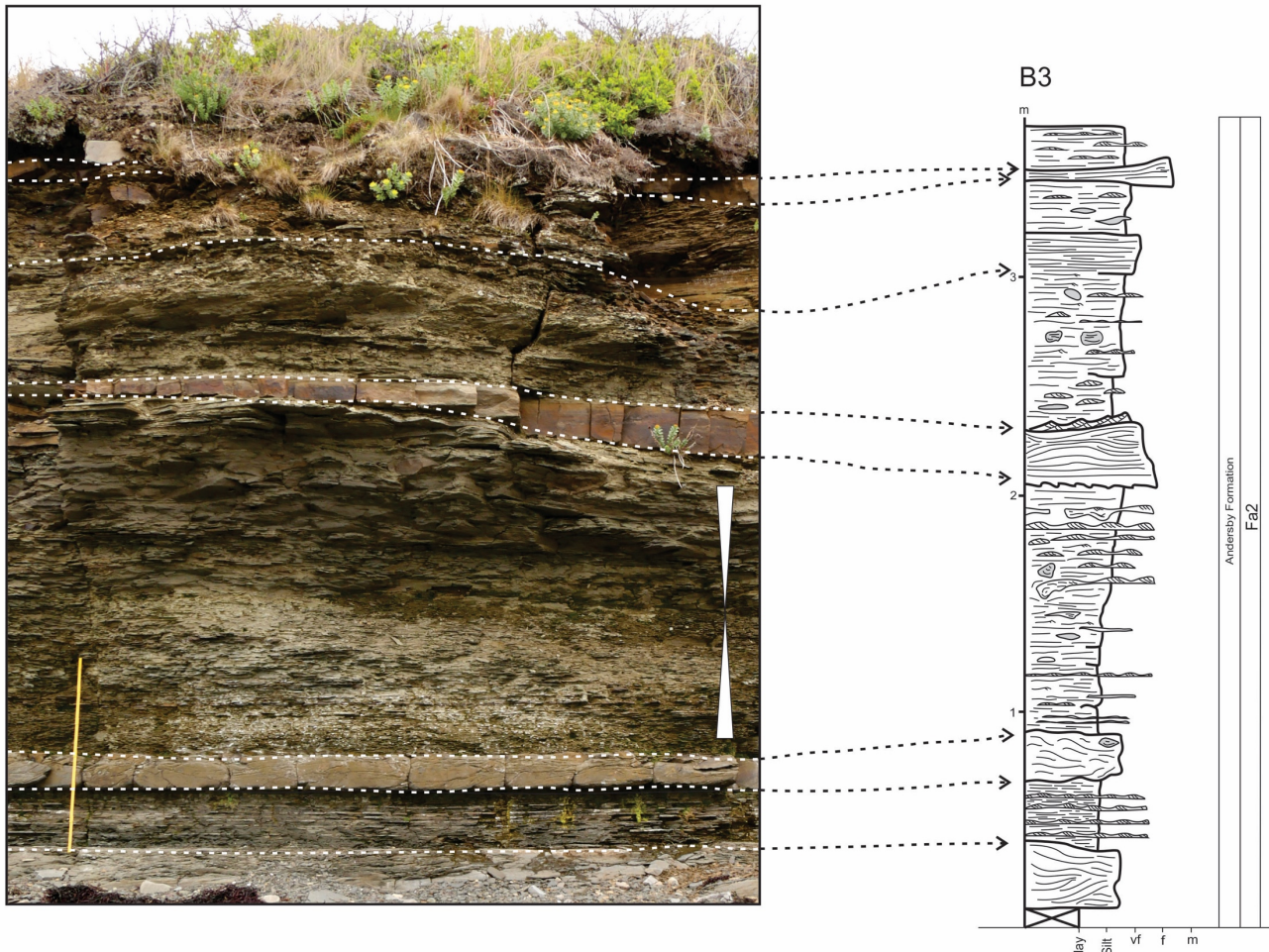


Figure 15. Overview photo from the Bergelva locality displaying the typical characteristics of a prodelta succession (FA2), which is correlated with log B3 (Fig. 17 and 18). White triangles indicate a fining to coarsening upward trend. Meter stick for scale (1 m).

#### 4.2.2 Facies association 2: Storm-influenced prodelta deposits

##### **Description:**

Facies association 2 (FA2) comprises 0.5 to 4 m thick upward coarsening and occasionally upward fining units of laminated sand-streaked siltstone (heterolithic, <100 cm) (lithofacies 1 and lithofacies 2) and both thin and thick interbedded sandstones, sporadically interrupted by beds of hummocky cross-stratified/deformed sandy siltstone (<70 cm, lithofacies 3) (Figs 15 and 16F). FA2 is normally restricted to the middle and upper successions of the Bergelva (Figs 15 and 18) and Vadsø locality (Figs 35 and 36), whereas in the Klubbnasen locality, FA3 primarily makes up the lower to middle part (Fig. 21). Both the thin-bedded and thick-bedded sandstones are typically lenticular or tabular and increases in both thickness and number upwards in the units (Figs 16 and 19). In the Andersby Formation (Bergelva and Vadsø locality) these beds can be traced laterally for tens of meters throughout the extent of

the outcrop with a meter-scale wavelength (Figs 19 and 36). The sandstone beds are normally graded with sharp to erosional bases typically containing flute casts of various sizes and rare load casts. The thin-bedded sandstones (2-10 cm thick) commonly obtain a lower massive base (lithofacies 4) and/or planar lamination (lithofacies 5) frequently capped with combined-flow ripples (lithofacies 8) at the top (Fig. 9C). Locally, HCS occur. Thin sandstone beds with wave ripples are sporadically observed in all three localities, typically in the lower part. The thick-bedded sandstone of FA2, dominates the middle to upper part of the facies association, are 10 to 40 centimetres thick constituting a diversity of lithofacies (Fig. 10A, 10B, 10D, 11B, 16C, 16D and 16E). The majority of these sandstone beds exhibit a typical vertical stacking pattern consisting of a lower structureless division (lithofacies 4) grading upwards into planar to quasi-planar lamination (lithofacies 5) and HCS (lithofacies 6) frequently capped with combined-flow ripples and rare climbing-ripple lamination (lithofacies 8). The beds commonly display variations in the typical bed architecture, which may lack one or more interval. In some cases, certain lithofacies (e.g. planar lamination (lithofacies 5)) may also be repeated in the bed sequence. Overall, the thick sandstone beds typically increase in concentration upwards in the formations, especially at the Klubbnasen locality (Fig.19 and 21) where they also have a tendency to become amalgamated (Figs 12A, 12B, 12C, 12D, 12E). However, the sandstone beds of the Klubbnasen locality typically obtain a simpler bed architecture, normally displaying only planar to quasi-planar lamination or anisotropic HCS (Fig. 12A and 12B). At the Bergelva locality the sandstone beds are usually gradually deformed eastward (Fig. 17 and 18), displaying both syn-sedimentary faults (Fig. 31) and soft sediment deformation structures such as different load structures and convolute lamination (Fig. 25). Similar trends are also present at the Vadsø and Klubbnasen localities, but at the Vadsø locality the sediments are usually severely deformed (Fig. 36). FA2 is also characterized by a sparse number of HCS sandy siltstone units (lithofacies 3, Figs 9E, 9F and 18), which are restricted to the lower and middle part of the FA2, typically overlying laminated siltstone/mudstone with an erosive base. SSDS (e.g. ball-and-pillow structures) associated with liquefaction and fluidization processes together with the presence of rare meter-scale erosive scours occur throughout the facies association. In all three localities, FA2 is transitionally overlying the fine-grained offshore facies association (FA1) (Fig. 21).



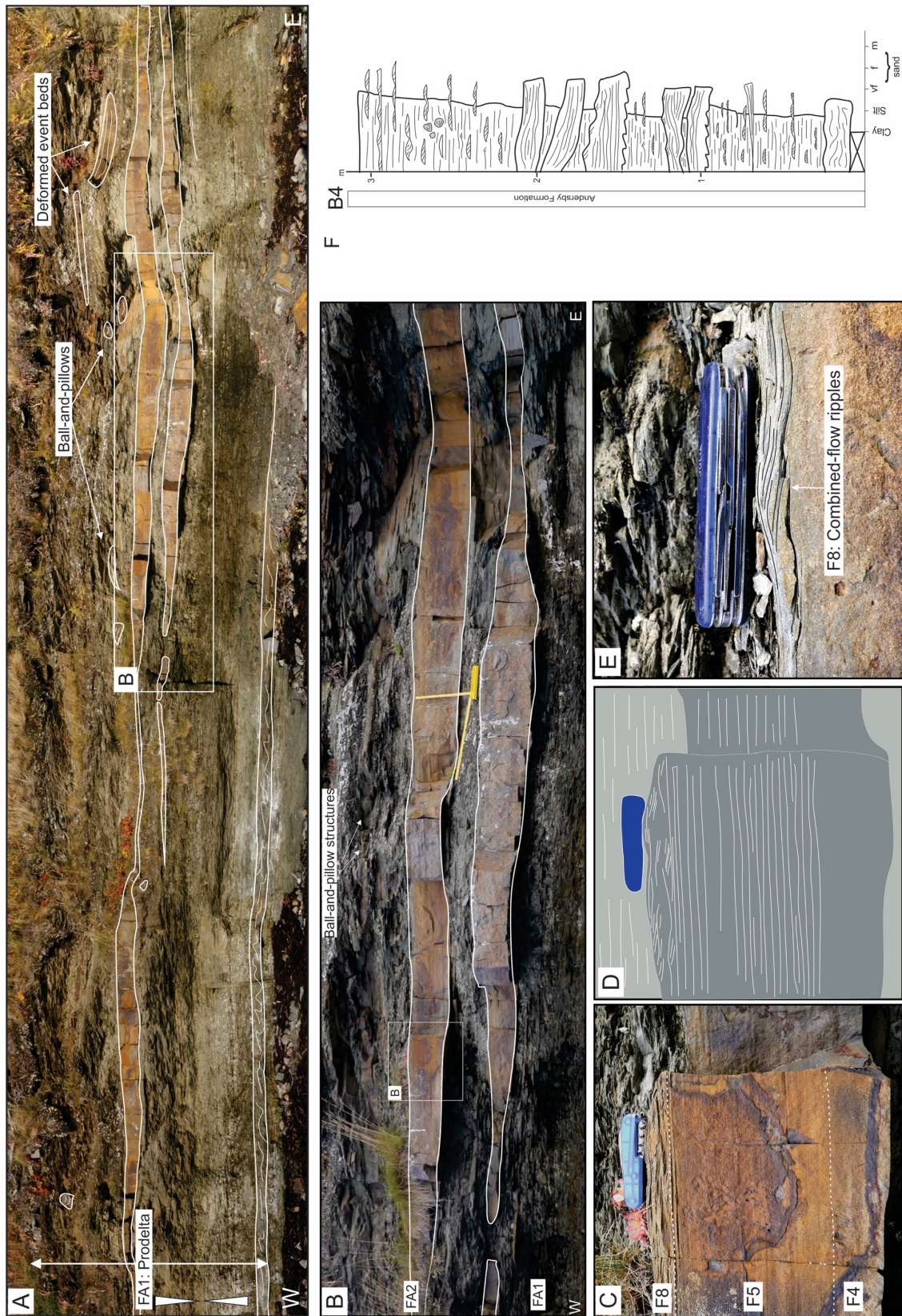


Figure 16 Representative photos of facies association 2 (prodelta). 16A) Panorama of prodelta successions at the Bergelva locality. Notice the pinch-and-swell geometry of the isolated event beds. 16B) Close-up view of event beds showing undulating to planar lamination. 16C) Close-up view of bed architecture of the event bed with a massive base (lithofacies 4) overlain by planar- to quasi-planar lamination (lithofacies 5) capped with combined-flow ripples (lithofacies 8). Pocket knife for scale (8 cm). 16D) Interpretative sketch of 15C. 15E) Event bed capped with combined-flow ripples (lithofacies 8). Notice the rounded crests. 15F) Log B4 of the section (see Fig. 17 and 18 for overview).

*Interpretation:*

The heterolithic nature of FA2, together with the presence of thick bedded sandstones, indicate a depositional environment with frequent alternations between hemipelagic fall-out and deposition governed by storm-generated currents combined with rare dilute, low-density turbidity flows. The thin sandstone beds are considered to have been formed during weak/distal storms capable of emplacing sand and silt in suspension clouds and transporting it onto the shelf before being deposited during the waning stage (Dott Jr and Bourgeois, 1982; Nelson, 1982; Myrow, 1992). Based on the occurrence of flute casts together with HCS, some of these beds may also be associated with a combination of both turbidity currents and later reworking by storms. The seafloor was also frequently disrupted by more violent storms leading to the generation of the thicker sandstone beds observed dominating the middle to upper part of the FA2. These beds obtain classical features of event beds generated mainly by storm-ebb surges (e.g. Dott Jr and Bourgeois, 1982; Cheel, 1991; Duke, 1991; Brenchley et al., 1993; Myrow, 2005; Morsilli and Pomar, 2012). Deposition of these types of beds was most likely preceded by deep bottom scour suggesting the presence of an initial powerful unidirectional current eroding the sea floor originating from either strong downwelling currents related to coastal set-up during storms or gravity flows (e.g. turbidity currents and hyperpycnal flows) (Myrow et al., 2002; Pattison, 2005; Lamb et al., 2008). Erosion was followed by transport and deposition of sand onto the shelf forming the typical vertical bed sequence consisting of a massive base, followed by planar- to quasi-planar lamination, HCS and combined-flow ripples. The frequent occurrence of this typical vertical bed sequence, as well as dominantly isotropic HCS indicate the presence of a waning oscillatory-dominated combined-flow during accumulation, while the initial unidirectional rapidly waned (e.g. Southard et al., 1990; Arnott and Southard, 1990; Myrow and Southard, 1991). The presence of different stacking patterns within different bed sequences is believed to be a result of hydrodynamic variations during transport and deposition. Similar vertical bed sequences are observed in several ancient deposits around the world (e.g. the Hatch Mesa succession (Pattison, 2005), Utah, USA and Starshot Formation, Antarctica (Myrow et al., 2002)) and are interpreted to be wave-modified turbidites (e.g. tempestites) typically identified in prodeltaic settings. The lack of pure oscillatory structures capping the beds indicate that post-depositional reworking by waves rarely occurred in this environment. FA2

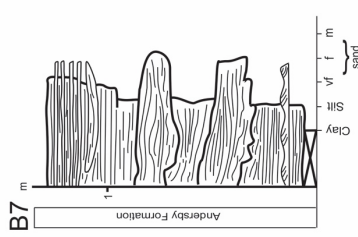
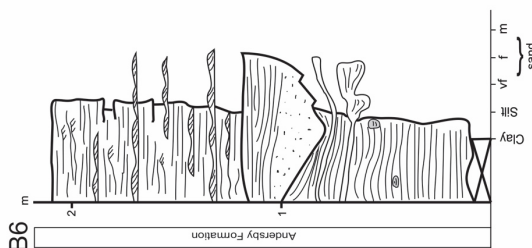
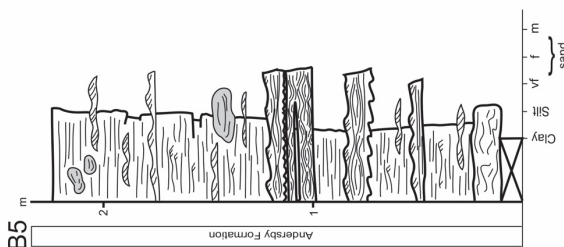
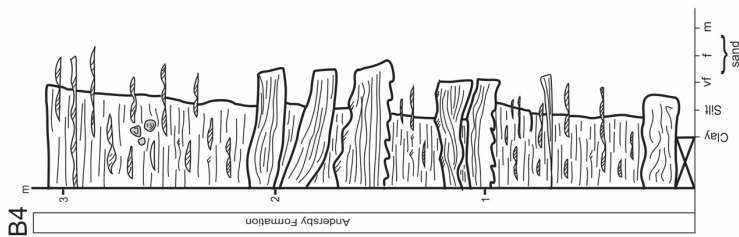
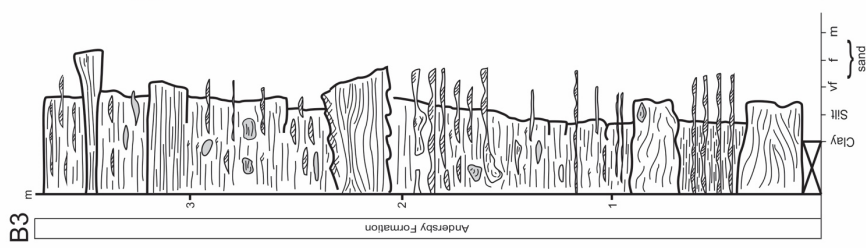
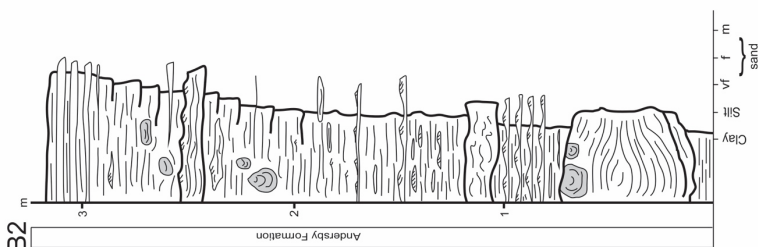
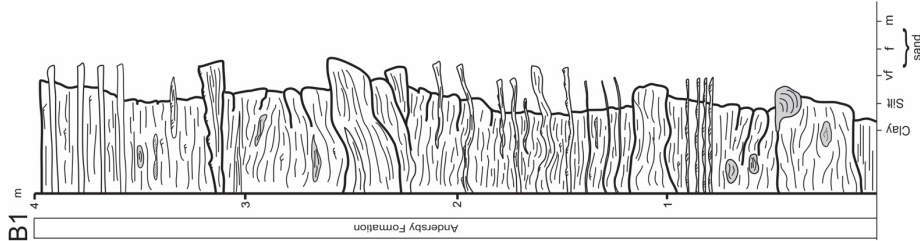


normally represents upward-coarsening successions indicating an upward increase in energy and thereby a prograding and shallowing environment. The common occurrence of SSDS (e.g. ball-and-pillow structures and convolute stratification) is indicative for an environment exposed to high sedimentation rates, which is typical deposition in prodeltaic environments (Bhattacharya and Davies, 2001). The depositional feature characterising FA2 is consistent with deposition in storm-dominated prodelta, where frequent storms and gravity-driven processes emplaced and reworked sands.

**Legend**

**Sedimentary structures**

- Masseive structureless
- Parallel planar lamination/bedding
- Combined-flow ripple cross-lamination
- Hummocky cross-stratification
- Quasi planar lamination
- Climbing-ripple lamination
- Self-sediment deformation
- Tabular/tangential cross-lamination/bedding
- Through cross-lamination/bedding
- Flute casts
- Load casts
- Bell and pillow structures
- Sand lenses
- Syneresis cracks
- Mud clasts



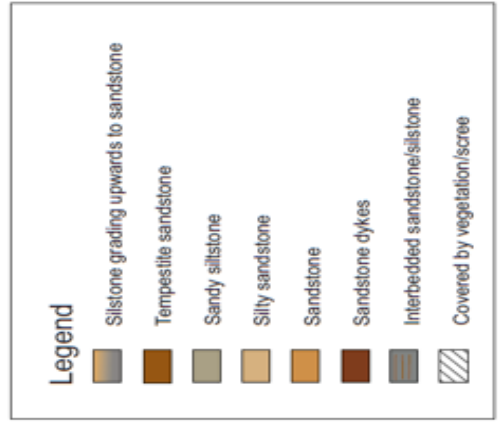
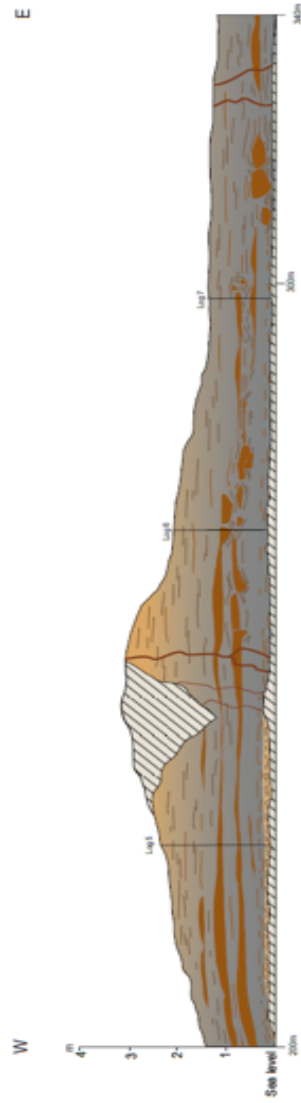
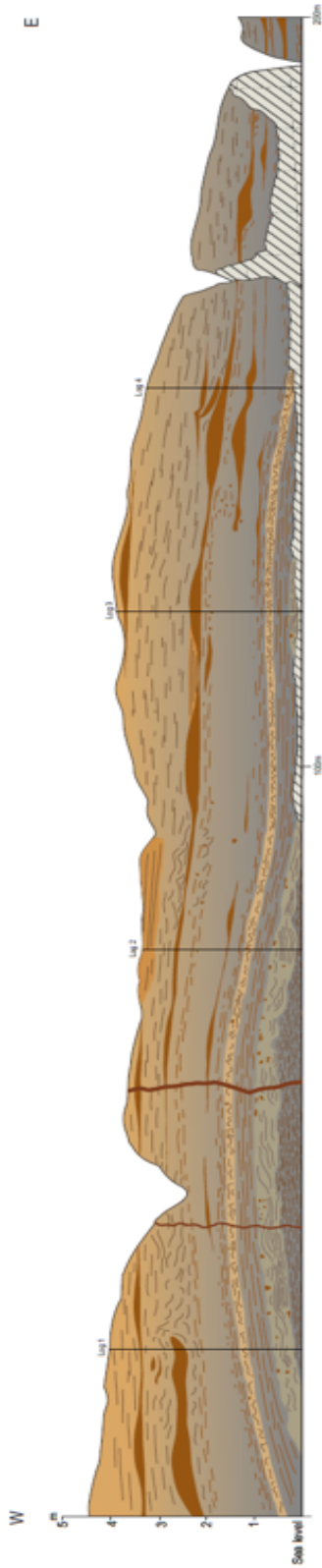


*Figure 17. Figure 17 Detailed, sedimentological logs of the Bergelva locality, Andersby Formation, representing a mainly prodeltaic deposits displaying regressive conditions. FA1 is only represented in the lower part of log B1 and B2. The logs are numbered from west to east.*

*Figure 18. A 340 meter long panel of the Bergelva locality showing both vertical and lateral distribution of the typical event bed, in addition the fair-weather lithofacies and deformed units in the lower part. Notice the increase in deformation of the event beds towards east. The sedimentological logs of Fig 17 are marked with corresponding numbers.*

#### 4.2.3 Facies association 3: Storm-influenced delta front

##### **Description:**

Facies association 3 (FA3) is characterized by stacked tabular to lenticular beds of both non-amalgamated and amalgamated fine to medium grained sandstone (<40 cm) and frequent lenses and thin beds of laminated and rippled siltstone (< 50 cm). The association is only observed in the middle to upper part in the Klubbnasen locality (Fig. 21, Klubbnasen Formation) making up an approximately three meters thick overall upward-coarsening unit. The amalgamated sandstone commonly displays interbedded anisotropic HCS (lithofacies 6) and SCS (lithofacies 7) (Figs 12A, 12b, 12C and 12D) with abundant mudstone intraclasts at their base (12E). The sandstone beds typically contain several internal truncation surfaces (Fig. 12B) and record migration toward the east. When traced laterally eastward, the amalgamated bed sets commonly thins and divides into isolated units separated by siltstone lenses/beds (Fig. 19). In contrast, when traced toward west, the anisotropic HCS lamina changes to a predominant preferred dip-direction eastward, resembling sigmoidal cross-bedding. A unit of stacked light-grey fine to medium grained sandstone beds (<20 cm) is observed in the western part of the Klubbnasen outcrop (Figs 14A, 14B, 19 and 20A). The unit includes both tangential- and trough-cross sets (lithofacies 9) and inclined planar bedding (lithofacies 10) (Figs 20B and 20C). These sandstone beds are typically wedge- to tabular shaped frequently capped by millimetre thick beds or lenses of laminated siltstone (lithofacies 1). Plan-view exposures of the stacked beds frequently displays characteristic rib-and-furrow structures (Fig. 14D) with a migration direction eastward. Several of the units of cross-bedding display both erosional scours and syn-sedimentary faults (Fig. 30) with a dip direction towards east. The syn-sedimentary faults are restricted to a 0.5 meter thick unit overlain by non-deformed cross-bedded sandstone. FA3 also include several other soft-sediment deformation structures, such as load structures and convolute/contorted stratification. This facies association also comprises a large-scale filled scour truncating into an apparently massive sandstone unit with pinch and swell beds. The scour is tens of

centimetres deep and several meters wide filled with muddy siltstone containing numerous ball-and-pillow structures of sandstone. The sandstone beds of tangential- and through cross-bedding and planar bedding with siltstone partings overlies the siltstone-filled scour. Although uncommon, climbing ripple cross-lamination may be seen sporadically throughout FA3.

*Interpretation:*

Based on the occurrence of sandstones displaying structures affected by both oscillatory and unidirectional flows interbedded with units of laminated to rippled silty sandstone, FA3 is interpreted to represent delta front deposits in a wave-dominated setting. The silty sandstone exhibiting both planar-lamination and ripples indicates that deposition predominantly took place immediately above fair-weather wave base (FWWB) where wave currents were able to promote sediments motion (Pemberton et al., 2012). The anisotropic nature of the HCS in FA4 suggests that deposition took place from an intermediate oscillatory flow with a sufficient unidirectional current leading to bed form migration (Duke, 1991; Dumas et al., 2005; Dumas and Arnott, 2006). The unidirectional component of the flow may have its origin from coastal set up leading to downwelling storm flows (Duke, 1991; Myrow and Southard, 1996) or density induced currents down the delta front (Myrow and Southard, 1996). Additionally, the amalgamation of the anisotropic HCS beds potentially reflects frequent reworking of both event beds (internal truncations) and fair-weather deposits based on the presence of truncations. The amalgamated units are thus interpreted to be produced by multiple storm events generating strong erosive flows, both unidirectional and oscillatory, transporting and depositing considerable amount of sand leading to both vertical aggradation and bed form migration (Cheel and Leckie, 1992; Cheel and Leckie, 2009). The amalgamated beds have a tendency to laterally grade into thinner beds separated by thin beds of silty sandstone/sandy siltstone reflecting deepening towards east. The predominance of cross-bedded sandstone in in the upper part of FA3 is indicative for a prograding, proximal delta front overlying the prodelta deposits of FA2.



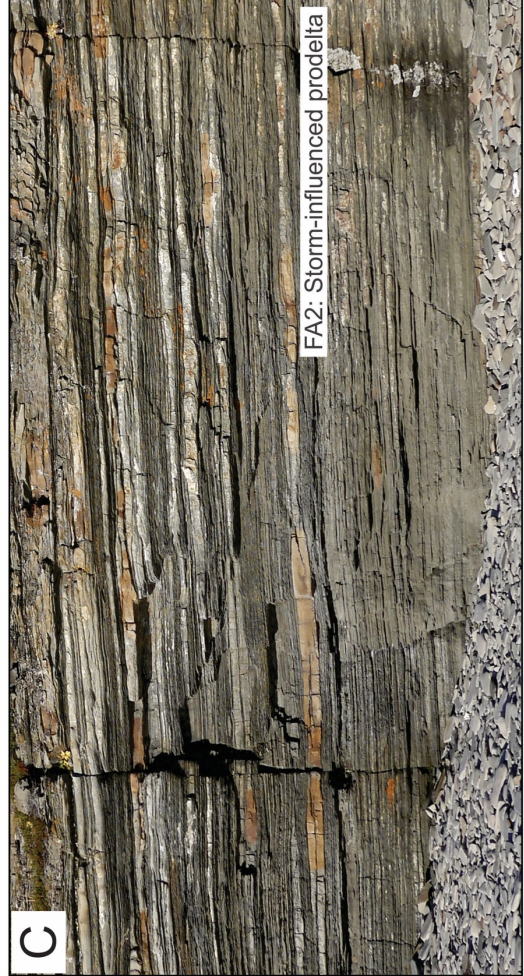




*Figure 19. 19A) Panorama displaying distal to proximal facies associations (FA2-FA3), Klubbnasen locality. White triangle indicate a coarsening-upward trend. 19B) Close-up view of FA3. 19C) Close-up view of FA2.*

The delta front was affected by both fluvial- and gravity driven processes (delta front instabilities) based on the occurrence of current-dominated structures, syn-sedimentary faults and scours (Røe, 1995; Coleman et al., 1998a; Coleman et al., 1998b). The occurrence of sandstones containing cross- and planar bedding are attributed to offshore-directed migration of subaqueous dunes (both 2D and 3D dunes ) (Best, 2005) formed as mouth bars or in terminal distributary channels (Olariu and Bhattacharya, 2006). Small scours/truncations between some of the cross-sets indicate that the dunes were formed in an environment with repeated erosion, while the frequent interbedded siltstone likely characterises significant variations in river discharge over time. Additionally, the large scour structure observed in FA3 may be attributed to major erosion by larger gravity flows (slumps) associated with an unstable delta front (Bhattacharya and Davies, 2001). Although, they may also be the result of erosion from hyperpycnal flows originating from distributary channels on the delta front (Pattison et al., 2007; Eide et al., 2014). The apparent lack of wave-formed structures in the upper part of FA3 indicate deposition characterized by either a high unidirectional flow suppressing any oscillatory flow or deposition in a wave-sheltered setting (Bowman and Johnson, 2014).

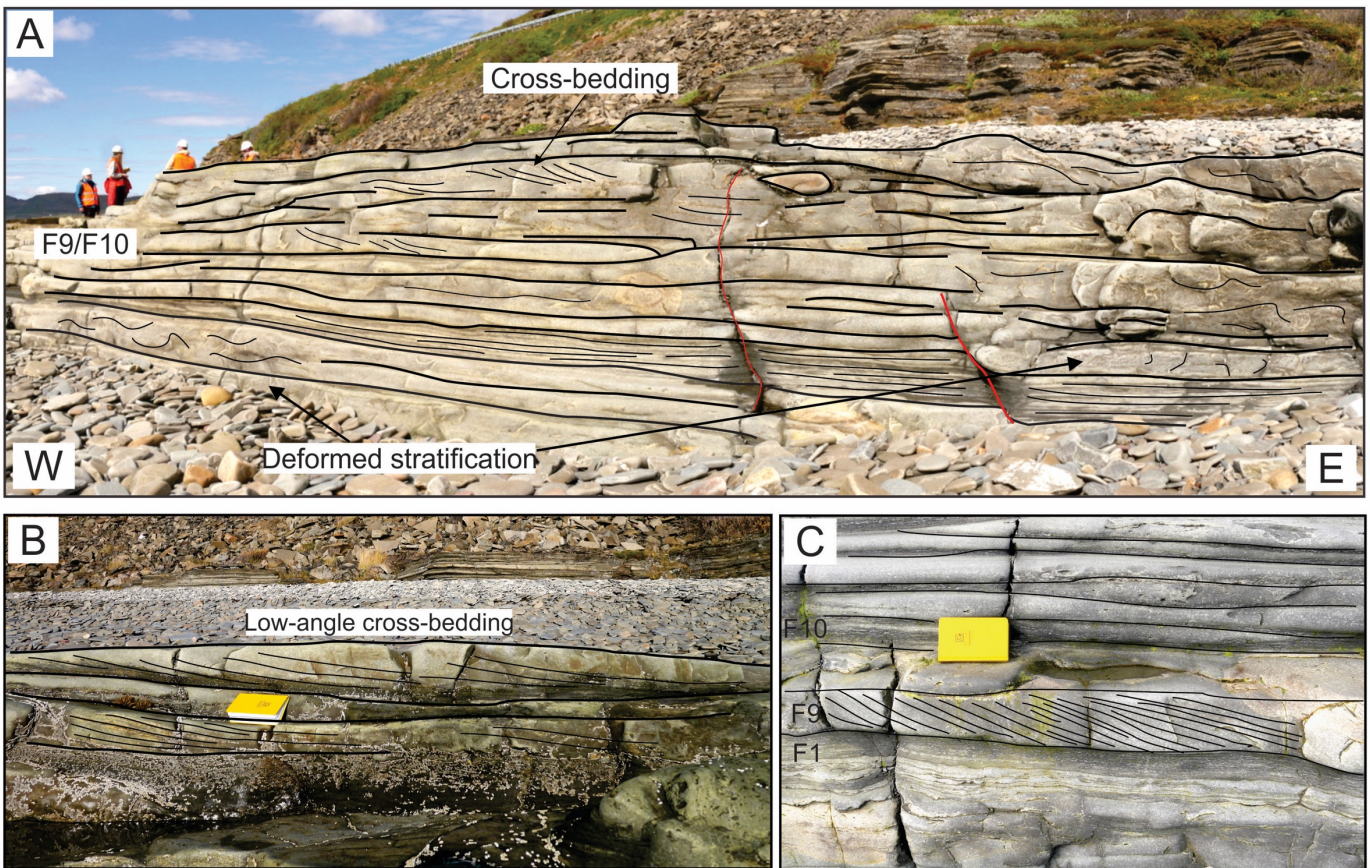


Figure 20. Sandstone beds of the upper part of the Klubbnasen Formation displaying both cross-bedding (lithofacies 9) and planar bedding (lithofacies 10) likely reflecting a delta front succession. 20A) Medium-grained stacked sandstone beds with frequent cross- and planar-bedding and deformed stratification. Deformation typically increases towards east. 20B) Dune scale low-angle cross-bedding. 20C) Planar cross-bedding. Notice the distinct difference in dip-angle and geometry between the cross-bedding in fig. 20B and 20C. Note book for scale (18 cm).

#### 4.2.4 Facies association 4: Braided river deposits

##### *Description:*

Facies association 4 (FA4) is recognized in the lower part of the Fugleberget and Paddeby formations at the Klubbnasen, Paddeby and Vadsøya localities (Figs 2C, 21 and 22), marking a drastic change in lithology from siltstone dominated units to beds of medium-grained sandstone, and thus represent the stratigraphic boundary between the Klubbnasen and Fugleberget formations, and the Andersby and Paddeby formations. Considering this facies association is not recognized in neither the Klubbnasen nor Andersby formations, it is only described superficially in order to achieve knowledge about the stratigraphic relationship between the two formations and the overlying units (i.e. the Fugleberget and Paddeby formations, respectively). The association consists of medium-grained thick sandstone beds



and rare thin siltstone beds (Fig. 15C). The sandstone beds range in thickness from 50 cm to 200 cm with an average thickness of 60 cm. FA4 is dominated by medium- to large-scale cross-bedding (F10; both through- and tangential cross-bedding) as well as planar bedded sandstone (F11) and occasionally laminated siltstone (F1). Parting lineations are frequently observed on bedding planes of the planar bedded sandstone displaying a paleocurrent direction representing east-west (Fig. 14D). Additionally, a single occurrence of a 50 cm thick bed of contorted to massive sandstone is identified in the middle of the unit. It consists of weak convolute bedding with vergence and does not continue into the underlying or overlying beds.

*Interpretation:*

The stratigraphic position of FA4 on top of FA2 with an erosional contact, together with the abundant cross-bedded sandstones and absence of wave-generated sedimentary structures, suggest that this unit is of fluvial origin. This is also supported by the predominate aggradational character of the units, which is typical for fluvial deposits (e.g. Jensen and Pedersen, 2010). The medium- and large-scale cross bedding together with planar bedding implies deposition by medium- to high-velocity currents carrying considerable amount of sediments in suspension (Miall, 1977; Røe, 1995; Cant and Walker, 1978). The cross-bedded sandstone represents both the migration of 2D and 3D dunes of different scale (Best, 2005), while the planar strata and parting lineations most likely has its origin from currents of upper flow regime (Allen, 1983). The single occurrence of a deformed to massive sandstone bed is attributed to suggest local liquefaction (Owen, 1996). Similar successions are commonly associated with braid plain deposits consisting of different architectural elements such as channels, bars and dune complexes (Hjellbakk, 1997; Cant and Walker, 1978; Williams and Rust, 1969). This interpretation is also consistent with former studies of the Fugleberget Formation (Røe and Hermansen, 1993; Hobday, 1974; Røe, 1987; Røe, 2003).

# Klubbnasen locality

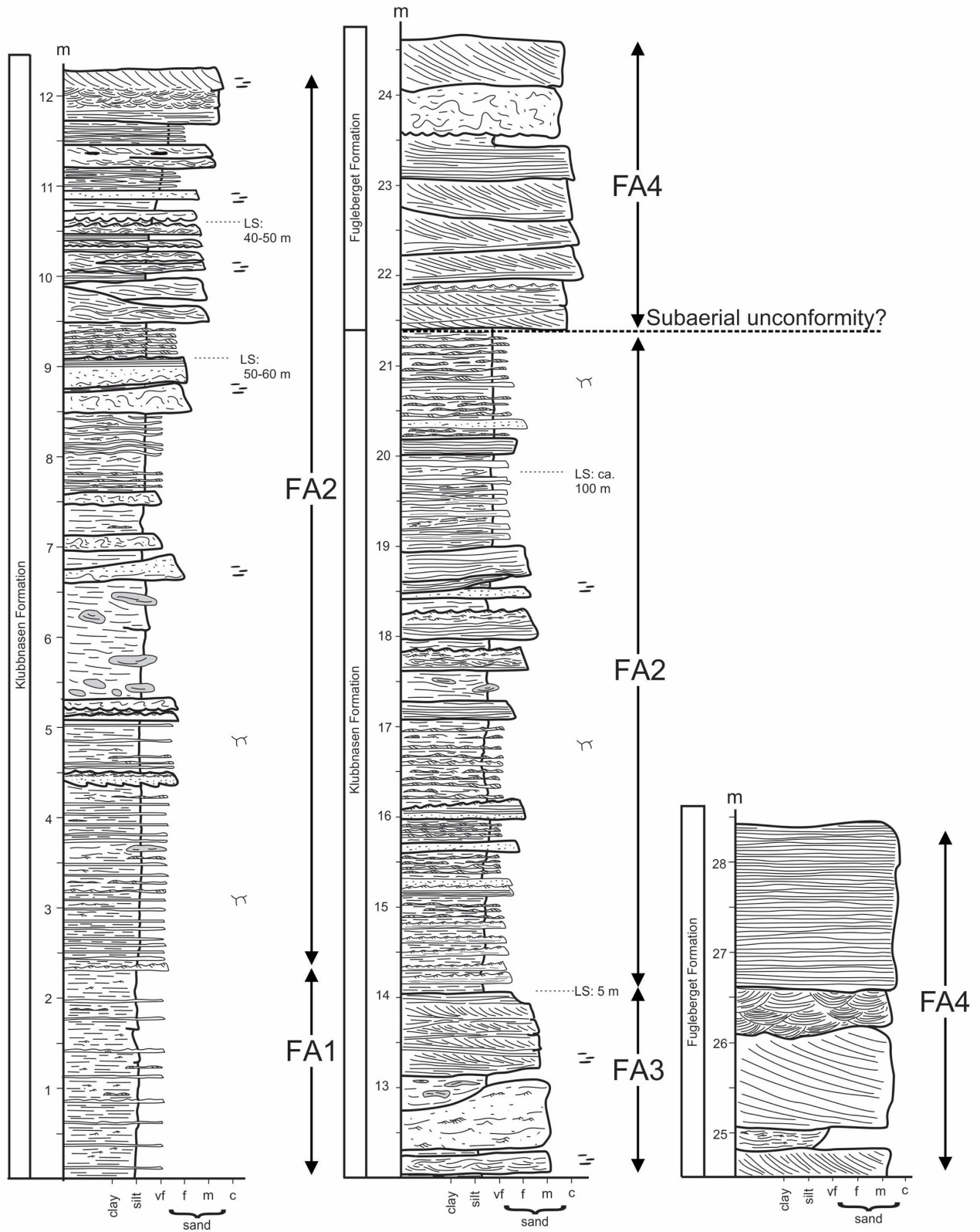


Figure 21. Detailed sedimentological log of the Klubbnasen locality (Fig. 3C for location). The upper seven meters of the log represent the lower part of the Fugleberget Formation (consisting of FA4). Notice the sharp boundary between the two formations at 21.5 meters. LS: lateral step in the log.

### 4.3 Stratigraphic development of the Klubbnasen and Andersby formations

#### *The Klubbnasen Formation:*

The Klubbnasen Formation can be divided into depositional units (K1 and K2) reflecting an overall upwards-coarsening and upward-shallowing depositional environment. Both the lower unit K1 and the upper unit (K2) can be traced across the Klubbnasen locality. Together the two depositional units makes up the Klubbnasen Formation (Fig. 22), which is restricted to the top by the Fugleberget Formation.

Outer shelf deposits (FA1), storm-influenced prodelta deposits (FA2) and storm-influenced delta front deposits (FA3) together form the K1 unit, displaying an overall distal to proximal trend. The lowermost part of K1 is approximately two meter thick consisting of outer shelf deposits (FA1) displaying limited variations in facies distribution (lithofacies 1 and lithofacies 2). The siltstone dominated FA1 is overlain by an upward-coarsening FA2 deposits, which makes up the majority of the K1 (8 m thick, Klubbnasen locality (Fig. 2C). The FA2 record a larger range of lithofacies, where the storm-emplaced lithofacies are dominating the upper part (Fig. 19). A two meter-thick interval within the FA2 contain abundant soft-sediment deformation structures (e.g. ball-and-pillows), which are bounded by undeformed sediments. The deposits of FA2 grades upwards into delta front deposits (FA3) which marks the upper and last interval of the lower depositional unit (K1). The FA3 deposits are characterized by sandstone beds, grading upwards from wave-influenced structures (HCS and SCS) to unidirectional-dominated structures (i.e. cross-bedded sandstone). Prodeltaic deposits (FA2) sharply overly the cross-bedded sandstone of FA3, marking the onset of the next depositional unit (K2). The contact between K1 and K2 is interpreted to be a marine flooding surface recording an abrupt deepening of the lithofacies assemblage from cross-bedded sandstone (FA3) to interbedded siltstone and sandstone (FA2) (Fig. 21). The relatively thin depositional unit (K2) overlying the marine flooding surface mainly consists of FA2 deposits dominated by thin to medium thick sandstone beds interbedded with siltstone.



The K2 is bounded to the top by a sharp and erosional surface marking the formation boundary between the Klubbnasen Formation and Fugleberget Formation (FA4; braided river deposits; Fig.22). Based on the abrupt shift from marine to fluvial environments the boundary is believed to represent a subaerial unconformity.

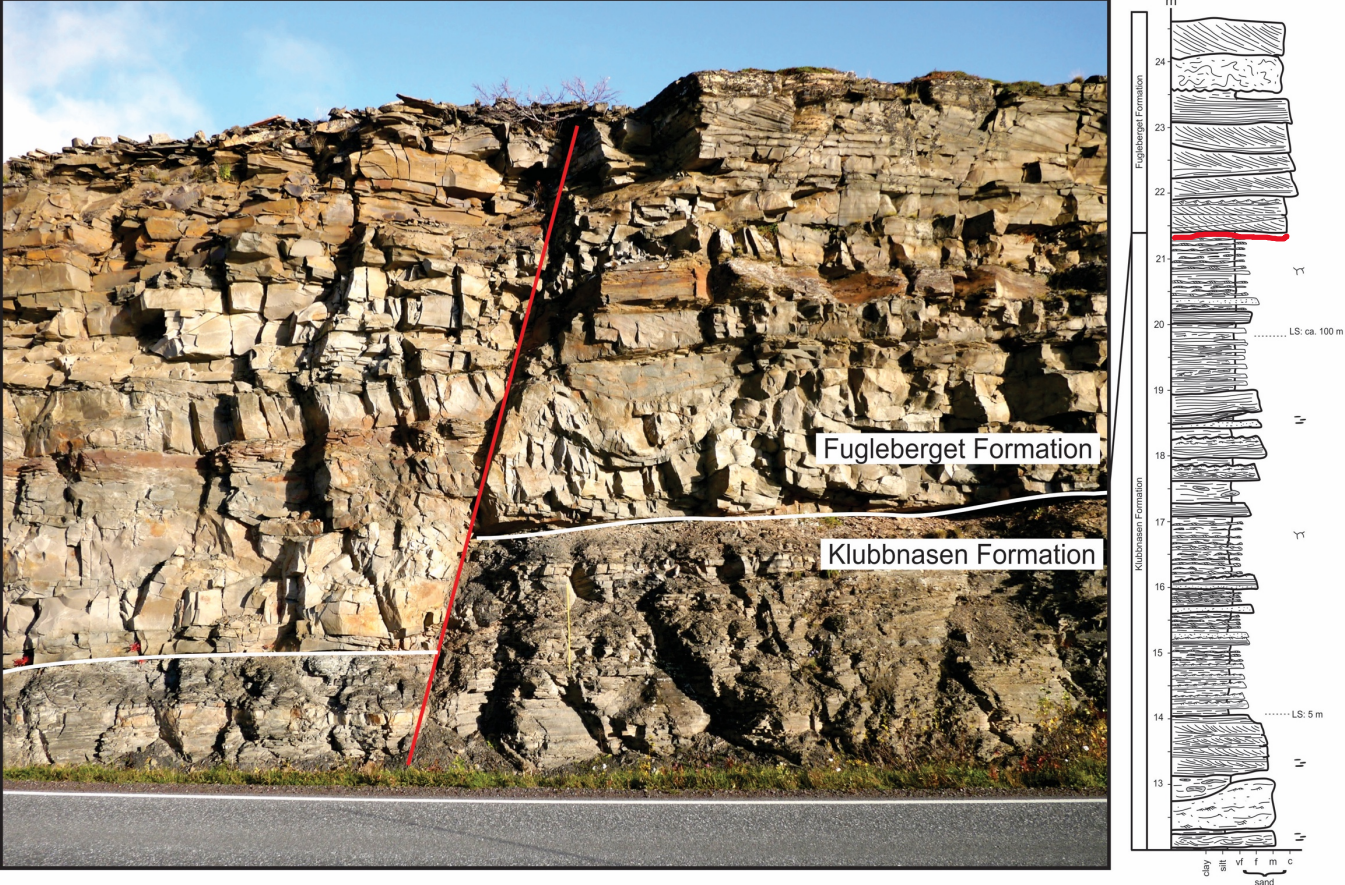


Figure 22. The stratigraphic boundary between the Klubbnasen and Fugleberget formations, Klubbnasen locality. Red line in photo marks a brittle normal fault of much younger age than the investigated succession). A vertical log of the upper part of the Klubbnasen Formation and lower part of the Fugleberget Formation. Red line marks the formation boundary.

### *The Andersby Formation:*

The Andersby Formation shares many similarities with the Klubbnasen Formation and can be divided into two depositional units (A1 and A2). The formations contain deposits of both FA1 and FA2 where the storm-influenced prodelta deposits (FA2) are volumetrically the most important FA within the Andersby Formation, making up the majority of the thickness.

The lower depositional unit of the Andersby Formation (A1) can be traced across both the Bergelva locality and the Vadsø coastal section (Figs 2C, 18 & 36) indicating a large lateral extent of the unit. The lower part of A1 consists of fine-grained deposits of outer shelf FA origin (FA1), which grades upwards into more sandier deposits of FA2 reflecting an overall prograding depositional environment. The overlying storm-induced prodelta deposits (FA2) are characterized by thicker sandstone beds (i.e. event beds), which are coupled with abundant soft-sediment deformation structures (Fig. 17). The number and thickness of the sandstone beds, typically attributed to storm-events, gradually increases upwards in unit. The top of the lower depositional unit (A1) is defined by an abrupt transition to the overlying finer-grained outer shelf deposits (FA1) marking the onset of the next depositional unit (A2). The sudden change in lithology, from sand-rich lithofacies to mudstone/siltstone-dominated lithofacies, most likely represent a marine flooding surface. The thinner and less developed A2 overlying the flooding surface consists of a relatively homogenous deposit of mainly siltstone/mudstone of outer shelf (FA1) origin (Fig.23).

The fine-grained upper depositional unit (A1) of the Andersby Formation is unconformably truncated by stacked units of thick sandstone beds representing the stratigraphic boundary between the Andersby Formation and the Paddeby Formation (FA4) (Fig. 23). Based on the abrupt shift from marine to fluvial environments the boundary is believed to represent a subaerial unconformity.



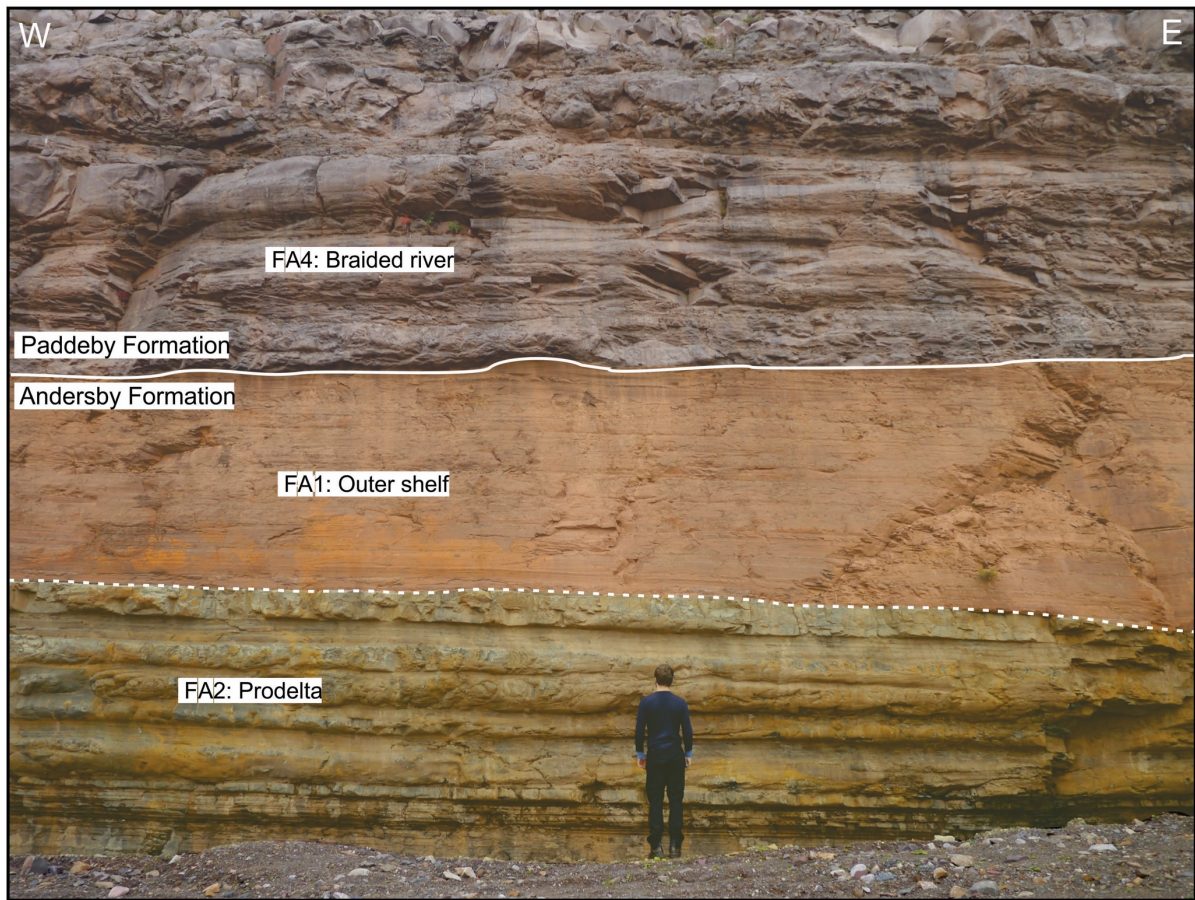


Figure 23. The stratigraphic boundary between the Andersby and Paddeby formations, Paddeby locality.

## 4.4 Soft-sediment deformation structures (SSDS)

Both the Klubbnasen and Andersby formations contain frequent soft-sediment deformation structures (SSDS), which morphologically vary in both size and style of deformation when traced laterally and vertically. Determining the deformation mechanism and driving force of the SSDS occurring in the investigated sections are important for understanding the processes and depositional environments under which the Klubbnasen and Andersby formations were formed. The SSDS occur in multiple stratigraphic intervals of the two formations, typically alternate with non-deformed layers. The SSDS typically occur in sandstone beds, although, some siltstone beds also display contorted and folded beds. The dominant SSDS structures in the Klubbnasen and Andersby formations will be described and interpreted below. Additionally, a lateral extensive unit consisting of various SSDS occurring in the Andersby Formation at the Vadsø locality will be further elaborated and interpreted.

### 4.4.1 Load structures

In both the Klubbnasen and Andersby formations, load structures (Fig. 24) of different morphologies occur frequently, representing the most commonly observed SSDS. The load structures typically occur as ball-and-pillow structures and load casts consisting of reddish-brown, very-fine to fine-grained sandstone fully or partly encapsulated by siltstone or mudstone. The ball-and-pillow structures are detached (i.e. from its associated bed base) load structures varying in sizes from only a couple of centimetres to tens of centimetres in diameter. They frequently occur as irregular pillows, either isolated or connected, and are fully surrounded by contorted mudstone or siltstone (Figs 24A, 25C and 25D). In addition, numerous meter-scale ball-and-pillow structures occur at the Vadsø locality (Fig. 31). Although severely deformed, several of the ball-and-pillow structures contain well-developed internal structures, such as planar-laminations, ripple cross-lamination and occasionally HCS, which normally turns concentric towards their outer contour (Fig. 24B and 25E). Piled load-casted ripples occur sporadically (Fig. 25F). These are typically rotated and underlying partly preserve deformed internal cross-laminations.



At the intersection between very-fine to fine-grained sandstone beds and siltstone/mudstone beds load casts occur frequently. These features are attached to the base of the overlying sandstone beds and are typically observed in association with flame structures. The flame structures typically consist of upward-pointing siltstone flames. Locally, the flame structures exhibit an inclination towards east (Figs 25A and 25B).

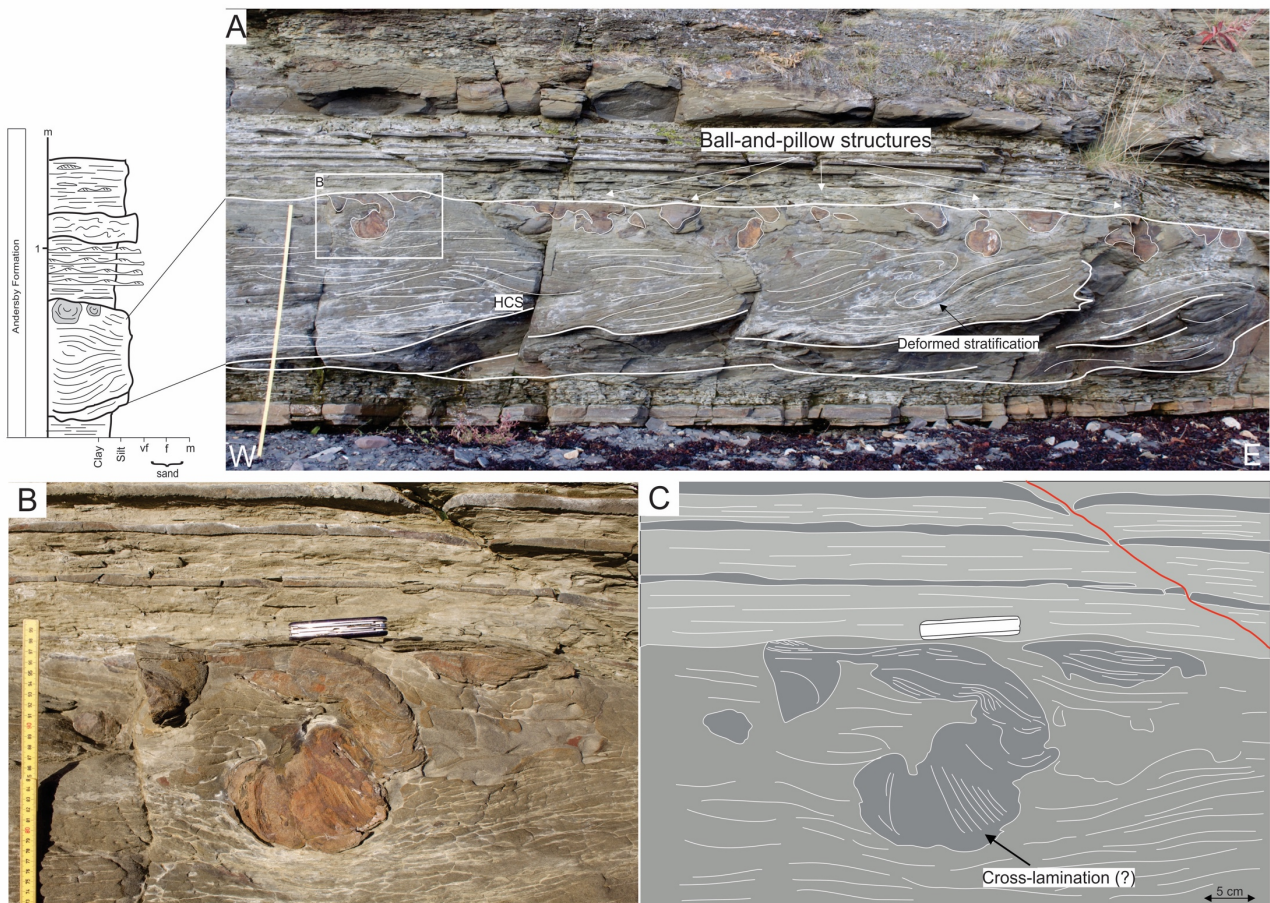
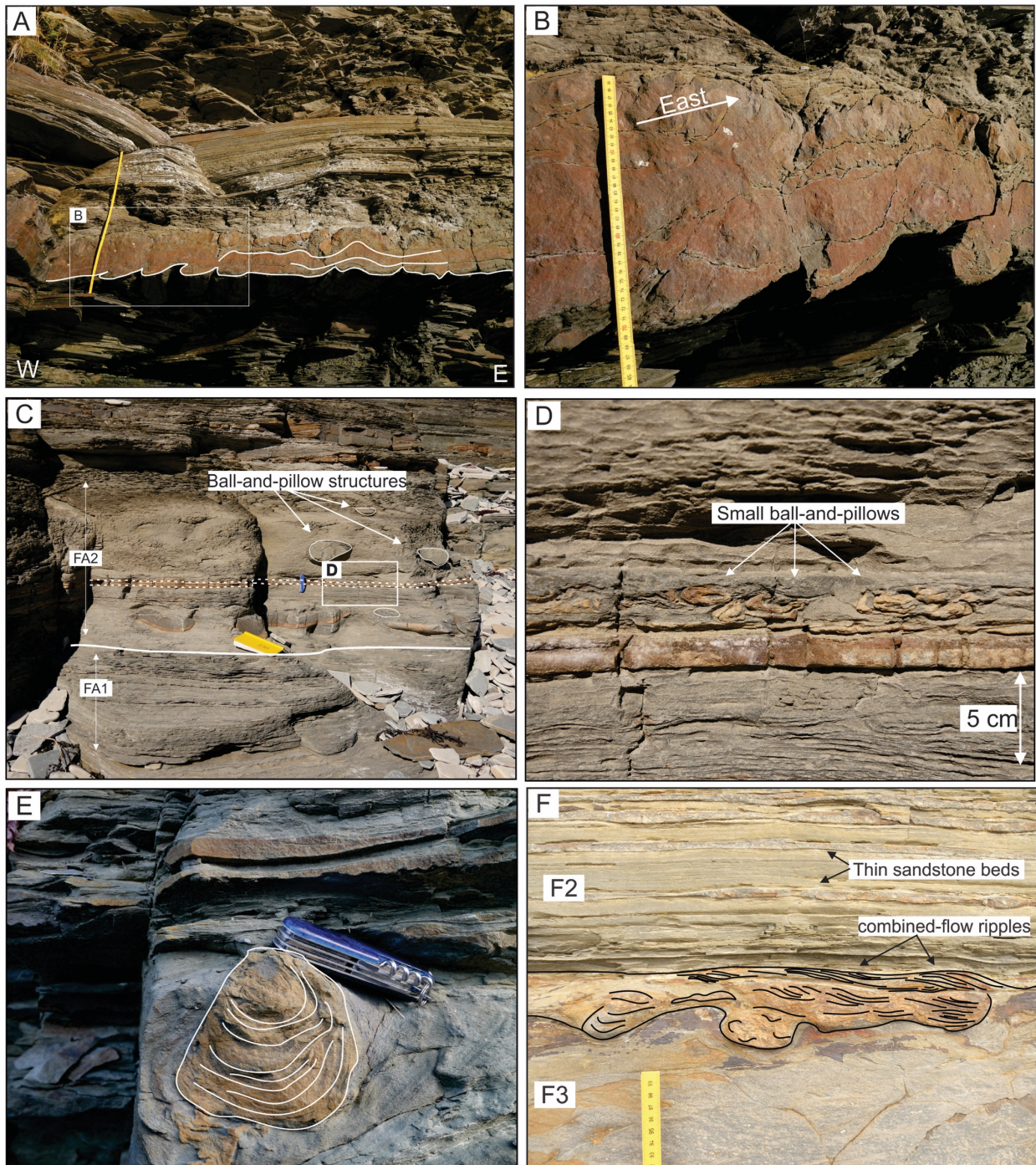


Figure 24. Figures show the deformed unit with abundant ball-and-pillow structures, Andersby Formation, Vadsø locality 24A) An overview of ball-and-pillow structures in partly deformed sandy siltstone with HCS (lithofacies 3). 24B) Close up of ball-and-pillow structure containing internal structures resembling cross-lamination. 24C) An interpretative sketch of the ball-and-pillow structure shown in Fig.24B. The red line marks a syn-sedimentary fault. Pocket knife for scale (8 cm).

*Interpretation:*

Load structures are well-known soft-sediment deformation structures from the literature, which are formed in response to either an unstable density inversion between two contrasting layers (e.g. sand and silt) or from lateral variation in load (e.g. ripples) (Allen, 1982; Owen, 2003). The formation of the load structures is commonly initiated by a drastic reduction of shear strength or in response to liquefaction and fluidization processes. If the deformation is adequately intense, isolated ball-and-pillow structures may be formed. There exist different causes for load-induced deformation and several trigger mechanism such as storm waves, earthquakes or overloading may lead to liquefaction of the upper denser layer and thus generating a gravitational readjustment resulting in the formation of load structures, including flames (Molina et al., 1998; Moretti et al., 2001; Alfaro et al., 2002; Owen, 2003). The presence of piled load-casted ripples indicate lateral variation in load caused by thickness differences in the overlying rippled sandstone bed, which may have undergone loading during continuous deposition of the ripples (Owen, 2003). The common occurrence of flame structures indicates the presence fluidization processes during deformation. The less dense layer (siltstone/mudstone) will normally migrate upwards due to fluidization of the underlying sediments and thus creating water escape-structures (*sensu* Lowe, 1975) such as flame structures (Owen, 2003). Several of the flames and load casts obtain an inclination towards east, which is probably related to a component of horizontal shear during deformation. Contrasts in sediment density alone are probably not efficient enough in creating load structures, as evident by the presence of the many beds with no load structures. Therefore, a trigger mechanism most likely has attributed to the deformation in combination with a density contrast (Berra and Felletti, 2011).





Figur 25. 25A & 25B) Flames structures with a vergence towards east. 25C) Overview photo of both large and small ball-and-pillow structures. Note book for scale (18 cm). 25D) Closer-view of the small ball-and-pillow structures. 25E) Ball-and-pillow structures with well-developed internal structures. Pocket knife for scale (8 cm). 25F) Loaded ripples with partly preserved combined-flow ripple lamination.

#### 4.4.2 Convolute and contorted lamination/bedding (deformed lamination)

Convolute and contorted lamination occur frequently within intervals of sandy siltstone and very-fine to fine-grained sandstone (Figs 26A-F). The structures are normally restricted to certain intervals (e.g. sandstone event beds) commonly underlain and overlain by undeformed finer-grained deposits (Figs 26 A, 26E & 26F). They are observed in all three localities (and both the Klubbnasen and Andersby formations) and vary in both scale and degree of distortion, from mildly disrupted to complete loss of primary stratification (Figs 26A & 26E). The convolute and contorted units are 5 cm to 50 cm thick commonly affecting the whole bed where the magnitude of distortion typically increases towards east.

Convolute lamination characterized by complex and overturned lamination (Fig. 26D), asymmetric folds and heavily contorted lamination are typically restricted to sandy siltstone- and sandstone beds (both thin-bedded and thick-bedded; 5 cm to 50 cm thick) in the Andersby Formation. The folds range from open to close, exhibiting both antiforms and synforms, where some antiforms may be tilted in the downcurrent direction (eastward) (Fig 32). The convolute and contorted lamination are frequently observed in association with ball-and-pillow structures and oriented flame structures, as well as occasionally mudstone clast and clastic dykes. The deformed units containing convolute and contorted lamination may extend laterally for several meters and occasionally several tens of meters, typically affecting the whole length of the exposed bed. Similar convolute and contorted structures are also observed at the Klubbnasen locality where they usually are restricted to sandstone beds throughout the succession. Although, the degree and magnitude of deformation appears to be lower in this locality. Small-scale convolute lamination (Figs 26A & B), which may affect single thin beds or several interbedded sandstone and siltstone beds, is typically observed within some units where they display discontinuous and sinuous lamination occasionally containing small-scale syn-sedimentary faults (Figs 30A & 30D). In addition, the lower unit of the Fugleberget Formation (Fig. 21) contains sandstone beds displaying complex and overturned cross-bedding, achieving the shape similar to recumbent folds, which laterally transfer into complete loss of stratification (Fig. 26G).



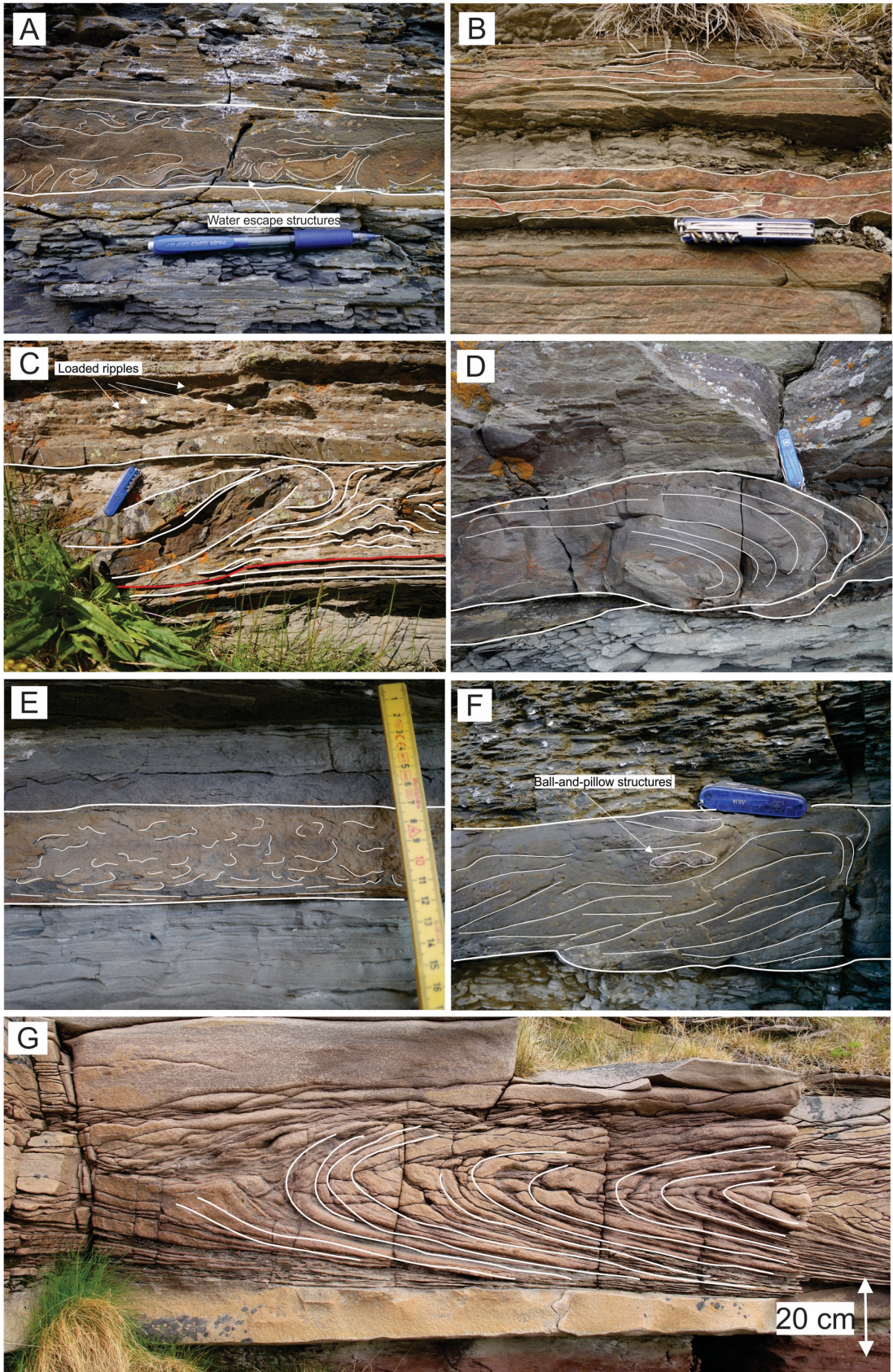




*Figure 26. Convolute and contorted stratification in sandstone, the Klubbnasen and Andersby formations. 26A) Small-scale convolute lamination and fluid-escape structures in the Vadsø locality. The layer is partly liquefied indicated by the massive appearance. Pocket knife for scale (8 cm) 26B) Small-scale deformation in thin massive sandstone beds. 26C) and 26D) Event bed displaying contorted and overturned lamination in the Klubbnasen locality and Vadsø locality, Andersby Formation. Pocket knife for scale (8 cm). 26E) Completely liquefied sandstone bed obtaining no internal structures, Klubbnasen Formation. 26F) Convolute and contorted silty sandstone with ball-and-pillow structures. The bed can be followed throughout the outcrop. Bergelva locality, Andersby Formation. Pocket knife for scale (8 cm). 26G) Recumbent folds of the Fugleberget Formation.*

### *Interpretation:*

The convolute and contorted lamination observed within the formations are interpreted to have been formed through liquefaction and fluidization processes where the sediments behaved in plastic manner due to increase in fluid pressure leading to disruption of the primary stratification (Allen, 1977; Brenchley and Newall, 1977; Owen, 1987; Owen and Moretti, 2011). The deformation probably occurred shortly after deposition when the applied stress exceeded the yield strength of the sediments and thus resulting in liquefaction and fluidization (Owen, 1995). Based on the variation in both dimension and degree of distortion, the sediments were most likely subjected to different amount and duration of stress during deformation, varying from only discrete and localized liquefaction to complete fluidization of entire beds (e.g. resulting massive beds). The deformation structures consisting of complex and asymmetrical folds and chaotic contorted lamination belonging to the Andersby Formation can most likely be attributed to a combination of a vertical shear stress (Owen, 2003) together with presence of a lateral shear component during deformation (Allen, 1977; Owen, 1987). The occurrence of load structures within the convolute and contorted lamination implies the presence of an inverse density contrast between two layers reinforcing the deformation (Owen, 2003). The small scale convolute and contorted lamination observed within the Klubbnasen Formation are also considered to be related to vertical shear stress during deformation, although the driving forces were most likely weaker than during the deformation in the Andersby Formation based on the size and distribution. The overturned cross-bedding in the lower part of the Fugleberget Formation is attributed to tangential shear stress formed by fast flowing water (i.e. upper flow regime conditions) close to the depositional surface (liquefied sand bed) creating structures similar to recumbent folds (Allen and Banks, 1972; Owen, 1987). This is consistent with earlier interpretations/studies of the Fugleberget Formation (e.g. Røe and Hermansen, 1993).

#### 4.4.3 Sandstone dykes

In the Andersby Formation, several vertical to steeply inclined clastic dykes of red to light brown sandstone penetrate the succession (Figs 27A-C). They are commonly found at the Bergelva locality, although a small number have also been observed at the Vadsø locality. The dykes are typically composed of fine-grained sandstone with a massive appearance and diameters ranging from 3 to 30 centimetres. Locally, a small proportion of siltstone clasts are present within the sandstone. In the Bergelva locality, the dykes typically cut through several meters of the succession (Fig. 27A), with a maximum visible height of 3 metres. The contacts between the dykes and the surrounding sediments is sharp consisting of grey siltstone commonly with a bulky and fractured morphology (Figs 27B & 27C). In several cases, the dykes display both upward and downward weak pinch-out geometries, where they sometimes bifurcate. However, neither the upper or lower termination is fully exposed and therefore the host sediments are not visible. In addition, rare small-scale scour-like structures with diffuse shapes, some similar to irregular flute casts, occur along the sharp contacts of the dykes (Fig. 27C). The structures surrounding the dykes commonly either display an upward inclination towards the interface or no inclination (Figs 27A & 27B). The dykes typically occur isolated with variable spacing along the outcrop, although in rare cases, they occur in pairs. The dykes are commonly associated with other SSDS such as load structures, contorted lamination and syn-sedimentary faults.



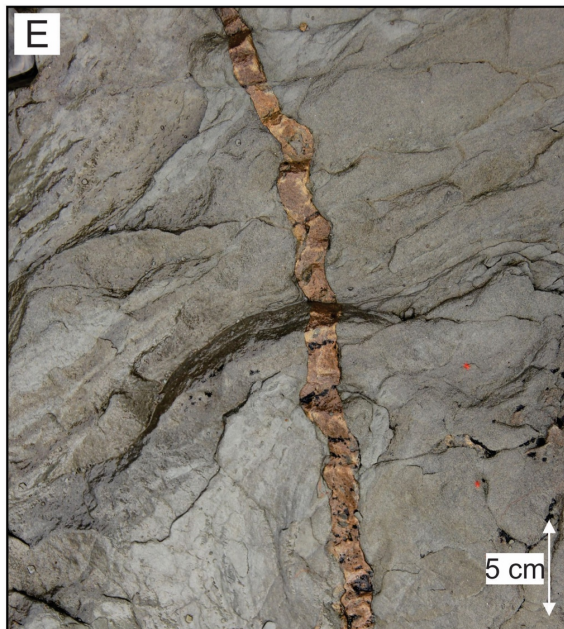
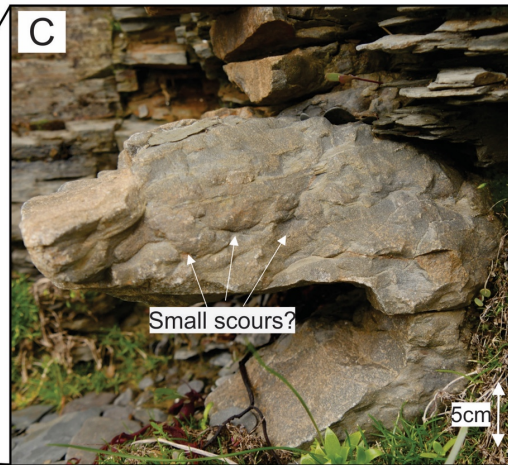
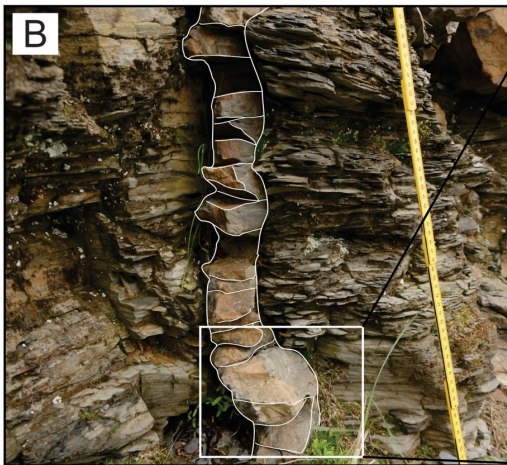


*Figure 27. Representative photos of sandstone dykes in the Andersby Formation. 27A) Two sandstone dykes cutting through the FA2 succession at the Bergelva locality. Notice the upward inclined event bed in connection to the right dyke. Ruler for scale (20 cm). 27B) Close-up view of one dyke at the Bergelva locality. Notice the fractured appearance as well as the inclined surrounding stratification. 27C) Close-up view of the interface (contact) of the dyke in 27B. Notice the small scour-like structures and finer-grained appearance. 27D) Close-up view of the sharp contact between dyke and the surrounding sediments. 27E) Close-up view of a dyke bed surface (plan view).*

### ***Interpretation:***

Clastic dykes are dewatering structures interpreted to have been formed by both liquefaction and fluidization processes after deposition (meta-depositional SSDS) (Owen, 1987). Liquefaction results from a temporary reduction in sediment strength related to an increase in pore fluid pressure equalling the overburden pressure, while fluidization processes are related to the frictional drag an upward moving fluid exerts on the surrounding particles (Owen, 1987; Duranti and Hurst, 2004; Owen and Moretti, 2011; Ross et al., 2014; Wheatley and Chan, 2018). The dykes observed in the Andersby Formation were probably developed when the saturated host bed was buried by low-permeability sediments, such as silt and mud, creating an overpressure in the sandy sediments causing them to liquefy. The sandstone was during the liquefied state most likely exposed to an external mechanical trigger (e.g. seismic shock) governing fluidization. As a result of the build-up overpressure (hydrostatic pressure), the sediments were forced upwards through cracks (hydraulic fracturation) leading to the formation of vertical to sub-vertical dykes (Owen and Moretti, 2011; Wheatley and Chan, 2018). The siltstone and mudstone clasts observed within the sandstone dykes are presumably eroded from the adjacent sidewalls during deformation before being incorporated into the dykes (Scott et al., 2009; Gao et al., 2019). This further indicates that the surrounding sediments were partly consolidated during the formation as mudstone clasts were formed. The common occurrence of inclined stratification surrounding the dykes is consistent with the upward drag force the escaping pore fluid exerted on the surrounding sediments (Hildebrandt and Egenhoff, 2007). In addition, the structures observed at the interfaces of the dykes similar to sole marks (small scours) may be the result of the fast-upward transport of fill material eroding the borders.

#### **4.4.4 Syneresis cracks**

In both the Klubbnasen and Andersby formations abundant well-developed sandstone-filled cracks are observed within the heterolithic fine-grained sediments (FA1 and FA2) (Figs 28A, 28B, 29A and 29B). These are commonly recognized as irregular sandstone-filled cracks penetrating mudstone or sandstone/siltstone beds (Figs 28B and 29B). They are also visible

on sandstone to siltstone and mudstone bedding planes (Fig. 28A). Locally, both sole marks (load casts and flute casts) and syneresis cracks are observed at the same basal sandstone surface (Fig. 10C). The syneresis cracks vary in both size and pattern morphology. In plan view, they are usually between 0.5 to 5 mm wide and 1 to 20 mm deep normally filled with fine-grained sandstone (28A). The cracks are randomly orientated and discontinuous, commonly displaying 1 to 10 cm long lines, either straight, curved or sinusoidal (Figs 28A & 29A). They typically intersect each other forming incomplete polygons and triple-junctions (Figs 28A & 29B). Where the cracks are observed in cross-section, they are commonly lenticular to V-shaped, although they commonly display a more irregular and folded geometry (Figs 4B & 5B).



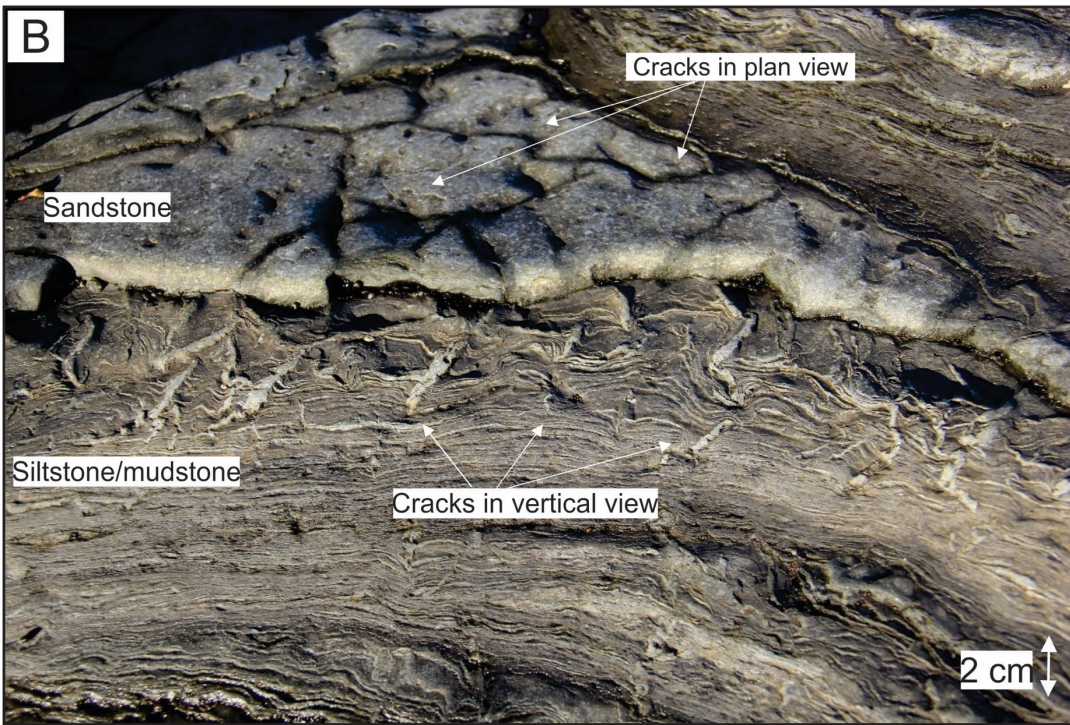
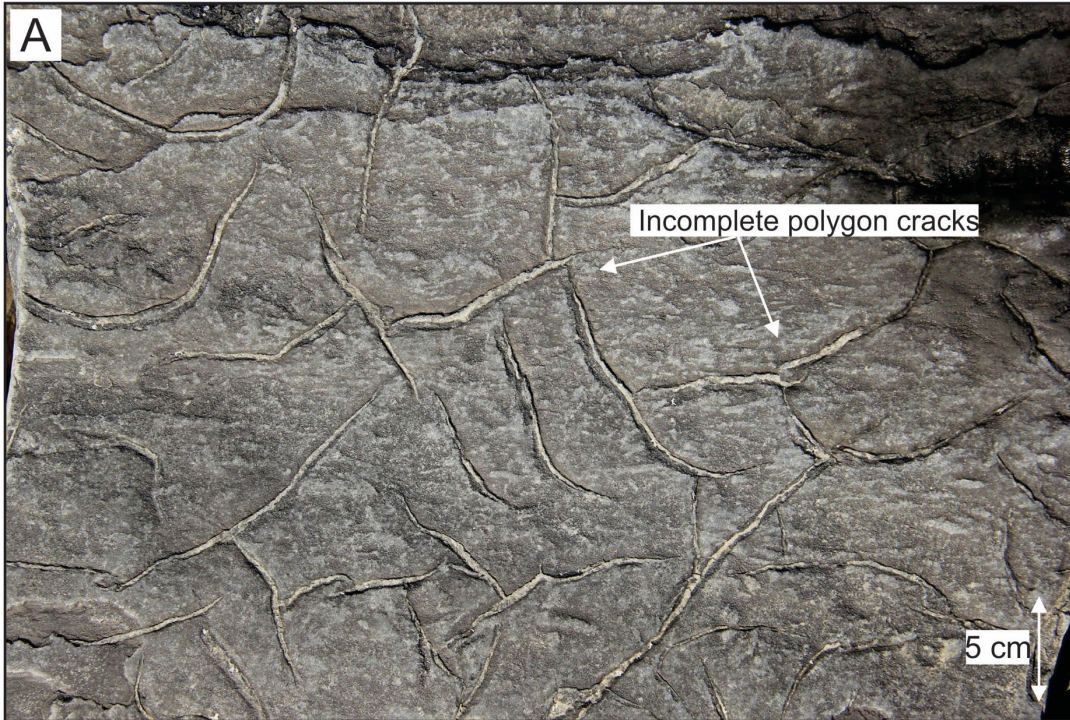


Figure 28A). Syneresis cracks observed on a bedding surface. Note the incomplete network of polygons. 28B) Syneresis cracks observed in both plan view on a sandstone bed surface and vertical view in siltstone/mudstone. Note the irregular geometry of the cracks in cross-section.





Figure 29. 29A) Syneresis cracks observed on the base of a sandstone bed, Vadsø locality, Andersby Formation. Notice the variation in width of the several of the cracks. 29B) Vertical view of the syneresis cracks. Note the V-shaped crack (black arrow). Pen for scale (13 cm).



*Interpretation:*

Syneresis sedimentary cracks are commonly attributed to shallow subaqueous settings close to the water-sediment interface induced by fluctuation in paleosalinity stress within the water column (Burst, 1965; Donovan and Foster, 1972; Astin and Rogers, 1991; Bhattacharya and MacEachern, 2009). Changes in salinity may generate deflocculation or intracrystalline de-watering of muddy to silty sediments resulting in shrinkage and thus the formation of cracks. However, several ancient syneresis cracks may also be attributed de-watering and grain reorientation processes related to seismic disturbance, wave-induced stress or burial-compaction (Plummer and Gostin, 1981; Pratt, 1998; McMahon et al., 2017). These cracks are commonly interpreted to formed substratally and may therefore obtain a high preservation potential in ancient successions (McMahon et al., 2017). The occurrence of sole marks in association with the cracks indicate an intrastratal origin where the casts have developed first (flute casts) or at the same time (load casts) (Plummer and Gostin, 1981). Similar cracks are commonly observed in several other Precambrian successions around the world and is believed to be related to the absence of bacteria binding sediments (Pratt, 1998). During the Phanerozoic the sediment-binding bacteria increased, which may be the reason why syneresis cracks are more rare in these successions.

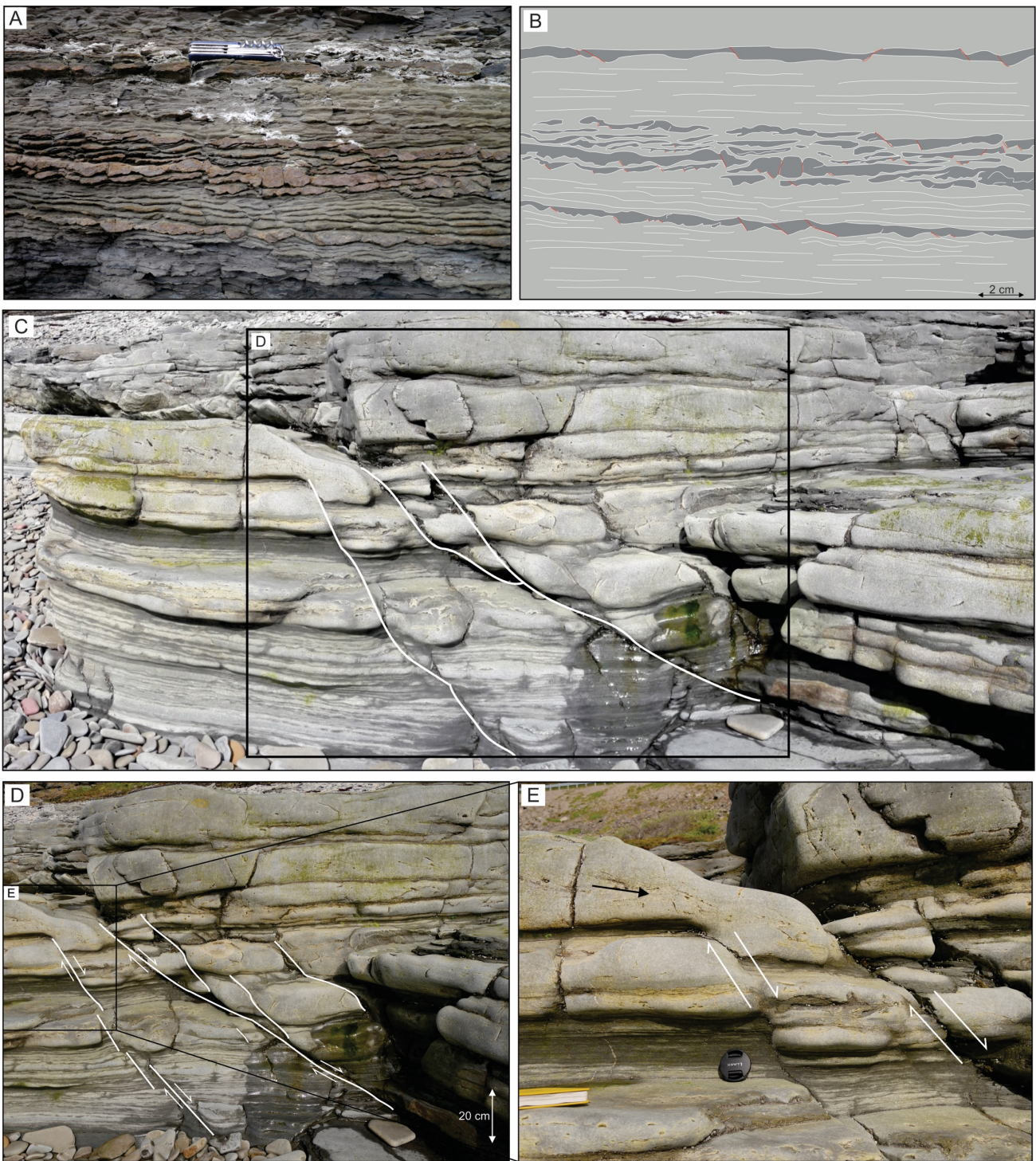


Figure 30. Small-scale syn-sedimentary faults, Klubbnasen and Andersby formations. 30A & 30 B) Micro-faults in thin sandstone beds at the Vadsø locality. Pocket knife for scale (8 cm). 30C) Overview of the faults shown in Fig. 30D and 30E. 30D) Multiple syn-sedimentary faults in sandstone beds (lithofacies 9, cross-bedded sandstone), Klubbnasen locality. 30E) Close-up view of syn-sedimentary fault from Fig. 30D. Note the overlying deformed (not faulted) sandstone bed (black arrow). Lens cap for scale (5 cm).



#### 4.4.6 Syn-sedimentary faults

Several syn-sedimentary faults affect both the Klubbnasen and Andersby formations (Figs 30 & 31). They are observed in all three localities, commonly restricted to sandstone beds where the siltstone surrounding the faults is plastically deformed (Figs 30A & 30B). They are usually planar normal to listric faults with an offset that range in sizes from a few millimetres to a maximum of 18 centimetres, typically obtaining a dip direction towards east (Figs 30C & D, 31A). The faults usually affect individual event beds (Fig. 31A), but may also affect several stacked beds (Figs 30A-30D). At the Bergelva and Vadsø localities, the faults are normally restricted to the sole of several event beds where they obtain a step-like (and occasionally boudinage-like) geometry (Fig. 31A). Several places the beds affected by the faulting typically thicken towards the fault plane (Fig. 30D). The faults are commonly associated with other SSDS, mainly contorted lamination and load structures. All of the faults sole out downward.



Figure 31. Syn-sedimentary faults at the Bergelva locality, Andersby Formation. 31A) Repeatedly faulted sandstone bed. Fault planes are directed towards east, marked by white lines. Note the undeformed sandstone underlying the faulted sandstone bed. Ruler for scale (20 cm). 31B) Close-up view of a small fault (eastward, white line) containing micro faults with opposite dip direction (towards west) on the bedding sole. 31C) Bedding sole with micro faults. Pocket knife for scale (8 cm).

At the Klubbnasen locality, several faults with curved and intersecting fault planes (offset of 10-20 cm) are observed in a sequence of stacked sandstone beds in the upper part of the Klubbnasen Formation. These faults typically constitute several fault blocks each with a lateral extent of several meters (usually < 10 m).

*Interpretation:*

The presence of frequent syn-sedimentary faults in the two formation indicates that brittle deformation of either unconsolidated or partly consolidated sediments took place in addition to hydroplastic processes (Seilacher, 1969; Owen, 1987; Rossetti and Góes, 2000). The deposition of the sediments and the faulting most likely occurred simultaneously based on the frequent existence of beds thickening towards the fault plane. The majority of the faults in the both Klubbnasen and Andersby formations are normal faults indicating an extensional stress field during deformation with a short-lasting fault activity based on the majority of small-scale faults. The common occurrence of SSDS in association with syn-sedimentary faults suggests a transition between brittle and ductile deformation (Mohindra and Bagati, 1996). Similar structures have been attributed to both seismic activity as well as slope failure, typically in basinward-dipping prodelta and delta front settings (Nemec et al., 1988; Bhattacharya and Bandyopadhyay, 1998; Rossetti, 1999; Onderdonk and Midtkandal, 2010; Korneva et al., 2016; Jiang et al., 2016; Ogata et al., 2018).



#### 4.4.5 Large-scale deformation - the Vadsø locality

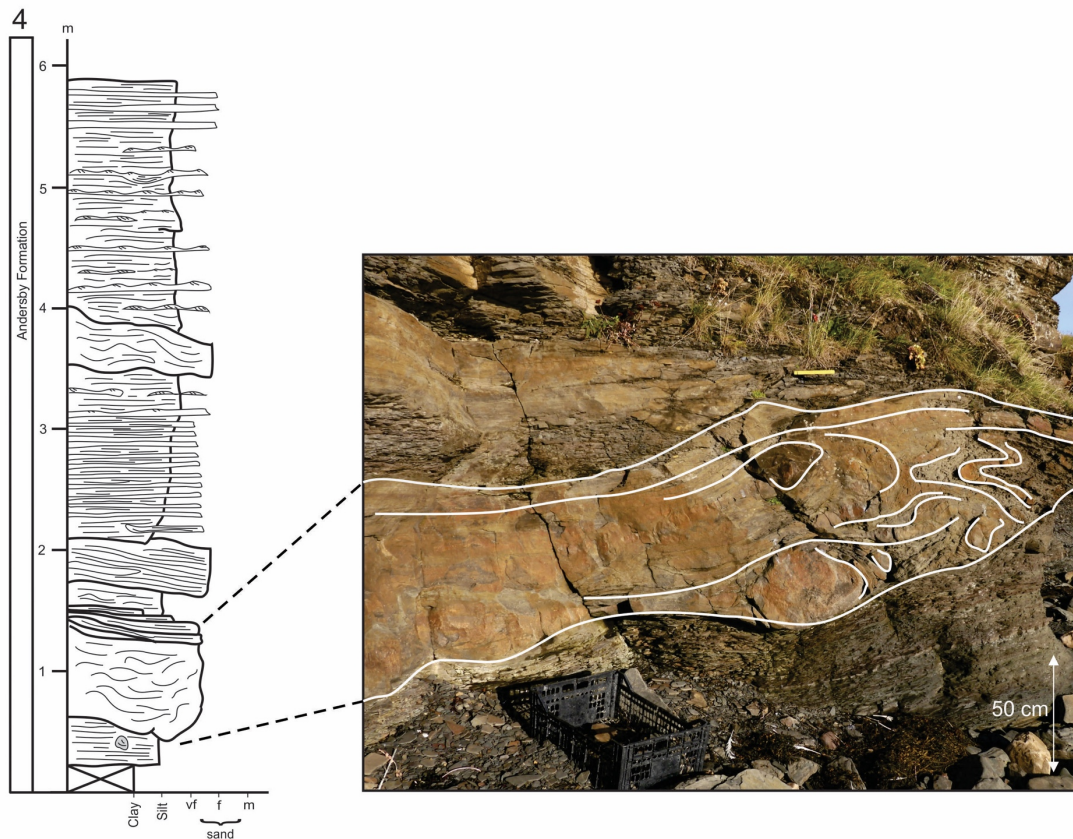


Figure 32. Large-scale deformation structures with contorted and folded bedding correlated with log 4, Vadsø locality, Andersby Formation.

In the Vadsø locality (Andersby Formation), a major chaotically deformed and partly discontinuous unit of light brown to red coloured, medium to very-fine grained sandstone and light grey siltstone can be traced throughout the extent of the outcrop (ca. 900 meters) (Figs 35 and 36). The unit contains several of the SSDS described above, but considering the lateral extensiveness and complexity of the unit, it will be described and interpreted separately herein. The deformed unit is restricted to a single stratigraphic horizon (Fig. 36), which ranges in thickness from 0.2 to 3 metres generally increasing in thickness towards east. A similar unit is also observed higher up in the Andersby formation (Vadsø locality), but it is not described in this thesis. The deformation ranges from only weakly distortion of primary structures (Fig. 26B) to complete loss of stratification (Fig. 33). Relatively undeformed units (consisting of FA1 & FA2) with irregular and mainly discordant contacts

typically confine the upper and lower part, where the basal surface appears to occasionally be scoured into the undeformed underlying unit, as well as being frequently loaded forming a distinct and irregular base (Fig. 33, 35 and 36).

The deformed unit is characterized by frequently steeply dipping and sometimes truncated layers together with rotated blocks, folds, syn-sedimentary faults, large-scale load structures, contorted and convolute stratification and rare water-escape structures. They typically appear in sandstone beds (0.15 to 2 metres), commonly obtaining internal deformed or undeformed stratification (e.g. lithofacies 5 (planar lamination) and lithofacies 6 (HCS)), while deformed siltstone (lithofacies 1) or heterolithics (lithofacies 2) commonly occur between the deformed sandstone beds. Locally, the upper part of the unit consists of relatively poorly sorted (mixed) sandstone and siltstone displaying heavily disrupted and deformed structures with no primary stratification typically containing abundant sandstone clasts. The contorted and convolute stratifications within the sandstone contain small-scale folds and overturned lamination (Figs 26A & 26B), which typically change into larger and more complex folds when followed laterally towards east (Fig. 32). The folds observed occur at different scales and obtain a diverse fold geometry, ranging from tens of centimetres to several metres. They vary from only weak gentle folds with long wavelengths (Fig. 34A) to intensely contorted, complex and overturned folds, some recumbent, frequently obtaining east-verging fold axis (Figs 34B & 34C). As the folds become further deformed, they transform into more heterogeneous units with more random orientations. In addition, several of the folds contain smaller ball-and-pillow structures (Fig 34B) of coarser material together with incorporated lenses and thin layers of deformed/folded siltstone (Figs 34A & 34C). In the middle to eastern part of the unit, numerous large-scale load casts and ball-and-pillow structures (0.5 to 2 meter in diameter) with irregular morphologies occur in association with other SSDS. They commonly consist of siltstone and very-fine to fine grained sandstone with rare internal structures. Some of these load structures may obtain a vergence towards east, which is also evident for some of the flame structures observed in association with the load structures. In addition, several isolated blocks, some rotated and disoriented with respect to normal horizontal beds, with contained internal structures and only weakly deformed, are observed sporadically within the unit.

The blocks/slabs vary in sizes from a couple decimetres to a few meters and occasionally overlap and thrust over one another. Locally, water-escape structures, typically consisting of mixed sandstone and siltstone, are found.

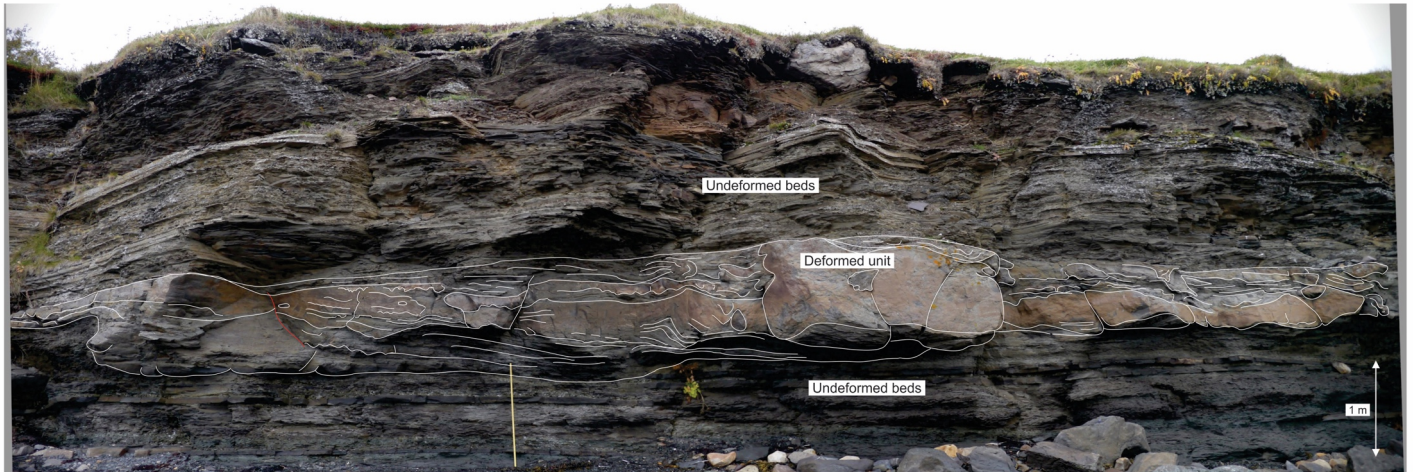


Figure 33. Panorama showing parts of the deformed unit at the Vadsø locality, Andersby Formation. Note the large-scale ball-and-pillow structures in the middle of the picture. Red line indicates a small fault plane. Meter stick for scale (1 m).

#### *Interpretation:*

The highly deformed and complex unit displaying variable horizontal and vertical deformation is most likely induced by liquefaction and fluidization processes with a component of lateral shear stress/slope failure (Allen, 1982; Owen, 1987; Owen and Moretti, 2011). The deformed unit is confined to one single horizon with undeformed stratification above and below, indicating an origin related to a single instantaneous event such as earthquakes, slump events or catastrophic storms, which occurred when the sediments were still unconsolidated and saturated with water (Mastrogiacomo et al., 2012; Lowe, 1975; Allen, 1982). These processes may either cause in situ deformation (liquefaction and/or fluidization) (Sims, 1975; Moretti et al., 2014; Allen, 1982; Lowe, 1975; Rossetti, 1999) or deformation and reduction of shear strength associated with lateral shear or downslope gravitational movements (Allen, 1982; Mulder and Cochonat, 1996; Shanmugam, 2019). Several trigger mechanism may have acted either individually or together during deformation (Rossetti, 1999), generating a variety of both small- and large-scale SSDS obtaining extensional and compressional features.



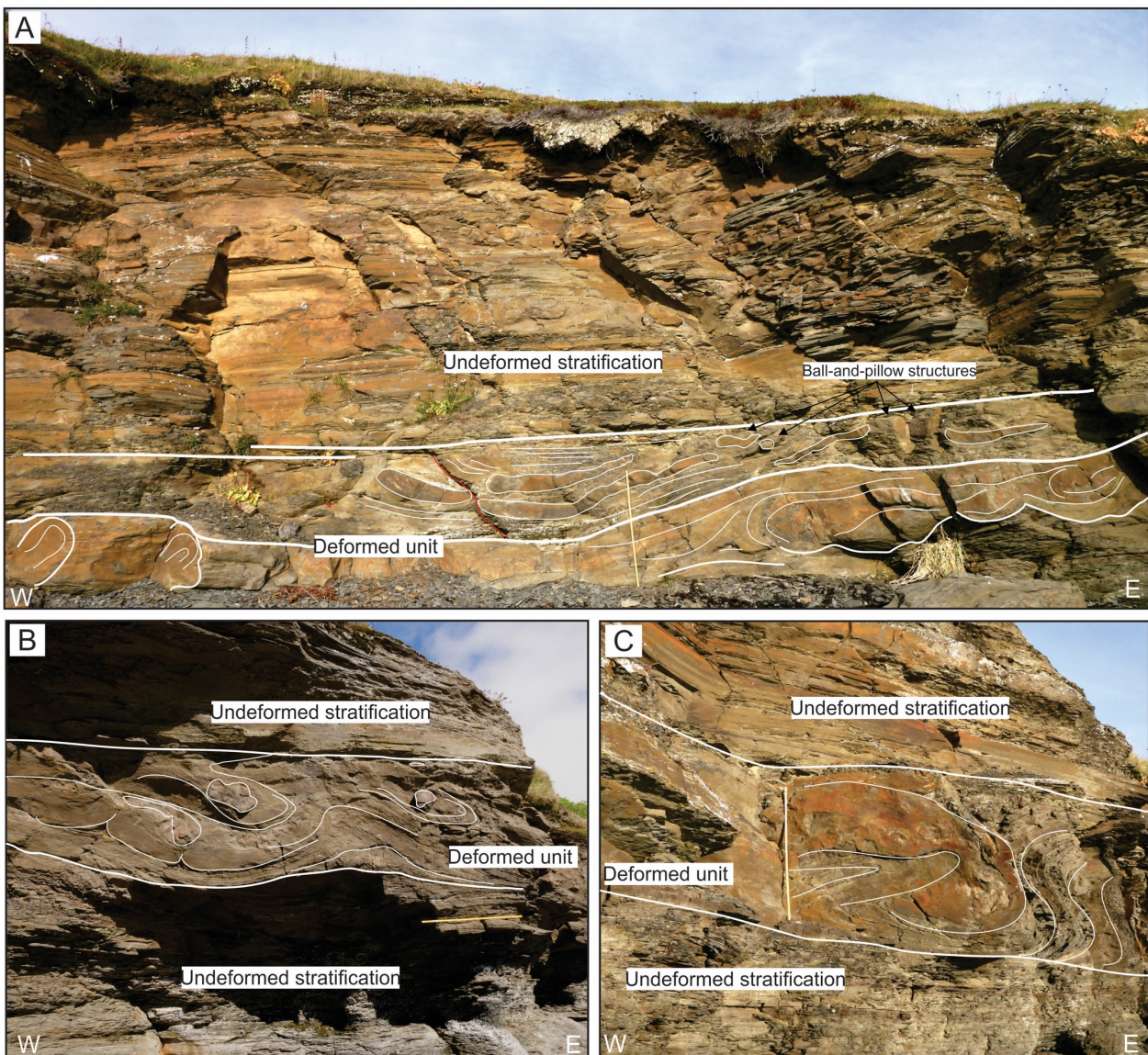


Figure 34. Large-scale folds observed in the deformed unit, Vadsø locality, Andersby Formation. 35A) Large-scale open fold with isolated sandstone blocks and smaller ball-and-pillow structures. 35B) Folds containing a vergence towards east. Notice the ball-and-pillow structures incorporated into the folds. 35C) Overturned fold towards east with an almost horizontal axial plane. Meter stick for scale (1 m).

The convolute and heavily contorted stratification observed within the unit may be attributed to partial liquefaction and fluidization induced deformation, while the general occurrence of massive sandstone beds and rare water-escape structures indicate that complete fluidization developed in several zones of the unit (Owen, 1987). The convolute and contorted structures typically transform eastward into fold structures obtaining variable sizes and degree of folding, which is indicative for a continuous hydroplastic or a laminar



liquefied flow where the primary stratification of the folded layers are deformed, but not completely destroyed (Lowe, 1975). Several of these folds are recumbent or obtain vergence towards east produced by shear stress during deformation, which may be associated with seismic surface waves (Rayleigh waves), subaqueous surface waves or downslope gravitational forces during deformation. In addition, the common development of large ball-and-pillow structures and load casts suggest the presence of reverse density mechanism between the sandstone and siltstone. Although, the density contrast between the layers is presumably not efficient enough in creating these structures alone based on the presence of non-deformed similar stratification surrounding the deformed unit, and consequently an external trigger mechanism must have caused liquefaction/fluidization of the sediments (Molina et al., 1998; Moretti et al., 2001; McLaughlin and Brett, 2004). This further supports the interpretation of an instantaneous nature of the deformation. Similar large-scale load structures, both symmetrical and asymmetrical, have been observed in several ancient successions (i.e.: Bowman et al., 2004; Taşgın et al., 2011; Mohindra and Bagati, 1996) and are typically interpreted as seismically induced deformation structures or in rare cases caused by storm induced stress (Molina et al., 1998). Additionally, several of the ball-and-pillows observed together with flame structures frequently obtain a verging trend towards east, which may be attributed to the presence of a lateral-driving force system during deformation such as shear stress (from seismic waves or subaqueous currents) or the presence of a slope (downslope gravitation force) (Moretti et al., 2001; Mohindra and Bagati, 1996). The rotated and disorientated blocks obtaining only weak distortion of the primary stratification indicate that the blocks were most likely consolidated or partly consolidated during deformation and thus acted rigid while the surrounding finer sediments were unconsolidated. In addition, the occurrence of thrusting and overlapping imply that compressional stresses developed during deformation, which may be indicative for localized slumping (McLaughlin and Brett, 2004).

Based on these interpretations, the deformed unit at the Vadsø locality can most likely be attributed to a single instantaneous slump event resulting in both vertical and horizontal shear stress caused by liquefaction and fluidization processes accompanied by local deformation of consolidated sediment.

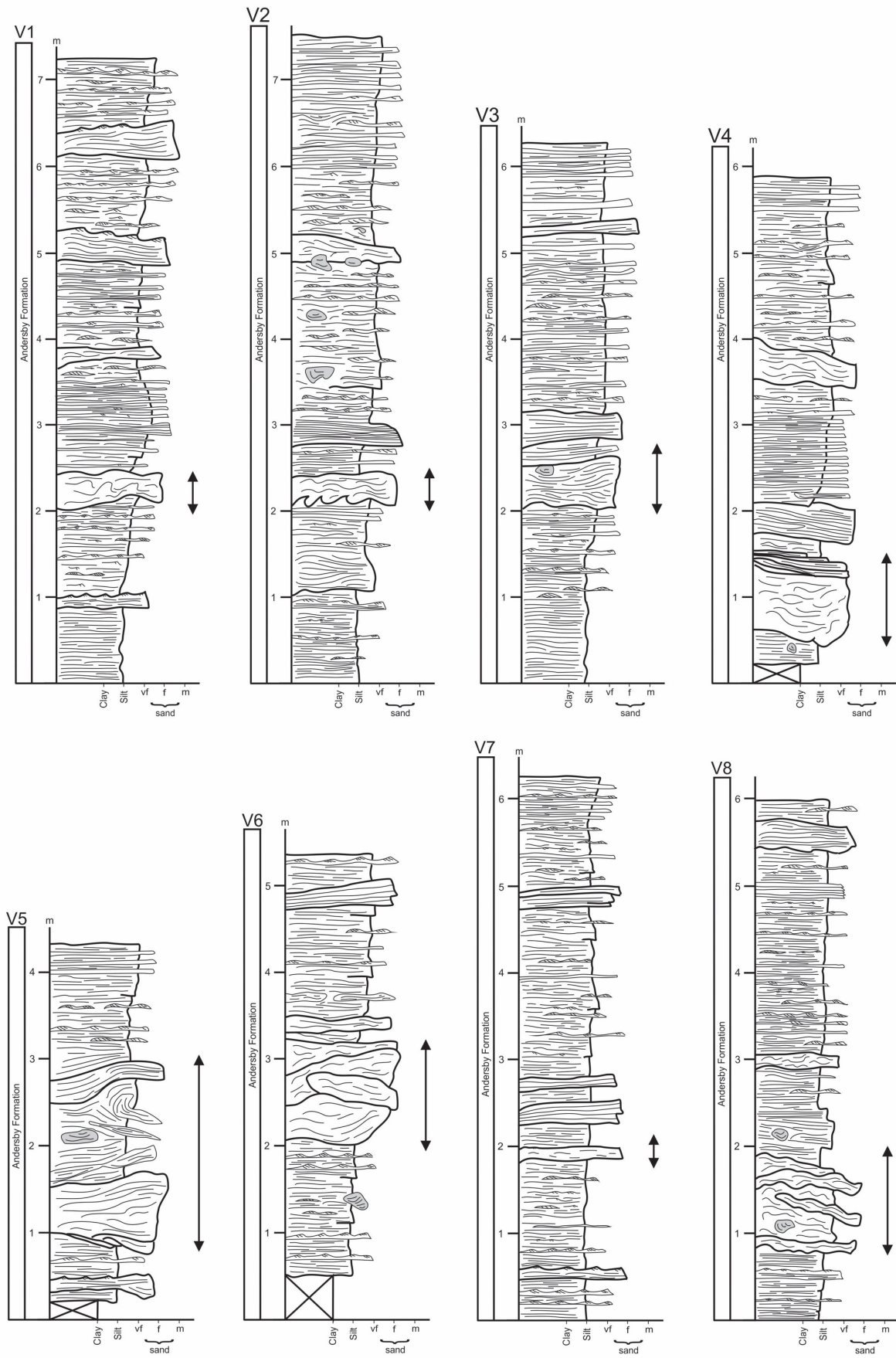
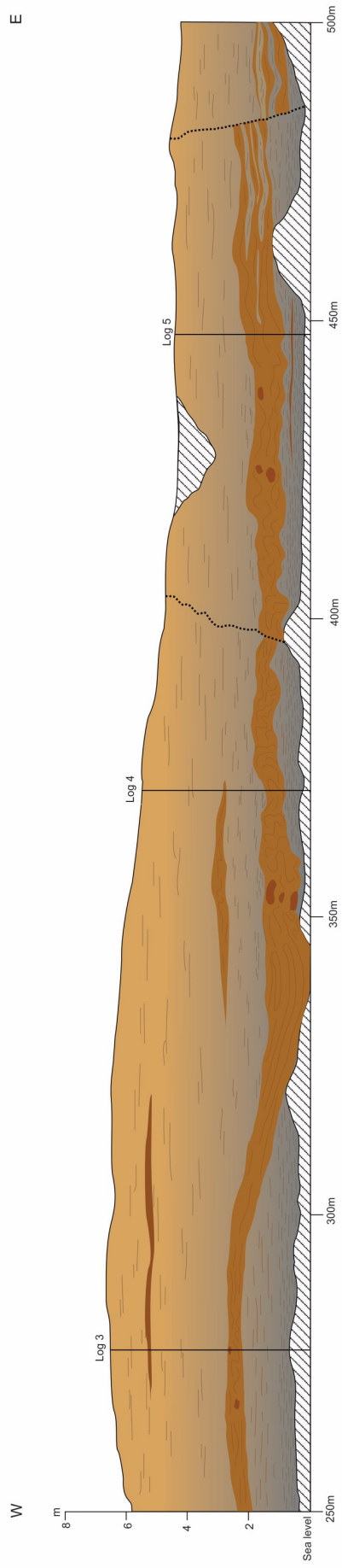
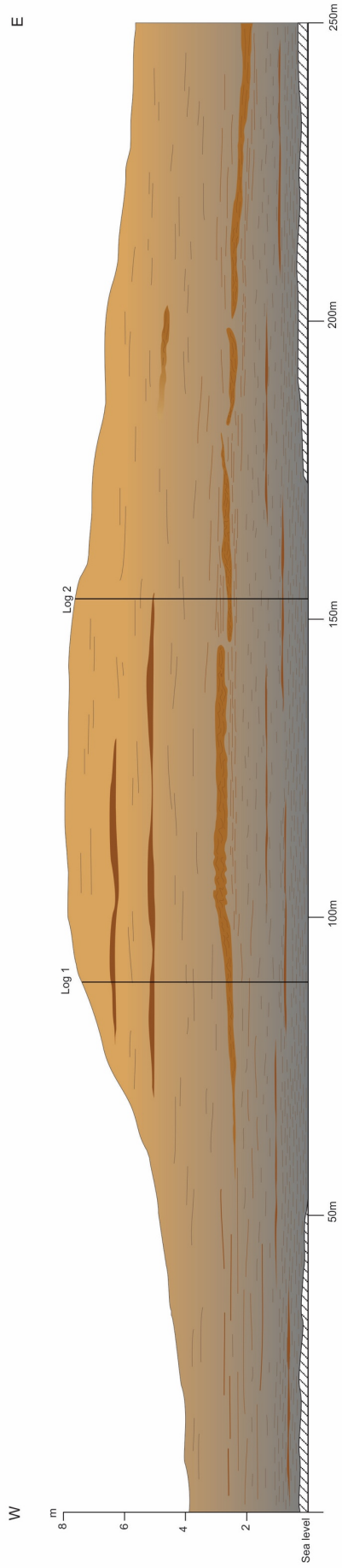


Figure 35. Detailed sedimentological logs of the Vadsø locality recording the development of the slump unit from west (V1) to east (V8). The black arrows mark the slump unit within logs. Correlation panel shown in Fig. 37.



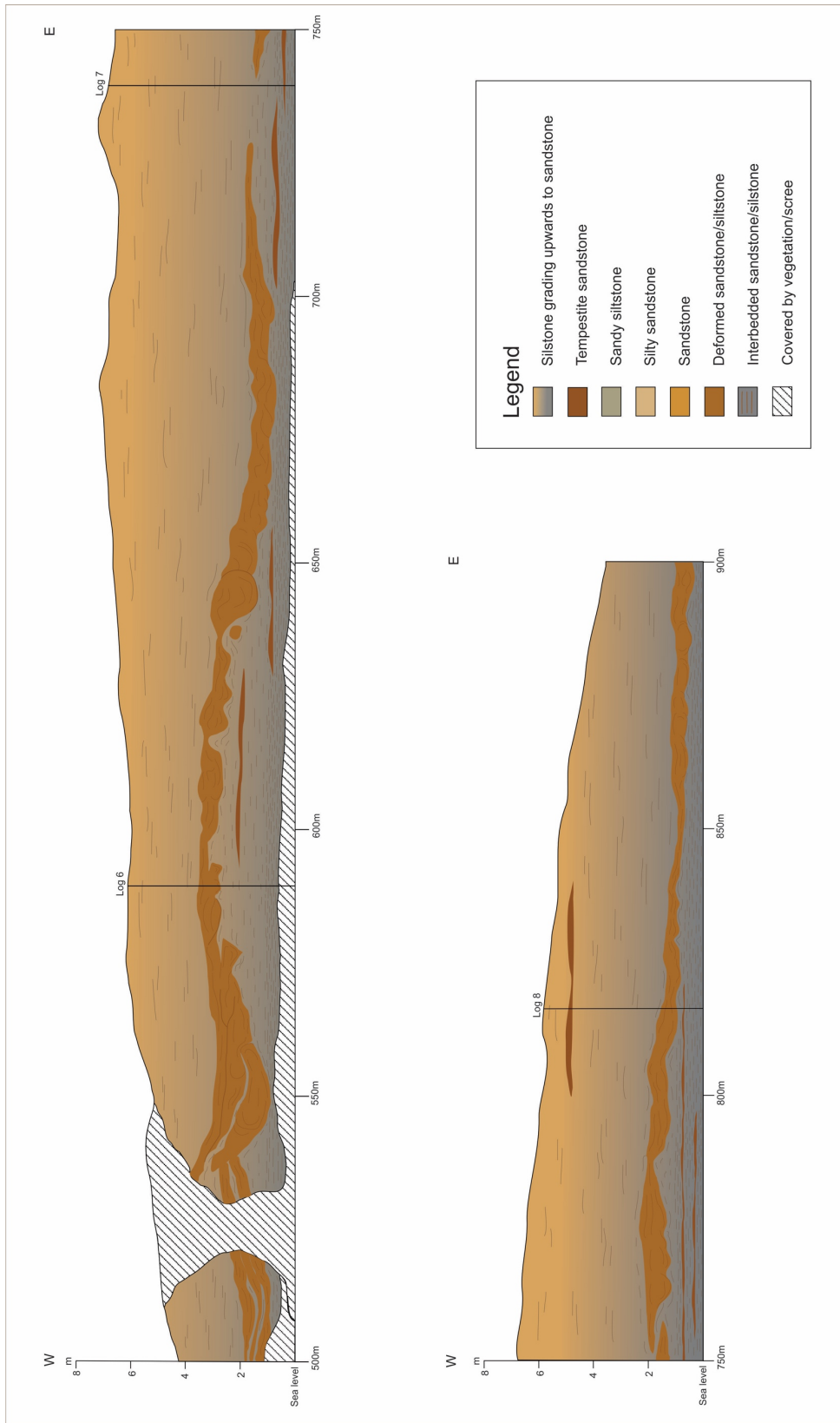


Figure 36. A 900 meter long panel displaying the lateral development of the slump unit at the Vadsø locality. The sedimentological logs (Fig. 36) are marked with black lines and corresponding numbers.



## 5. Discussion

### 5.1 Origin of the event beds of the Klubbnasen and Andersby formations

For the past decades, several studies have been published regarding the hydrodynamic mechanisms attributing in transporting and depositing sand onto the shelf. However, the subject has been and still is controversial and the debate is ongoing (e.g. Dott Jr and Bourgeois, 1982; Leckie and Walker, 1982; Swift et al., 1983; Duke, 1985; Arnott and Southard, 1990; Myrow, 1992; Dumas and Arnott, 2006; Lamb et al., 2008). Both geological and oceanographic studies have been conducted to give a better understanding on the depositional dynamics and the lithofacies patterns on continental shelves. While the oceanographic point of view focuses on modern shelf investigations (e.g. Snedden et al., 1991; Siringan and Anderson, 1994), the geological studies are based on investigations concerning ancient shelf successions (e.g. Brenchley and Newall, 1982; Myrow and Southard, 1991; Myrow et al., 2002; Pattison, 2005), leading to two radically different findings.

The oceanographic studies from modern shelves emphasise geostrophic currents as an important agent in governing sediment transport. Geostrophic currents are the product of an offshore-pressure gradient resulting from coastal set-up during storms (e.g. storm surges), which is further deflected by the Coriolis effect making nearly shore-parallel currents (low angle to the coast, parallel or oblique) (Swift and Niedoroda, 1986; Leckie and Krystinik, 1989; Myrow, 2005). In combination with strong oscillatory flows, these currents are believed to be the main mechanism in transporting sediments onto modern shelves. However, in many ancient storm-influenced shoreline sequences, paleocurrent data from mainly sole marks, at the base of storm-generated event beds (e.g. tempestites) are commonly oriented normal to the paleo-shoreline. This indicate a dominance of offshore directed flows, which contradicts with the oceanographic observations on modern shelves (Leckie and Krystinik, 1989; Duke, 1990).

Thus, the early facies models derived from ancient shelf successions suggested that offshore transportation and deposition were governed by storm-generated turbidity currents induced by excess weight forces (Wright and Walker, 1982; Dott Jr and Bourgeois, 1982; Leckie and Walker, 1982). The offshore-directed paleocurrent data from solemarks, as well as the similarities to deep-water turbidites and proximal (lower shoreface) tempestites, supported

this interpretation (Dott Jr and Bourgeois, 1982; Leckie and Walker, 1982; Myrow, 2005). Although, many oceanographers disagree with this interpretation because autosuspension seems unlikely on low-gradient slopes typical for modern shelf environments (Swift and Niedoroda, 1986) and considering that geostrophic currents are nearly shore-parallel. Several studies document a variety of internal structures and bed geometries of tempestites suggesting that three different processes act upon the sediments during a single storm event. These are (1) geostrophic currents, (2) storm-generated waves and (3) excess-weight forces (downwelling density flows, e.g. turbidity currents) (Myrow et al., 2002; Dumas et al., 2005; Pattison, 2005; Dumas and Arnott, 2006; Mulder et al., 2009; Jelby et al., 2020). The facies architecture of the resulting deposit is attributed to the temporal and spatial evolution of the three transport agents.

The tempestites of the Klubbnasen and Andersby formations display a diversity of sedimentary structures and bed architectures (Figs 9 to 13, 15 and 16; Table 1) representing unidirectional, oscillatory and combined-flows. The beds, notably in the Andersby Formation, are normally graded displaying various combined-flow-generated structures (as described in FA2; Fig. 17). The typical bed architecture obtains an erosional base with eastward directed sole marks (flute casts, Fig. 19C), which is typically overlain by interval of normally graded, massive sandstone (lithofacies 4; Figs 10A & 10B). The massive sandstone is further covered by planar-lamination (lithofacies 5; Figs 10B, 10D, 16C & 16D) grading into quasi-planar lamination and/or HCS (lithofacies 6; Fig. 11), which is further capped by combined-flow ripple cross-lamination or climbing ripple cross-lamination (lithofacies 8; Fig. 13). Several of the beds typically obtain a pinch-and-swell bed geometry (Figs 16, 17 & 18) indicating reworking by storm waves (e.g. Brenchley et al., 1993). Although, a small number also obtain a more tabular geometry (Figs 15, 17 & 18), which typically characterizes deposition dominantly by turbidity flows with little wave-reworking (e.g. Mutti and Ricci Lucchi, 1978).

The presence of erosional bases and sole marks on several event beds is indicative for an initially powerful, unidirectional, near-bottom flow during the pre-depositional phase of the bed, which gradually waned (Myrow, 1992; Myrow and Southard, 1996). The origin of this unidirectional component may be attributed to either wind-induced hydrostatic pressure gradients (geostrophic currents) or density-induced gravity flows (e.g. turbidity currents)

(Myrow and Southard, 1996). The eastward oriented solemarks of the two formations (Fig. 10C) thus reflect strong offshore-directed currents according to the regional paleogeographic reconstructions by Røe (2003) (Fig. 8), excluding shore-parallel geostrophic currents as a possible transporting agent in the present case. In prodeltaic environments, offshore-directed currents are typically related to turbidity currents down the delta front governed by excess weight forces (Pattison, 2005; Lamb et al., 2008; Bhattacharya and MacEachern, 2009; Basilici et al., 2012). The excess weight force producing these flows is a function of excess weight per unit volume of the sediment suspension as well as the gradient of the slope (Myrow and Southard, 1996). Although, Swift (1985) argued that turbidity currents are not dense enough to obtain strong currents on low-gradient slopes such as the prodeltas the Klubbnasen and Andersby formations represent. However, if a storm-induced oscillatory flow is superimposed on the turbidity currents, it may enhance the turbulence and boundary-layer shear stress and thus maintain the driving force for relatively large distances across the shelf (Myrow and Southard, 1996; Macquaker et al., 2010). Such turbidity currents, referred to as wave-modified turbidity currents, seem to be a common feature of many modern and ancient shelf systems (e.g. Myrow et al., 2002; Pattison, 2005; Lamb et al., 2008). These beds are typically characterized by a Bouma-like sequence containing abundant well-developed offshore-directed flute casts and are normally graded where several display climbing-ripple cross-lamination. However, in contrast to deep-sea turbidities, the wave-modified turbidites are commonly deposited above SWB and typically contain structures associated with oscillatory flows such as hummocky cross-stratification (HCS), quasi-planar lamination and combined-flow ripples (Myrow et al., 2002). Despite the characteristics of the beds of the Klubbnasen and Andersby formations are highly variable (Figs 10, 11, 13 & 16), the overall bed architecture strongly resembles wave-modified turbidite beds reported elsewhere (e.g. Myrow et al., 2002; Jelby et al., 2020). The variety in bed architecture may be related to variable flow mechanisms such as wave unsteadiness (Jelby et al., 2020) and temporal evolution of the turbidity flow as well as proximity to the delta front (Eide et al., 2015; Lamb et al., 2008; Grundvåg et al., 2020).

The wave-modified turbidites may be generated by several different processes, including both fluvial and storm-related processes on the delta front (Plink-Björklund and Steel, 2004). Several ancient wave-modified turbidites are interpreted to be the result of hyperpycnal

river floods, termed oceanic floods, which is typically associated with fluvio-deltaic environments (Wheatcroft and Borgeld, 2000; Collins et al., 2017). These flows are produced by the catastrophic introduction of sediment-laden floodwater into the sea via distributary channels presumably during storm events (Mulder et al., 2003; Myrow, 2005; Collins et al., 2017). The lack of plants and vegetation binding up sediments during the Late Precambrian times would additionally have enhanced the sediment load in the flow during floods. Deposits by these types of coupled flood-storm-induced currents typically result in beds with alternating sedimentary structures indicative for a fluctuating flow (i.e. multiple wax-wane cycles resulting in inverse-normal grading). Although, this depositional model may be important in cross-shelf sediment transport in several cases (Mulder et al., 2003; Myrow et al., 2004; Bhattacharya and MacEachern, 2009; Wilson and Schieber, 2014; Collins et al., 2017), it may not be applicable for the tempestites of the Klubbnasen and Andersby formations, considering their predominantly waning bed architecture (i.e. sharp-base, normal grading, massive to HCS lower part, rippled bed tops etc.). However, under certain circumstances it has been suggested that the waxing bed division, typically observed as inverse grading, is not preserved as a result of erosion during peak flow (Mutti et al., 2002) and thereby achieving the Bouma-like sequence reported from many wave-modified turbidites (Mulder et al., 2003; Myrow et al., 2008). Based on these considerations, as well as the relatively close proximity to fluvial systems (in this case the Fugleberget and Paddeby formations, respectively (Figs 8, 21, 22 & 24)), storm-induced hyperpycnal flows cannot be excluded as a possible trigger for the investigated event beds. Although inverse grading related to waxing flow have not been observed.

Another plausible process governing turbidity currents are high pore-fluid pressures associated with cyclic wave loading during storms (Prior et al., 1989; Bhattacharya and Giosan, 2003; Traykovski et al., 2007). The increasing pressure within the sediments on the delta front may lead to liquefaction and nearshore slumps, which may further generate turbidity currents (Plink-Björklund and Steel, 2004). The occurrence of several syn-sedimentary faults (FA3; Fig. 30) and meter-scale scours in the delta front deposits (FA3, Figs 19A & 19B) indicate that the environment were frequently subjected to sediment failure, which may have been triggered by storm-induced stress. However, sediment failure on the delta front may also be related to seismically-induced liquefaction. Both the Klubbnasen and



Andersby formations have previously been interpreted to be part of a syn-rift succession (Røe, 2003) indicating a seismically active basin at the time of deposition. Additionally, the formations display abundant and widespread soft-sediment deformation at several stratigraphic levels, which could potentially be related to seismic activity. There have been reported several turbidite successions related to seismically induced stress, in both active rift-basins and deltaic environments (Gorsline et al., 2000; Gibert et al., 2005). Subsequently, the turbidity currents may also have been triggered by seismic-induced stress. According to these observations, the complex mixture of wave-modified turbidites documented in the Klubbnasen and Andersby formations may be attributed to a combination of several different trigger mechanisms where the most plausible are hyperpycnal flows and cyclic stress related to storm waves and seismic activity.

Based on the assumption given above, a general model regarding the hydrodynamic processes during the formation of the wave-modified turbidites of the Klubbnasen and Andersby formations is proposed (Fig. 37). The model illustrates conditions during a progressively waning storm event with high aggradation rates where deposition took place between FWWB and SWB (intermediate settings; FA2). The model does not consider waxing-waning cycles related to coupled storm-flood-generated hyperpycnal flows, as inverse grading lack in nearly all the investigated event beds. Moreover, beds deposited in proximal (FA3) or distal (FA1) settings will naturally deviate from this model. The proximal to distal storm-variability trends will be further discussed in the next chapter.

The predepositional phase during the development of a typical wave-modified turbidites was most likely dominated by highly erosional unidirectional flows in the form of a fully turbulent flow, leading to the formation of offshore-directed flutes (Fig. 37A). As the flow rapidly waned and deposition commenced with high rates of sediment fallout and aggradation, the lowermost unit of massive graded sand were formed, locally filling in the flutes (Fig. 37B). As the deposition continued, the influence of oscillatory flows increased, and planar lamination was deposited (Fig. 37C). At one point, the oscillatory component of the flow exceeded the unidirectional component (i.e. oscillatory-dominated combined-flow) leading to the formation of quasi-planar lamination and nearly isotropic HCS (Fig. 37D) as observed in the Andersby Formation. During the last phase of the storm, the oscillatory component decelerated, which further promoted the formation of last unit consisting of

combined-flow ripples or climbing-ripple cross-lamination (Fig. 37E). The formation of climbing-ripple cross-lamination may have been promoted during rapid sediment fallout generated by quickly decelerating flows governing both high aggradation rates and bedform migration. This would typically occur when the storm-generated flow shift from confined to unconfined, commonly when the flow reaches the base of the slope or leaves a confined channel (Bouma, 2004).

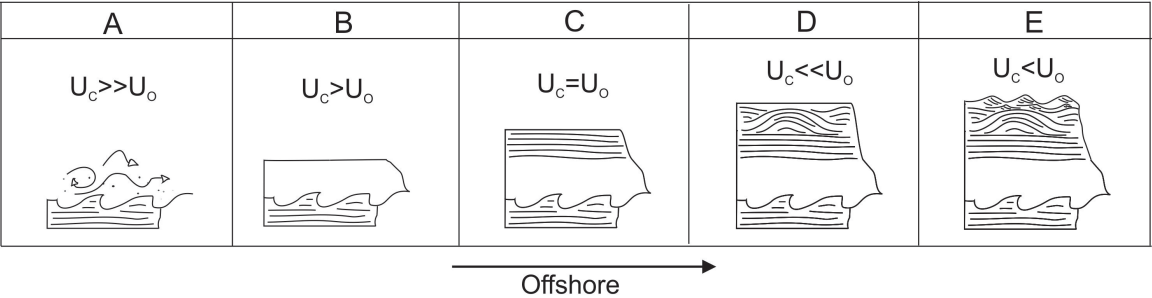
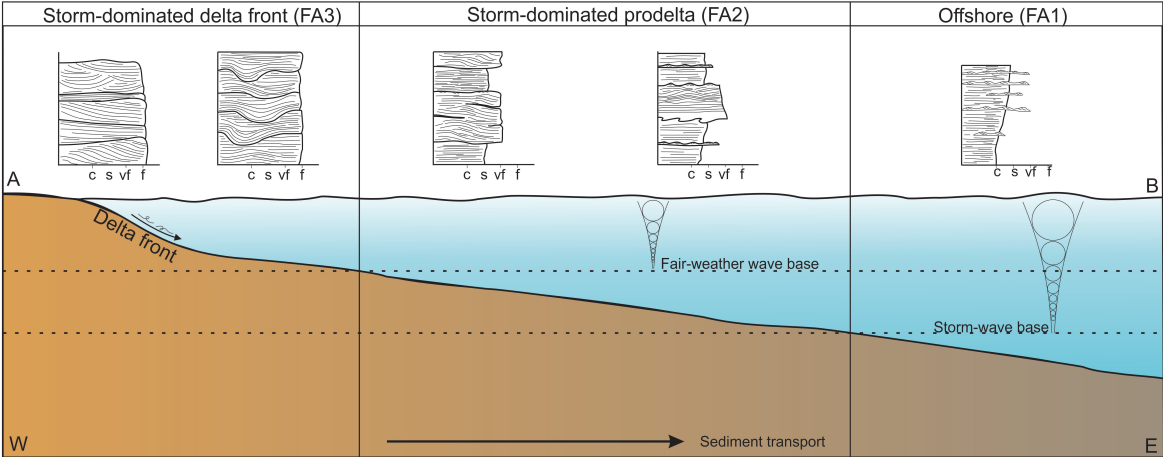


Figure 37. Model displaying the typical formation of a typical wave-modified turbidite during a waning storm event.  $U_c$ = unidirectional component and  $U_o$ = Oscillatory component.

### 5.2 Storm-bed variability across the shelf

During storms, nearshore areas experience erosion where large waves and strong unidirectional currents (e.g. turbidity currents and other associated down-welling currents) transport and deposit large amount of sand onto the shelf. Combined, these processes contribute to progradation of the shoreface environments (also in storm-dominated delta settings). The resulting deposits commonly occur as HCS-bearing progradationally stacked and upward-coarsening successions reflecting the lateral variation in hydrodynamic processes from distal to proximal settings (Dott Jr and Bourgeois, 1982; Brenchley et al., 1986; Myrow and Southard, 1991; Dumas and Arnott, 2006). In general, the sandstone beds increase in thickness and complexity from distal to proximal settings. Thinner isotropic HCS-bearing beds generally grade landward into anisotropic HCS, which gradually become more amalgamated towards the lower and middle shoreface zone. The most proximal settings above FWFB (i.e. upper shoreface), are commonly dominated by amalgamated swaley-cross stratification (SCS) overlain by large-scale, high angle cross-stratification (Dumas and Arnott, 2006; Bowman and Johnson, 2014).

Both the Klubbnasen and Andersby formations display clear distal to proximal trends with variations in the lateral distribution of lithofacies association (Fig. 38) resembling similar trends as the typical storm-dominated sequence described above (e.g. Figs 17, 18, 19 & 21). The lowermost units of the two formations represent the distal deposits (FA1, offshore), dominated by thin, normally graded sandstone beds separated by fair-weather deposits (e.g. Figs 9A & 9B), which are either structureless (fig. 9D) or exhibiting combined-flow ripples and/or planar lamination (Fig. 9C). These beds are linked to relatively quiet condition in deep waters where both the oscillatory flow and turbidity currents are considerably weaker and thus the formation of both erosional structures (e.g. flute casts) and HCS are dismissed. Similar thin-bedded sandstone related to storm-dominated shelf successions have typically been ascribed to purely unidirectional currents represented by dilute turbidity currents where the oscillatory flows are absent (Dott Jr and Bourgeois, 1982; Myrow et al., 2002; Myrow, 2005; Pattison, 2005). However, in contrast to standard storm depositional models, the thin beds of this study display structures typically associated with combined-flows (e.g. combined-flow ripple lamination). It is thus believed that the majority of the thin beds were deposited by wave-enhanced turbidity currents during intensive storms that reached considerable depth.



Figur 38. Figure displaying the proximal to distal relationship of tempestite beds. Not to scale.

The distal deposits are typically overlain by variations of the typical wave-modified turbidite facies sequence (*sensu* Myrow et al., 2002) indicating the presence of a powerful, but decelerating combined-flow above mean SWB. The beds are typically observed in the middle to upper part of the Andersby Formations (FA2, Figs 16, 17 & 18) where they are interbedded with fair-weather deposits. Further proximally (i.e. stratigraphic upwards in the investigated successions), the isotropic HCS is succeeded by beds of anisotropic HCS where several contain evidence of amalgamation (internal second-order truncations). This suggests an increase in the unidirectional component promoting bedform migration where the sediments were frequently subjected to erosion and reworking by successive storms. In the more proximal settings above FWWB (i.e. FA3), amalgamated and anisotropic HCS and SCS typically occur coincidentally in the same unit (Fig. 12), reflecting a relatively shallow environment where strong unidirectional-dominated combined-flows controlled deposition. However, according to Dumas and Arnott (2006) SCS are commonly developed in units above anisotropic HCS, reflecting shallower settings with lower aggradation rates. Although, the SCS in the middle/upper part of the Klubbnasen Formation typically occur interbedded in the same units as the anisotropic HCS (Fig. 12), which differ from standard progradational storm sequences (Dott Jr and Bourgeois, 1982; Leckie and Walker, 1982; Dumas and Arnott, 2006). These observations suggest that the aggradation rates frequently alternated during deposition, which may be a result of seabed variations causing variable bedform stabilities across the shelf. Further shoreward the units of HCS and SCS merge into stacked units of low-angle dune-scale cross-bedded and planar bedded sandstone (Figs 14A, 14B & 14F) recording stronger unidirectional currents with little wave influence, which is further consistent with a delta front setting. The proximal to distal lithofacies distribution is summarized in Fig. 38.

### 5.3 Formative mechanisms and possible triggers of the SSDS

A diversity of syn-sedimentary deformation structures, differing in both scale and type of deformation, have been observed throughout the Klubbnasen and Andersby formations at nearly all stratigraphic levels (Figs 22 to 25, 35 and 36). They are interpreted to have been developed in sediments deposited in storm-dominated prodeltaic to deltaic environments where the SSDS are observed in both storm-emplaced lithofacies and fair-weather



lithofacies. The interpretation of the formative processes and generation (trigger mechanism) of SSDS may be important in understanding the hydrodynamic and sedimentological processes as well be an aid in determining the presence of rift-related seismic activity during formation. The development of SSDS is commonly divided into three components, which consequently must be simultaneously fulfilled to generate deformation of the sediments (Owen, 1987; Owen and Moretti, 2011). The given components are 1) deformation mechanism, 2) a driving force and 3) a trigger mechanism. The trigger mechanism typically initiates the deformation mechanism or/and driving force, where the primary mechanisms contributing to deformation are liquefaction and fluidization, reverse density gradients, slope failure/slumping and shear stress (Owen and Moretti, 2011). The trigger mechanisms can be divided into two categories; endogenic (e.g. overloading and storm waves) and exogenic (earthquakes and tsunamis) (Owen, 1996; Rossetti, 1999; Alfaro et al., 2002; Moretti et al., 2014). The majority of the structures of the Klubbnasen and Andersby formations, including different load structures and convolute stratification, are interpreted to have developed in unconsolidated sediments during or shortly after deposition. Additionally, the presence of sandstone dykes (Fig. 27) and slump deposits (Fig. 35 and 36) is indicative for the occurrence of local post-depositional deformation of partly consolidated sediments. Determining the origin of the SSDS may be a difficult task, particularly since different trigger mechanisms can generate similar SSDS and one single trigger mechanism may generate a wide range of different structures.

The variety of SSDS in Klubbnasen and Andersby formations may be indicative for several different trigger mechanisms where the most plausible for similar settings are earthquakes, storm waves, overloading (rapid sedimentation) and tidal shear (Owen and Moretti, 2008). However, tidal shear can be excluded considering there exists no sign of tidal-related structures in neither the Klubbnasen Formation nor the Andersby formation and it is therefore unlikely that tidal current promoted deformation in these settings.

Overloading related to rapid sedimentation by turbidity currents (e.g. wave-modified currents) and storm waves have been reported to be a common cause of soft-sediment deformation in several ancient prodeltaic successions (Moretti et al., 2001; Lamb et al., 2008; Oliveira et al., 2009). Load structures, such as ball-and-pillows and various convolute and contorted stratification have commonly been attributed to rapid sand-accumulation

onto water-saturated muddy sediments (Allen, 1982). Moretti et. al 2001 interpreted several SSDS, including large ball-and-pillow structures from the Guadix Basin (southern Spain), to have been triggered by rapid sedimentation of single high-concentration turbidites. The ball-and-pillow structures of these deposits all display a vergence downslope, and thus indicating the influence of a current drag force from the turbidites in addition to the density induced deformation. Hypothetically, rapid sedimentation from turbidity currents could have caused several of the soft-sediment deformation of the Klubbnasen and Andersby formations. For instance, some of the beds displaying convolute and contorted lamination obtain a vergence toward east and may have been developed due to overloading caused by rapid sedimentation from turbidity currents. Although, overloading seems like an unlikely trigger mechanism for several of the structures present. Most of the SSDS are not displaying any clear evidence of preferred orientation apart from the structures mentioned above and those observed within the large deformation unit at the Vadsø locality (Figs 25A, 25B, 34B & 34C). Also, there are several wave-modified turbidite beds displaying considerable thickness, containing no deformation or load structures. Furthermore, overloading does not explain several of the observed SSDS in the heterolithic units where the sandstone beds are very thin and sedimentation rates are inferred to have been low. Overloading caused by rapid sedimentation may therefore be an inadequate trigger mechanism for several of the SSDS of the Klubbnasen and Andersby formations. Although, locally high sedimentation rates might have played a role in generating liquefaction and fluidization forming SSDS.

Deformation may also be triggered by pore pressure-related variations caused by the cyclic effect of storm waves or passing currents (Molina et al., 1998; Alfaro et al., 2002; Owen and Moretti, 2011). Several of the beds of both of the Klubbnasen and Andersby formations contain storm-related structures such as HCS and SCS indicating an environment frequently affected by storm events. During storms, the interstitial pressure within the sediments may increase as a result of pressure differences between the crest and trough of the cyclic effect of waves and subsequently generate liquefaction and/or fluidization within the sea bed (Molina et al., 1998; Alfaro et al., 2002). There are few studies concerning storm waves as the trigger mechanism, but in the few published studies load structures (e.g. ball-and-pillows) associated with tempestites are typically linked to the cyclic stress from storms (e.g. Molina et al., 1998; Alfaro et al., 2002). In both the Klubbnasen and Andersby formations,

ball-and-pillow structures are frequently associated with the wave-modified turbidites beds, which may under certain circumstances be the result of cyclic stress from storm waves where the induced stress from waves were adequate in generating liquefaction and/or fluidization. However, storm waves cannot account for the SSDS observed in lithofacies deposited below the presumed storm-wave base and thus an additional trigger mechanism must be considered. Furthermore, several of the SSDS observed, such as large sandstone dykes, larger (dm to m-scale) ball-and-pillows, convolute folds and other water-escape structures, are rarely associated with storm waves.

Cyclic stress induced by the passage of seismic waves may contribute to a diversity of SSDS in tectonically active environments (Owen and Moretti, 2011). During earthquakes, the pore pressure within water-saturated sediments increases causing the sediments to behave like a fluid. SSDS observed within several ancient successions, representing various depositional environments, have been interpreted to be seismically induced (e.g. Mohindra and Bagati, 1996; Rossetti, 1999; Gibert et al., 2005; Hildebrandt and Egenhoff, 2007; Gao et al., 2019). The SSDS of these successions have several characteristics in common, including a lateral extensiveness, vertical repetition and close proximity to active faults. These characteristics are parts of the certain criteria suggested by Owen and Moretti (2011) to be indicative for seismically induced deformation, including zonation of complexity with distance from faults and morphology comparable with other structures described to be seismically induced. There are several limitations with these criteria (Moretti et al., 2014), but they give an overall idea in which settings seismically induced deformation typically occur.

The morphology and distribution of SSDS in the Klubbnasen and Andersby formations corresponds with several of the criteria mentioned above. The Andersby Formation displays a variety of different SSDS, which can be traced laterally along the entire length of the outcrop at the Bergelva locality (c. 400 m) (Figs 2, 17 & 18). Although not correlated, three to four kilometres further east, in the Vadsø locality (Figs 2, 35 & 36), which is also part of the Andersby Formation, similar trends are observed, in addition to the presence of a lateral extensive slump unit (900 meters; Fig. 36). Accordingly, the region was presumably subjected to a repetitive stress field affecting a larger area over different time spans, which thus facilitates deformation at different stratigraphic levels. The Klubbnasen Formation (Fig. 21) also display several different SSDS (Figs 25C & 25D) similar to the Andersby Formation,

including large-scale ball-and-pillow structures, convolute stratification and syn-sedimentary faults. These are commonly restricted to certain stratigraphic intervals interbedded with non-deformed stratification displaying similar sedimentological characteristics as the deformed intervals, thereby reflecting repetitive catastrophic events (Moretti and Ronchi, 2011; Owen and Moretti, 2011). In addition, both the Klubbnasen and Andersby formations contain a large number of syneresis cracks typically occurring in high density at specific intervals, which may indicate that the sediments were affected by some type of repeated stress. Based on these observations both the criteria of vertical repetition and lateral continuity are met.

Several of SSDS of both the Klubbnasen and Andersby formation are comparable to deformation structures reported from other areas affected by seismic activity (e.g. McLaughlin and Brett, 2004). These include ball-and-pillow structures of various sizes, contorted/convolute stratification, syn-sedimentary faults and sandstone dykes (Alfaro et al., 1997; Bhattacharya and Bandyopadhyay, 1998; Hildebrandt and Egenhoff, 2007; Gao et al., 2019). These SSDS may also be attributed to other individual trigger mechanism not related to seismic activity. However, it seems unlikely that a variety of SSDS produced by processes of different origins may have acted simultaneously. A seismic origin is thus a more appealing interpretation under which the sediments may have responded differently and consequently formed a diversity of SSDS, both brittle and ductile. The presence of multiple sandstone dykes along the Bergelva in the Andersby Formation reinforces the interpretation of a seismic-related trigger mechanism considering the frequent occurrence of clastic dykes in seismically induced successions (e.g. Neef, 1991; Scholz et al., 2009; Peterson et al., 2014). Furthermore, Pratt (1998) suggested that the occurrence of syneresis cracks formed intrastratal likely are result of strong ground motion from earthquakes.

The distinctive slump unit at the Vadsø locality, featuring both plastic and brittle deformation, may be attributed to several different processes related to overloading, oversteepening and/or seismic shock (Allen, 1982; Owen, 1987; Van Loon and Brodzikowski, 1987). Based on the facies analysis and field observations (e.g. Figs 35 & 36), the unit is interpreted to be deposited on low-angle paleoslope in a prodeltaic environment. A trigger mechanism associated with oversteepening is thus unlikely. Furthermore, overloading may also be of less importance based on the relatively small thickness of the deformed unit



(maximum 2.5 meters thick). However, slump structures have been reported to be produced on slopes with angles as low as  $0.25^\circ$  under the influence of seismic shock in subaqueous environments (Field et al., 1982). There are reported several slump horizons of low-angle slopes, which have been interpreted to be produced by earthquakes (Gibert et al., 2005; Alsop and Marco, 2011; Mastrogiacomo et al., 2012; Alberti et al., 2017) and several of these display structures resembling the features of the Vadsø slump (e.g. slump folds). It is therefore likely that the Vadsø slump was seismically triggered, which further strengthens the theory of widespread deformation associated with earthquakes.

Furthermore, the investigated area are in close proximity (30-40 km) to a large fault zone, respectively the TFKFZ (Figs 4 and 5), which presumably was seismically active at the time of deposition of the two studied formations (Karpuz et al., 1995b; Herrevold et al., 2009). Additionally, Røe (2003) proposed the presence of a NW—SE trending fault zone (rift basin) in the Varangerfjorden (Fig. 6) which supposedly was active during the Riphean period (Fig. 1). Thus, it seems likely that two active fault zones in close proximity during the time of deposition may have generated or strongly contributed to the extensive occurrence of the SSDS in the Klubbnasen and Andersby formations. Additionally, deformation produced by both overloading and cyclic stress associated with storm waves may have occurred.

## 5.4 Stratigraphic development of the Klubbnasen and Andersby formations

### *The Klubbnasen Formation:*

The facies associations within the Klubbnasen Formation are arranged into two overall coarsening-upward and shallowing-upward depositional units consisting of storm dominated facies associations (Fig. 21). The lower depositional unit (K1) displays a typical development of a storm dominated shelf succession (Dott Jr and Bourgeois, 1982), from muddy and silty offshore deposits (FA1) grading upwards into more sandier prodeltaic deposits (FA2), which are further capped by stacked beds of delta front deposits (FA3) (Figs 19 & 21). The boundaries between each lithofacies association are typically gradational suggesting a continuously shallowing environment. These characteristics further indicate a depositional environment controlled by a prograding shoreline towards east affected by frequent storm reflecting an overall normal regressive development (e.g. Van Wagoner et al., 1990; Walker and Plint, 1992; Bhattacharya and Giosan, 2003; Olariu and Bhattacharya, 2006). The top of the uppermost sandstone bed in the lower depositional unit (K1; Figs 14A & 14B), are overlain by beds of laminated siltstone (FA1/FA2) marking the onset of the second depositional unit (K2) of the Klubbnasen Formation. This distinct boundary (Fig. 21) is interpreted to represent a flooding surface associated with significant increase in water depth or a sudden decrease in sediment supply (Catuneanu et al., 2009; MacEachern et al., 2012). Such flooding surfaces are commonly related to delta lobe switching and abandonment, which is a typical processes affecting prograding deltaic systems where several upward-coarsening units are bounded by flooding surfaces (Correggiari et al., 2005; Bhattacharya, 2006; Charvin et al., 2010).. Although, given the proposed tectonic setting of the Klubbnasen Formation (i.e. syn-rift succession), the marine flooding surface may also be attributed to tectonic mechanisms (Martins-Neto and Catuneanu, 2010; Gawthorpe et al., 2018). In rift-basins, the accommodation space is partly controlled by tectonic subsidence and/or uplift (i.e. hanging wall and footwall movements), leading to either generation or loss of accommodation space. Additionally, tectonic activity may also generate shifts in the footwall source area, which consequently increases or decreases the sediment supply to the basin (Gawthorpe et al., 1994; Martins-Neto and Catuneanu, 2010; Henstra et al., 2016). The marine flooding surface may therefore be attributed to either a rapid creation of accommodation due to fault-controlled subsidence in the hanging-wall basin or due to tectonic shifts in the source area leading to a decrease in sediment supply.

The second unit of the Klubbnasen Formation (K2) comprises alternation of FA1 and FA2 recording deposition in more distal and intermediate settings. Considering the weakly upward-coarsening nature of K2, it is most likely related to normal regressive conditions with moderate sediment supply accompanied by hanging-wall subsidence. The upper part of K2, consisting of laminated siltstone and sandstone, is abruptly overlain by a stacked unit of thick-bedded sandstone, representing the lower part of Fugleberget Formation. The occurrence of coarser-grained and cross-bedded sandstone beds (FA4, braided river deposits (Fig. 14C)) overlying bed sets of prodeltaic origin (FA3) mark an abrupt and dramatic change in depositional environment, from marine to fluvial settings (Fig. 22). The distinct boundary represents a clear violation of Walther's law and may be regarded as a subaerial unconformity (i.e. a type 1 sequence boundary following the Exxon sequence stratigraphic terminology (SSM)). The unconformity was most likely developed during an episode of uplift or eustatic sea-level fall where the underlying marine succession was subjected to fluvial erosion (Plint, 1988; Catuneanu and Elango, 2001; Embry, 2002; Catuneanu et al., 2009). Considering the overall syn-rift nature of the Vadsø Group and the presence of seismically induced SSDs throughout the Klubbnasen Formation, it is likely that the stratigraphic development was influenced by the evolving rift-basin (Leeder et al., 1991; Gawthorpe et al., 1994; Carr et al., 2003; Henstra et al., 2016). Displacement of the basin-bounded normal faults may have induced footwall uplift, which consequently result in major changes in the depositional environment (Gawthorpe and Leeder, 2008). During footwall uplift, larger areas are exposed facilitating extensive erosion of the underlying sediments, which subsequently increases the sediment supply. Thus, tectonically-induced displacement, possibly associated with footwall uplift, seems like an adequate mechanism in generating the subaerial unconformity (Gawthorpe et al., 1994).

The Andersby Formation displays similar characteristics as the Klubbnasen Formation, although deposits of FA3 (delta front deposits) are seemingly lacking. Similar to the Klubbnasen Formation, the Andersby Formation consists of two depositional units (A1 and A2). The lower unit (A1) is dominated by mudstone/siltstone, which pass vertically into more sandstone-rich deposits of prodeltaic origin (FA2) (Figs 15, 17 & 18) reflecting an overall prograding succession. In contrast to the Klubbnasen Formation, the lower unit of Andersby Formation terminates after FA2. The unit is further overlain by depositional unit A2

consisting of mudstone- and siltstone-dominated outer shelf deposits (FA1) recording sudden decrease in sediment input and deepening of the lithofacies assemblage. The distinct boundary separating the two units resembles the observed flooding surface within the Klubbnasen Formation, indicating a similar origin of the surface. It is thus suggested that the contact represents a marine flooding surface associated with either delta lobe switching or as a result of tectonic activity leading to either an increase in the accommodation space (i.e. tectonic subsidence) or drastic changes in the source area (sudden decrease in sediment supply).

The upper depositional unit of A2 is a relatively thin depositional unit (maximum 3 meters) dominated by siltstone and mudstone of possible outer shelf origin (FA1; Fig. 24). The unit is further truncated by thick-bedded sandstone (lithofacies 9 and 10) marking a distinct transition (Fig. 24) into the overlying cross-bedded sandstone unit of the Paddeby Formation (Fig. 8), which is attributed to deposition in a braided river system (FA4; 13C, 22). Based on the sudden and dramatic facies shift, from outer shelf deposits (FA1) to braided river deposits (FA4), the surface is interpreted to represent a subaerial unconformity (i.e. type 1 sequence boundary) related to a relative sea-level fall. Similar to the subaerial surface of the Klubbnasen Formation, the generation of the unconformity is most likely the consequence of footwall uplift in the rift margin.

There are clear similarities between the stratigraphic evolution of the Klubbnasen and Andersby formations. Both of the formations contain overall upwards-coarsening units bounded by marine flooding surface, which in turn are overlain by deposits of fluvial origin separated by subaerial unconformities. It thus seems likely that the Klubbnasen-Fugleberget formations and the Andersby-Paddeby formations represent two stratigraphic successions of similar depositional trends, recording the cyclic infill history to the rift basin reflecting recurrent episodes of subsidence and uplift (Gawthorpe et al., 1994; Gawthorpe and Leeder, 2008; Martins-Neto and Catuneanu, 2010).

The finer-grained Klubbnasen and Andersby formations most likely record deposition following hanging wall subsidence where progressively new accommodation space was generated. Eventually, the sediment input outpaced the subsidence rate (i.e. periods of relatively tectonic quiescence) and consequently leading to the formation of a successively



progradation deltaic successions (Strachan et al., 2013). The presence of predominantly fine-grained material in the Klubbnasen and Andersby formations indicate relatively low sedimentation rates where only the finer-grained fraction reached the basin. Rift basins may experience such low rates of sediment supply due to low relief in the footwall source area or as result of longer transporting distances to the basin, which is both typical for marine rift basins (Ravnås and Steel, 1998; Martins-Neto and Catuneanu, 2010). During the gradual infill of the basin, minor episodes of subsidence may have occurred, generating a rise in the relative sea level, which further resulted in the formation of the marine flooding surfaces observed within both the formations.

The observed subaerial unconformities from a marine to a fluvial deposits, have been attributed to a sudden uplift of the footwall leading to a dramatic fall in base level, which further provoked extensive footwall erosion (Ravnås and Steel, 1998). As a result, the sediment supply to the basin increased, while the distance from the source area to the accommodation space and sediment accumulation decreased, governing high aggradation rates and the generation of fluvial deposits (i.e. Fugleberget and Paddeby formations). A following sea-level rise due tectonic subsidence of the hanging wall resulted in the drowning of the coarser-grained fluvial deposits (i.e. the Fugleberget and Paddeby formations) giving rise to a new depositional cycle.

It thus seems likely that fault displacement within in the rift-basin partly controlled the sequence stratigraphic evolution of the Klubbnasen-Fugleberget formations and the Andersby-Paddeby formations successions. Although, this is a simplified interpretation and does not consider various external forcing mechanisms (e.g. climate and base-level changes) and internal feedback mechanisms affecting the sedimentation.

## 5.5. Depositional environment

The clear similarities between the Klubbnasen and Andersby formations regarding both hydrodynamic processes and stratigraphic development (Fig. 39) indicate that the two formations represent overall similar depositional environments. Based on the lithofacies and facies association analysis including the including a soft-sediment deformation investigation presented here, a storm-influenced prodeltaic and delta front origin are proposed as the

depositional environments for the two formations (Fig.39). The deltas were presumably deposited in a seismically active basin where the main sedimentary processes were storm-generated waves and currents, river-fed flows (i.e. hyperpycnal flows) and gravity-driven flows. The depositional environment can roughly be divided into three, which record the proximal settings above FWWB (FA3; delta front), intermediate settings above mean SWB (FA2, prodelta) and the outer shelf below mean SWB (FA1) representing the distal offshore (basinal) deposits (Figs 38 &39).

Wave-enhanced turbidity currents were most likely the main transporting agent in distributing sand eastward onto the delta front (FA3) and prodelta (FA2). The turbidity currents were most likely governed by hyperpycnal flows related to river floods (large storms) and/or triggered by cyclic stress from storm waves/seismic waves at the delta front. These processes are common in modern deltaic settings and have been inferred from ancient deltaic successions elsewhere (Mulder and Syvitski, 1995; Wheatcroft and Borgeld, 2000; Mulder et al., 2003; Bhattacharya and MacEachern, 2009).

Considering the previously proposed syn-rift origin of both the Klubbnasen and Andersby formations (Røe, 2003), the abundance of seismically induced SSDS and slumps, as well as the cyclic stacking pattern documented in this study, it seems likely that the basin evolution was subjected to periods of seismic activity (Leeder et al., 1991; Gawthorpe and Leeder, 2008; Martins-Neto and Catuneanu, 2010; Henstra et al., 2016; Gawthorpe et al., 2018). The deposition most likely took place in a hanging wall depocenter (e.g. half graben), which was frequently subjected to both fault-controlled subsidence and uplift. Based on the paleocurrent data from both of the formations and the overlying Fugleberget and Paddeby formations, the depositional environment was advancing dominantly eastward nearly along-strike with the proposed rift-basin, which have previously been interpreted to be NW—SE oriented. The sediment entry point from the source area may therefore originate from a relatively low-gradient relay ramp dipping eastward connecting two fault segments (Gawthorpe and Leeder, 2008). Although, other fault-controlled topographies may also have affected the sediment input from the source area (Ravnås and Steel, 1998; Gawthorpe and Leeder, 2000; Henstra et al., 2016).

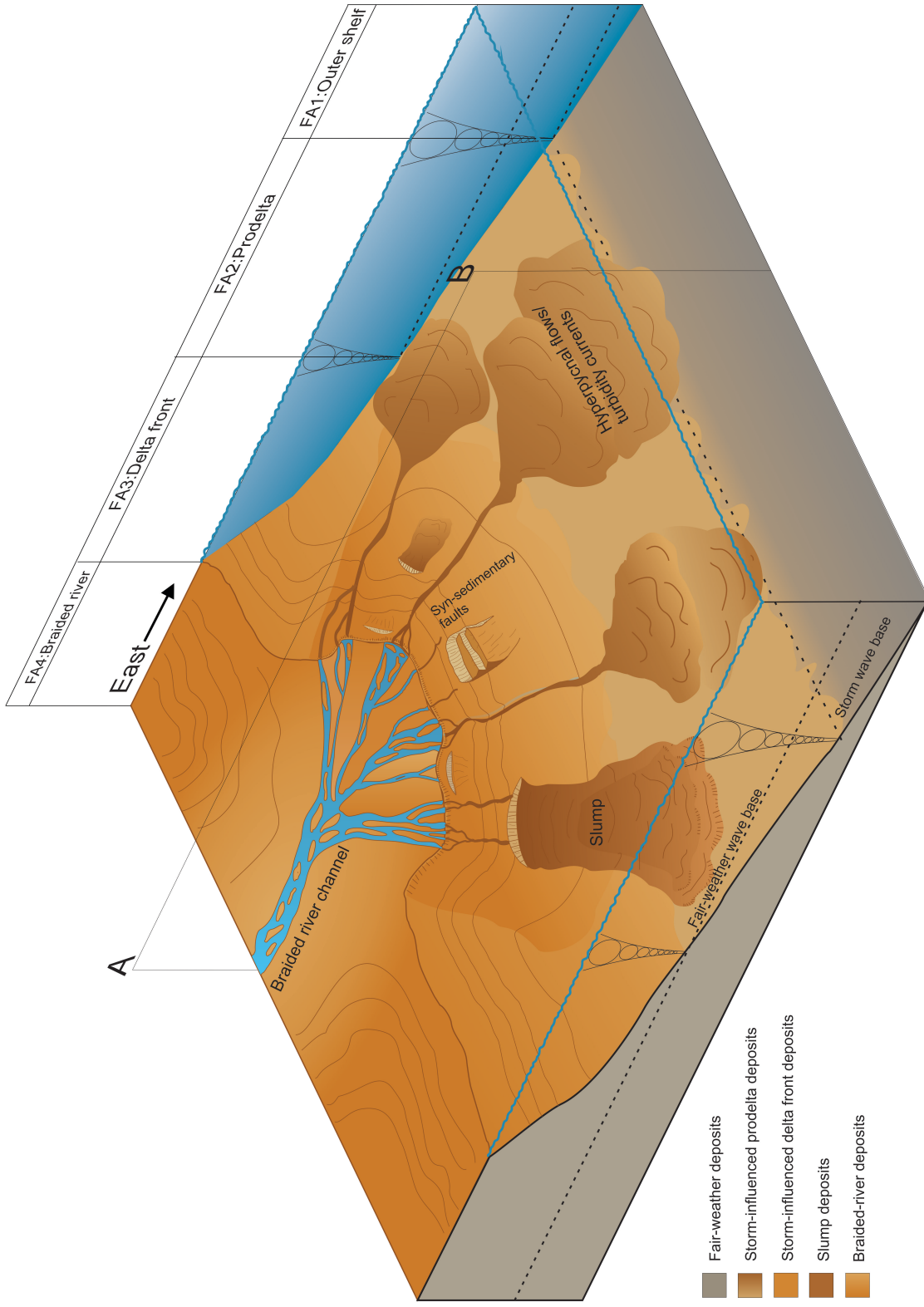


Fig. 39. Depositional model of the Klubbnasen and Andersby formations. Not to scale. Section A to B represent the profile in Figure 38.

## 6. Conclusion

This thesis presents a detailed sedimentological study of the Klubbnasen and Andersby Formations, Varanger Peninsula in eastern Finnmark. In addition, the lower part of Fugleberget and Paddeby formations were investigated superficially to establish the formation boundaries and sequence stratigraphic relationship. Based on the lithofacies and facies association analysis, including the soft-sediment deformation investigations, the depositional environment and sequence stratigraphic development were established.

The main conclusion of this study is summarized below:

- A total of ten lithofacies (Table 1) were recognized within the investigated sections. Laminated mudstone/siltstone (lithofacies 1) and interbedded siltstone/sandstone (lithofacies 2) reflect relatively quiet conditions during fair-weather deposition where only weak combined-flows occasionally emplaced sand. HCS siltstone (lithofacies 3), massive sandstone (lithofacies 4), planar laminated sandstone (lithofacies 5), HCS and SCS sandstone (lithofacies 6 and 7) and combined-flow rippled sandstone (lithofacies 8) reflects deposition during frequent storm events and typically represent intervals of a typical tempestite bed. Cross-bedded and planar-bedded sandstone (lithofacies 9 and 10) were mainly governed by strong unidirectional flows where the supply of sand was sufficient.
- The facies analysis revealed four lithofacies associations reflecting four different depositional settings. The facies associations include outer shelf (FA1), storm-influenced prodelta (FA2), storm-influenced delta front (FA3; only observed in the Klubbnasen Formation) and braided river deposits (FA4; only observed in the Fugleberget and Paddeby formations).
- The numerous tempestite beds are interpreted to be governed by a combination of oscillatory flows (i.e. storm waves) and unidirectional flows (i.e. turbidity currents) producing variations of the typical wave-modified turbidite bed. A typical storm bed (e.g. wave-modified turbidite) reflected an initial stage of strong, but decelerating offshore directed unidirectional flows (e.g. turbidity currents), which was followed by gradually increase in the oscillatory-component of flow (storm waves) governing an oscillatory-dominated combined-flow structures. The variation of storm-bed architectures is attributed to the temporal and spatial evolution of the two transporting agents, including the topography of the seafloor



and proximity to the delta front. Proximally, the beds become more amalgamated and anisotropic, favouring bed-form migration, while they distally become thinner and less complex.

- The abundance of soft-sediment deformation structures in both the Klubbnasen and Andersby formations, including ball-and-pillow structures and convolute/contorted lamination, support seismic activity as the main trigger mechanism. Additionally, the laterally extensive soft-sediment deformed unit in the Vadsø locality (exposing the Andersby Formation) is interpreted to represent seismically-induced slump evolving on a low-angle prodelta slope.
- Both the Klubbnasen and Andersby formations are characterised by an overall progradational and regressive stacking trend, with prodeltaic to deltaic deposits forming upward coarsening units. They are internally bounded by marine flooding surfaces, interpreted to represent periods of sudden tectonic subsidence of the hanging-wall or change in source area relief leading to a decrease in sediment input. Subaerial unconformities formed by sudden footwall uplift bound the Klubbnasen and Andersby formations to the overlying braided river deposits of the Fugleberget and Paddeby formations. The Klubbnasen-Fugleberget formations and the Andersby-Paddeby formations successions were most likely developed in hanging-wall depocenter within a seismically active rift-basin (NW—SE trending), which experienced episodes of both hanging-wall subsidence and footwall uplift.

## 7. References

- ALBERTI, M., PANDEY, D. K., SHARMA, J. K., SWAMI, N. K. & UCHMAN, A. 2017. Slumping in the upper Jurassic Baisakhi formation of the Jaisalmer Basin, western India: Sign of synsedimentary tectonics? *Journal of Palaeogeography*, 6, 321-332.
- ALFARO, P., DELGADO, J., ESTÉVEZ, A., MOLINA, J., MORETTI, M. & SORIA, J. 2002. Liquefaction and fluidization structures in Messinian storm deposits (Bajo Segura Basin, Betic Cordillera, southern Spain). *International Journal of Earth Sciences*, 91, 505-513.
- ALFARO, P., MORETTI, M. & SORIA, J. 1997. Soft-sediment deformation structures induced by earthquakes (seismites) in pliocene lacustrine deposits (Guadix-Baza Basin, Central Betic Cordillera). *Eclogae Geologicae Helvetiae*, 90, 531-540.
- ALLEN, J. 1977. The possible mechanics of convolute lamination in graded sand beds. *Journal of the Geological Society*, 134, 19-31.
- ALLEN, J. 1983. Studies in fluvial sedimentation: bars, bar-complexes and sandstone sheets (low-sinuosity braided streams) in the Brownstones (L. Devonian), Welsh Borders. *Sedimentary Geology*, 33, 237-293.
- ALLEN, J. 1984. Parallel lamination developed from upper-stage plane beds: a model based on the larger coherent structures of the turbulent boundary layer. *Sedimentary Geology*, 39, 227-242.
- ALLEN, J. & BANKS, N. 1972. An interpretation and analysis of recumbent-folded deformed cross-bedding. *Sedimentology*, 19, 257-283.
- ALLEN, J. R. L. 1982. *Sedimentary Structures: Their Character and Physical Basis.*, Elsevier Science & Technology.
- ALSOP, G. I. & MARCO, S. 2011. Soft-sediment deformation within seismogenic slumps of the Dead Sea Basin. *Journal of Structural Geology*, 33, 433-457.
- ARNOTT, R. 1993. Quasi-planar-laminated sandstone beds of the Lower Cretaceous Bootlegger Member, north-central Montana; evidence of combined-flow sedimentation. *Journal of Sedimentary Research*, 63, 488-494.
- ARNOTT, R. & HAND, B. M. 1989. Bedforms, primary structures and grain fabric in the presence of suspended sediment rain. *Journal of Sedimentary Research*, 59, 1062-1069.
- ARNOTT, R. W. & SOUTHARD, J. 1990. Exploratory flow-duct experiments on combined-flow bed configurations, and some implications for interpreting storm-event stratification. *Journal of Sedimentary Research*, 60, 211-219.
- ASTIN, T. & ROGERS, D. 1991. "Subaqueous shrinkage cracks" in the Devonian of Scotland reinterpreted. *Journal of Sedimentary Research*, 61, 850-859.
- BALL, M. M., SHINN, E. & STOCKMAN, K. 1967. The effects of Hurricane Donna in south Florida. *Journal of geology*, 75, 583-597.
- BANIAK, G. M., GINGRAS, M. K., BURNS, B. A. & GEORGE PEMBERTON, S. 2014. An example of a highly bioturbated, storm-influenced shoreface deposit: Upper Jurassic Ula Formation, Norwegian North Sea. *Sedimentology*, 61, 1261-1285.
- BANKS, N., HOBDAV, D., READING, H. & TAYLOR, P. 1974. Stratigraphy of the late Precambrian 'older sandstone series' of the Varangerfjord area, Finnmark. *Norges geologiske undersøkelse*, 303, 1-15.
- BASILICI, G., DE LUCA, P. H. V. & POIRÉ, D. G. 2012. Hummocky cross-stratification-like structures and combined-flow ripples in the Punta Negra Formation (Lower-Middle Devonian, Argentine Precordillera): A turbiditic deep-water or storm-dominated prodelta inner-shelf system? *Sedimentary Geology*, 267-268, 73-92.

- BERRA, F. & FELLETTI, F. 2011. Syndepositional tectonics recorded by soft-sediment deformation and liquefaction structures (continental Lower Permian sediments, Southern Alps, Northern Italy): stratigraphic significance. *Sedimentary Geology*, 235, 249-263.
- BEST, J. 2005. The fluid dynamics of river dunes: A review and some future research directions. *Journal of Geophysical Research: Earth Surface*, 110.
- BEUKES, N. 1996. Sole marks and combined-flow storm event beds in the Brixton Formation of the siliciclastic Archean Witwatersrand Supergroup, South Africa. *Journal of Sedimentary Research*, 66, 567-576.
- BHATTACHARYA, H. & BANDYOPADHYAY, S. 1998. Seismites in a Proterozoic tidal succession, Singbhum, Bihar, India. *Sedimentary Geology*, 119, 239-252.
- BHATTACHARYA, J. P. 2006. Deltas. *Facies models revisited*, 84, 237-292.
- BHATTACHARYA, J. P. & DAVIES, R. K. 2001. Growth faults at the prodelta to delta-front transition, Cretaceous Ferron sandstone, Utah. *Marine Petroleum Geology*, 18, 525-534.
- BHATTACHARYA, J. P. & GIOSAN, L. 2003. Wave-influenced deltas: Geomorphological implications for facies reconstruction. *Sedimentology*, 50, 187-210.
- BHATTACHARYA, J. P. & MACEACHERN, J. A. 2009. Hyperpycnal rivers and prodeltaic shelves in the Cretaceous seaway of North America. *Journal of Sedimentary Research*, 79, 184-209.
- BINGEN, B., SKÅR, Ø., MARKER, M., SIGMOND, E. M., NORDGULEN, Ø., RAGNHILDSTVEIT, J., MANSFELD, J., TUCKER, R. D. & LIÉGEOIS, J.-P. 2005. Timing of continental building in the Sveconorwegian orogen, SW Scandinavia. *Norwegian Journal of Geology*, 85.
- BJØRLYKKE, K. 1967. The Eocambrian "Reusch Moraine" at Bigganjårgga and the geology around Varangerfjord, northern Norway. *Studies on the latest Precambrian and Eocambrian Rocks in Norway*. NGU.
- BOGDANOVA, S., GORBATSHEV, R. & GARETSKY, R. 2016. EUROPE/East European Craton. *Reference Module on Earth Systems and Environmental Sciences*. Elsevier.
- BOGDANOVA, S., PISAREVSKY, S. & LI, Z. 2009. Assembly and Breakup of Rodinia (Some results of IGCP project 440). *Stratigraphy and Geological Correlation*, 17, 259-274.
- BOUMA, A. H. 1962. Sedimentology of some flysch deposits: A graphic approach to facies interpretation. *Elsevier, Amsterdam*, 168.
- BOUMA, A. H. 2004. Key controls on the characteristics of turbidite systems. *Geological Society, London, Special Publications*, 222, 9-22.
- BOURGEOIS, J. 1980. A transgressive shelf sequence exhibiting hummocky stratification; the Cape Sebastian Sandstone (Upper Cretaceous), southwestern Oregon. *Journal of Sedimentary Research*, 50, 681-702.
- BOWMAN, A. P. & JOHNSON, H. D. 2014. Storm-dominated shelf-edge delta successions in a high accommodation setting: The palaeo-Orinoco Delta (Mayaro Formation), Columbus Basin, South-East Trinidad. *Sedimentology*, 61, 792-835.
- BOWMAN, D., KORJENKOV, A. & PORAT, N. 2004. Late-Pleistocene seismites from Lake Issyk-Kul, the tien shan range, Kyrgyzstan. *Sedimentary Geology*, 163, 211-228.
- BRENCHLEY, P., PICKERILL, R. & STROMBERG, S. 1993. The role of wave reworking on the architecture of storm sandstone facies, Bell Island Group (Lower Ordovician), eastern Newfoundland. *Sedimentology*, 40, 359-382.
- BRENCHLEY, P. J. & NEWALL, G. 1977. The significance of contorted bedding in upper Ordovician sediments of the Oslo region, Norway. *Journal of Sedimentary Research*, 47, 819-833.
- BRENCHLEY, P. J. & NEWALL, G. 1982. Storm-influenced inner-shelf sand lobes in the Caradoc (Ordovician) of Shropshire, England. *Journal of Sedimentary Research*, 52, 1257-1269.
- BRENCHLEY, P. J., ROMANO, M. & GUTIERREZ-MARCO, J. C. 1986. Proximal and distal hummocky cross-stratified facies on a wide Ordovician shelf in Iberia. *Shelf Sands and Sandstones*.
- BRIDGE, J., SMITH, N., TRENT, F., GABEL, S. & BERNSTEIN, P. 1986. Sedimentology and morphology of a low-sinuosity river: Calamus River, Nebraska Sand Hills. *Sedimentology*, 33, 851-870.
- BURST, J. 1965. Subaqueously formed shrinkage cracks in clay. *Journal of Sedimentary Research*, 35.

- BYLUND, G. 1994. Palaeomagnetism of the Late Precambrian Vadsø and Barents Sea Groups, Varanger Peninsula, Norway. *Precambrian Research*, 69, 81-93.
- CANT, D. J. & WALKER, R. G. 1978. Fluvial processes and facies sequences in the sandy braided South Saskatchewan River, Canada. *Sedimentology*, 25, 625-648.
- CARR, I. D., GAWTHORPE, R. L., JACKSON, C. A. L., SHARP, I. R. & SADEK, A. 2003. Sedimentology and Sequence Stratigraphy of Early Syn-Rift Tidal Sediments: The Nukhul Formation, Suez Rift, Egypt. *Journal of sedimentary research*, 73, 407-420.
- CATUNEANU, O., ABREU, V., BHATTACHARYA, J., BLUM, M., DALRYMPLE, R., ERIKSSON, P., FIELDING, C. R., FISHER, W., GALLOWAY, W. & GIBLING, M. J. E.-S. R. 2009. Towards the standardization of sequence stratigraphy. *Earth-Science Reviews*, 92, 1-33.
- CATUNEANU, O. & ELANGO, H. N. 2001. Tectonic control on fluvial styles: the Balfour Formation of the Karoo Basin, South Africa. *Sedimentary Geology*, 140, 291-313.
- CAWOOD, P. A., NEMCHIN, A. A., STRACHAN, R., PRAVE, T. & KRABBENDAM, M. 2007. Sedimentary basin and detrital zircon record along East Laurentia and Baltica during assembly and breakup of Rodinia. *Journal of the Geological Society*, 164, 257-275.
- CAWOOD, P. A. & PISAREVSKY, S. A. 2006. Was Baltica right-way-up or upside-down in the Neoproterozoic? *Journal of the Geological Society*, 163, 753-759.
- CAWOOD, P. A. & PISAREVSKY, S. A. 2017. Laurentia-Baltica-Azania relations during Rodinia assembly. *Precambrian Research*, 292, 386-397.
- CHARVIN, K., HAMPSON, G. J., GALLAGHER, K. L. & LABOURDETTE, R. 2010. Intra-parasequence architecture of an interpreted asymmetrical wave-dominated delta. *Sedimentology*, 57, 760-785.
- CHEEL, R. J. 1990. Horizontal lamination and the sequence of bed phases and stratification under upper-flow-regime conditions. *Sedimentology*, 37, 517-529.
- CHEEL, R. J. 1991. Grain fabric in hummocky cross-stratified storm beds; genetic implications. *Journal of Sedimentary Research*, 61, 102-110.
- CHEEL, R. J. & LECKIE, D. A. 1992. Coarse-grained storm beds of the Upper Cretaceous Chungo Member (Wapiabi Formation), southern Alberta, Canada. *Journal of Sedimentary Research*, 62, 933-945.
- CHEEL, R. J. & LECKIE, D. A. 2009. *Hummocky Cross-Stratification*.
- COLEMAN, J. M., ROBERTS, H. H. & STONE, G. W. 1998a. Mississippi River delta: an overview. *Journal of Coastal Research*, 699-716.
- COLEMAN, J. M., WALKER, H. J. & GRABAU, W. E. 1998b. Sediment instability in the Mississippi River delta. *Journal of Coastal Research*, 872-881.
- COLLINS, D. S., JOHNSON, H. D., ALLISON, P. A., GUILPAIN, P. & DAMIT, A. R. 2017. Coupled 'storm-flood' depositional model: Application to the Miocene-Modern Baram Delta Province, north-west Borneo. *Sedimentology*, 64, 1203-1235.
- CORREGGIARI, A., CATTANEO, A. & TRINCARDI, F. 2005. The modern Po Delta system: lobe switching and asymmetric prodelta growth. *Marine Geology*, 222, 49-74.
- DONOVAN, R. N. & FOSTER, R. J. 1972. Subaqueous shrinkage cracks from the Caithness Flagstone Series (middle Devonian) of northeast Scotland. *Journal of Sedimentary Research*, 42, 309-317.
- DOTT JR, R. & BOURGEOIS, J. 1982. Hummocky stratification: significance of its variable bedding sequences. *Geological Society of America Bulletin*, 93, 663-680.
- DUFOIS, F., VERNEY, R., LE HIR, P., DUMAS, F. & CHARMASSON, S. 2014. Impact of winter storms on sediment erosion in the Rhone River prodelta and fate of sediment in the Gulf of Lions (North Western Mediterranean Sea). *Continental Shelf Research*, 72, 57-72.
- DUKE, W. L. 1985. Hummocky cross-stratification, tropical hurricanes, and intense winter storms. *Sedimentology*, 32, 167-194.



- DUKE, W. L. 1990. Geostrophic circulation or shallow marine turbidity currents? The dilemma of paleoflow patterns in storm-influenced prograding shoreline systems. *Journal of Sedimentary Research*, 60, 870-883.
- DUKE, W. L. 1991. Shelf sandstones and hummocky cross-stratification: New insights on a stormy debate. *Geology*, 19.
- DUMAS, S. & ARNOTT, R. 2006. Origin of hummocky and swaley cross-stratification—The controlling influence of unidirectional current strength and aggradation rate. *Geology*, 34, 1073-1076.
- DUMAS, S., ARNOTT, R. & SOUTHARD, J. B. 2005. Experiments on oscillatory-flow and combined-flow bed forms: implications for interpreting parts of the shallow-marine sedimentary record. *Journal of Sedimentary research*, 75, 501-513.
- DURANTI, D. & HURST, A. 2004. Fluidization and injection in the deep-water sandstones of the Eocene Alba Formation (UK North Sea). *Sedimentology*, 51, 503-529.
- EDWARDS, M. B. 1972. *Glacial, Interglacial, and Postglacial Sedimentation in a Late Precambrian Shelf Environment, Finnmark, North Norway*. University of Oxford.
- EIDE, C. H., HOWELL, J. & BUCKLEY, S. 2014. Distribution of discontinuous mudstone beds within wave-dominated shallow-marine deposits: Star Point Sandstone and Blackhawk Formation, Eastern Utah. *AAPG bulletin*, 98, 1401-1429.
- EIDE, C. H., HOWELL, J. A. & BUCKLEY, S. 2015. Sedimentology and reservoir properties of tabular and erosive offshore transition deposits in wave-dominated, shallow-marine strata: Book Cliffs, USA. *Petroleum Geoscience*, 21, 55-73.
- EINSELE, G. 2000. *Sedimentary basins: evolution, facies, and sediment budget*, Springer Science & Business Media.
- EMBRY, A. F. Transgressive-regressive (TR) sequence stratigraphy. Gulf Coast SEPM Conference Proceedings, Houston, 2002. 151-172.
- FIELD, M. E., GARDNER, J. V., JENNINGS, A. E. & EDWARDS, B. D. 1982. Earthquake-induced sediment failures on a 0.25° slope, Klamath River delta, California. *Geology*, 10, 542-546.
- FIELDING, C. R. 2006. Upper flow regime sheets, lenses and scour fills: extending the range of architectural elements for fluvial sediment bodies. *Sedimentary Geology*, 190, 227-240.
- GAO, Y., JIANG, Z., BEST, J. L., LIU, S. & ZHANG, J. 2019. Small-and large-scale soft-sediment deformations in a Triassic lacustrine delta caused by overloading and seismicity in the Ordos Basin, central China. *Marine Petroleum Geology*, 103, 126-149.
- GAWTHORPE, R. & LEEDER, M. 2008. Tectono-sedimentary evolution of active extensional basins. *Basin Research*, 12, 195-218.
- GAWTHORPE, R. L., FRASER, A. J. & COLLIER, R. E. L. 1994. Sequence stratigraphy in active extensional basins: implications for the interpretation of ancient basin-fills. *Marine Petroleum Geology*, 11, 642-658.
- GAWTHORPE, R. L. & LEEDER, M. R. 2000. Tectono-sedimentary evolution of active extensional basins. *Basin Research*, 12, 195-218.
- GAWTHORPE, R. L., LEEDER, M. R., KRANIS, H., SKOURTSOS, E., ANDREWS, J. E., HENSTRA, G. A., MACK, G. H., MURAVCHIK, M., TURNER, J. A. & STAMATAKIS, M. 2018. Tectono-sedimentary evolution of the Plio-Pleistocene Corinth rift, Greece. *Basin Research*, 30, 448-479.
- GEE, D. G., FOSSEN, H., HENRIKSEN, N. & HIGGINS, A. K. 2008. From the early Paleozoic platforms of Baltica and Laurentia to the Caledonide Orogen of Scandinavia and Greenland. *Episodes*, 31, 44-51.
- GIBERT, L., DE GALDEANO, C. S., ALFARO, P., SCOTT, G. & GARRIDO, A. L. 2005. Seismic-induced slump in Early Pleistocene deltaic deposits of the Baza Basin (SE Spain). *Sedimentary Geology*, 179, 279-294.
- GORSLINE, D., DE DIEGO, T. & NAVA-SANCHEZ, E. H. 2000. Seismically triggered turbidites in small margin basins: Alfonso Basin, western Gulf of California and Santa Monica Basin, California borderland. *Sedimentary Geology*, 135, 21-35.

- GRUNDVÅG, S. A., JELBY, M. E., OLAUSSEN, S. & ŚLIWIŃSKA, K. 2020. The role of shelf morphology on storm-bed variability and stratigraphic architecture, Lower Cretaceous, Svalbard. *Sedimentology*.
- HAMBLIN, A., DUKE, W. & WALKER, R. 1979. Hummocky Cross-Stratification--Indicator of Storm-Dominated Shallow-Marine Environments. *Bulletin of the Geological Society of America*, 63, 460-461.
- HARMS, J. 1969. Hydraulic significance of some sand ripples. *Geological Society of America Bulletin*, 80, 363-396.
- HARMS, J. C. 1975. Depositional environments as interpreted from primary sedimentary structures and stratification sequences. *Soc Econ Paleont Miner Short Course*, 2, 161p.
- HAYES, M. O. 1967. Hurricanes as geological agents, south Texas coast. *AAPG Bulletin*, 51, 937-942.
- HENSTRA, G. A., GRUNDVÅG, S.-A., JOHANNESSEN, E. P., KRISTENSEN, T. B., MIDTKANDAL, I., NYSTUEN, J. P., ROTEVATN, A., SURLYK, F., SÆTHER, T. & WINDELSTAD, J. 2016. Depositional processes and stratigraphic architecture within a coarse-grained rift-margin turbidite system: The Wollaston Forland Group, east Greenland. *Marine Petroleum Geology*, 76, 187-209.
- HERREVOLD, T., GABRIELSEN, R. H. & ROBERTS, D. 2009. Structural geology of the southeastern part of the Trollfjorden-Komagelva fault zone, Varanger Peninsula, Finnmark, north Norway. *Norsk Geologisk Tidsskrift, Norwegian Journal of Geology*, 89, 305-325.
- HILDEBRANDT, C. & EGENHOFF, S. 2007. Shallow-marine massive sandstone sheets as indicators of palaeoseismic liquefaction—An example from the Ordovician shelf of Central Bolivia. *Sedimentary Geology*, 202, 581-595.
- HILL, P. R., MEULÉ, S. & LONGUÉPÉE, H. 2003. Combined-flow processes and sedimentary structures on the shoreface of the wave-dominated Grande-Riviere-de-la-Baleine delta. *Journal of Sedimentary Research*, 73, 217-226.
- HJELLBAKK, A. 1997. Facies and fluvial architecture of a high-energy braided river: the Upper Proterozoic Segloddan Member, Varanger Peninsula, northern Norway. *Sedimentary Geology*, 114, 131-161.
- HOBDAV, D. 1974. Interaction between fluvial and marine processes in the lower part of the Late Precambrian Vadsø Group. *Norges geologiske undersøkelse*, 303, 39-56.
- HOLTEDAHL, O. 1918. Bidrag til Finnmarkens geologi. *Norges geologiske undersøkelse*, 84, 314.
- IDE, Y., MAEJIMA, W. & IDE, Y. 2011. Distal Storm Sedimentation of the Lower Cretaceous Arida Formation, Yuasa-Aridagawa Basin, Southwest Japan. *Journal of Geosciences Osaka City University*, 54, 31-41.
- JELBY, M. E., GRUNDVÅG, S. A., HELLAND-HANSEN, W., OLAUSSEN, S. & STEMMERIK, L. 2020. Tempestite facies variability and storm-depositional processes across a wide ramp: Towards a polygenetic model for hummocky cross-stratification. *Sedimentology*, 67, 742-781.
- JENSEN, M. A. & PEDERSEN, G. K. 2010. Architecture of vertically stacked fluvial deposits, atane formation, cretaceous, nuussuaq, central west greenland. *Sedimentology*, 57, 1280-1314.
- JIANG, H., ZHONG, N., LI, Y., XU, H., YANG, H. & PENG, X. 2016. Soft sediment deformation structures in the Lixian lacustrine sediments, eastern Tibetan Plateau and implications for postglacial seismic activity. *Sedimentary Geology*, 344, 123-134.
- JOHANSSON, Å. 2009. Baltica, Amazonia and the SAMBA connection—1000 million years of neighbourhood during the Proterozoic? *Precambrian Research*, 175, 221-234.
- JOHNSON, H., LEVELL, B. & SIEDLECKI, S. 1978a. Late Precambrian sedimentary rocks in East Finnmark, north Norway and their relationship to the Trollfjord-Komagelva fault. *Journal of the Geological Society*, 135, 517-533.
- JOHNSON, H. D. 1975. Tide and wave-dominated inshore and shoreline sequences from the late Precambrian, Finnmark, North Norway. *Sedimentology*, 22, 45-74.
- JOHNSON, H. D. 1978. Facies distributions and lithostratigraphic correlation in the late Precambrian Ekkerøey Formation, East Finnmark, Norway. *Norsk Geologisk Tidsskrift*, 58, 175-190.

- JOHNSON, H. D., LEVELL, B. K. & SIEDLECKI, S. 1978b. Late Precambrian sedimentary rocks in East Finnmark, north Norway and their relationship to the Trollfjord-Komagelv fault. *Journal of the Geological Society*, 135, 517-533.
- KARPUZ, M., ROBERTS, D., MORALEV, V. & TEREKHOV, E. 1995a. Regional lineaments of eastern Finnmark, Norway, and the western Kola Peninsula, Russia. *Norges geologiske undersøkelse Special Publication*, 7, 121-135.
- KARPUZ, M., ROBERTS, D., OLESEN, O., GABRIELSEN, R. & HERREVOLD, T. 1993. Application of multiple data sets to structural studies on Varanger Peninsula, Northern Norway. *International Journal of Remote Sensing*, 14, 979-1003.
- KARPUZ, M. R., ROBERTS, D., HERREVOLD, T., GABRIELSEN, R. H., KRILL, A. G. & LIPPARD, S. J. 1994. Structural diversity of the Trollfjorden-Komagelva fault zone, northern Norway and western Kola Peninsula. Oslo: Oslo, Norway: Universitetsforlaget.
- KARPUZ, R., ROBERTS, D., HERREVOLD, T., GABRIELSEN, R. & OLESEN, O. 1995b. Structural and geophysical characteristics of the Trollfjorden-Komagelv Fault Zone, Varanger Peninsula, northern Norway. *NGU Special Publication*, 7, 151-152.
- KORNEVA, I., TONDI, E., JABLONSKA, D., DI CELMA, C., ALSOP, I. & AGOSTA, F. 2016. Distinguishing tectonically-and gravity-driven synsedimentary deformation structures along the Apulian platform margin (Gargano Promontory, southern Italy). *Marine Petroleum Geology*, 73, 479-491.
- KRASSAY, A. A. 1994. Storm features of siliciclastic shelf sedimentation in the mid-Cretaceous epeiric seaway of northern Australia. *Sedimentary Geology*, 89, 241-264.
- LAMB, M., MYROW, P., LUKENS, C., HOUCK, K. & STRAUSS, J. 2008. Deposits from wave-influenced turbidity currents: Pennsylvanian Minturn Formation, Colorado, USA. *Journal of Sedimentary Research*, 78, 480-498.
- LECKIE, D. A. & KRISTINIK, L. F. 1989. Is there evidence for geostrophic currents preserved in the sedimentary record of inner to middle-shelf deposits. *Journal of Sedimentary Research*, 59, 862-870.
- LECKIE, D. A. & WALKER, R. G. 1982. Storm-and tide-dominated shorelines in Cretaceous Moosebar-Lower Gates interval--outcrop equivalents of Deep Basin gas trap in western Canada. *AAPG Bulletin*, 66, 138-157.
- LEEDER, M. R., SEGER, M. J. & STARK, C. P. 1991. Sedimentation and tectonic geomorphology adjacent to major active and inactive normal faults, southern Greece. *Journal of the Geological Society*, 148, 331-343.
- LEVELL, B. & ROBERTS, D. 1977. A re-investigation of the geology of north-west Varanger Peninsula, east Finnmark, north Norway. *Norges geologiske undersøkelse*, 334, 83-90.
- LI, Z., BOGDANOVA, S., COLLINS, A., DAVIDSON, A., DE WAELE, B., ERNST, R., FITZSIMONS, I., FUCH, R., GLADKOCHUB, D. & JACOBS, J. 2008. Assembly, configuration, and break-up history of Rodinia: a synthesis. *Precambrian research*, 160, 179-210.
- LOWE, D. R. 1975. Water escape structures in coarse-grained sediments. *Sedimentology*, 22, 157-204.
- MACEACHERN, J. A., DASHTGARD, S. E., KNAUST, D., CATUNEANU, O., BANN, K. L. & PEMBERTON, S. G. 2012. Sequence stratigraphy. *Developments in Sedimentology*. Elsevier.
- MACQUAKER, J. H., BENTLEY, S. J. & BOHACS, K. M. 2010. Wave-enhanced sediment-gravity flows and mud dispersal across continental shelves: Reappraising sediment transport processes operating in ancient mudstone successions. *Geology*, 38, 947-950.
- MARTINS-NETO, M. & CATUNEANU, O. 2010. Rift sequence stratigraphy. *Marine Petroleum Geology*, 27, 247-253.
- MASTROGIACOMO, G., MORETTI, M., OWEN, G. & SPALLUTO, L. 2012. Tectonic triggering of slump sheets in the Upper Cretaceous carbonate succession of the Porto Selvaggio area (Salento peninsula, southern Italy): Synsedimentary tectonics in the Apulian Carbonate Platform. *Sedimentary Geology*, 269, 15-27.

- MCLAUGHLIN, P. I. & BRETT, C. E. 2004. Eustatic and tectonic control on the distribution of marine seismites: examples from the Upper Ordovician of Kentucky, USA. *Sedimentary Geology*, 168, 165-192.
- MCMAHON, S., VAN SMEERDIJK HOOD, A. & MCILROY, D. 2017. The origin and occurrence of subaqueous sedimentary cracks. *Geological Society, London, Special Publications*, 448, 285-309.
- MERDITH, A. S., COLLINS, A. S., WILLIAMS, S. E., PISAREVSKY, S., FODEN, J. D., ARCHIBALD, D. B., BLADES, M. L., ALESSIO, B. L., ARMISTEAD, S. & PLAVSA, D. 2017. A full-plate global reconstruction of the Neoproterozoic. *Gondwana Research*, 50, 84-134.
- MIALL, A. D. 1977. A review of the braided-river depositional environment. *Earth-Science Reviews*, 13, 1-62.
- MIDTGAARD, H. H. 1996. Inner-shelf to lower-shoreface hummocky sandstone bodies with evidence for geostrophic influenced combined flow, Lower Cretaceous, West Greenland. *Journal of Sedimentary Research*, 66, 343-353.
- MOHINDRA, R. & BAGATI, T. 1996. Seismically induced soft-sediment deformation structures (seismites) around Sumdo in the lower Spiti valley (Tethys Himalaya). *Sedimentary Geology*, 101, 69-83.
- MOLINA, J., ALFARO, P., MORETTI, M. & SORIA, J. 1998. Soft-sediment deformation structures induced by cyclic stress of storm waves in tempestites (Miocene, Guadalquivir Basin, Spain). *TERRA NOVA-OXFORD*, 10, 145-150.
- MORETTI, M. & RONCHI, A. 2011. Liquefaction features interpreted as seismites in the Pleistocene fluvio-lacustrine deposits of the Neuquén Basin (Northern Patagonia). *Sedimentary Geology*, 235, 200-209.
- MORETTI, M., SORIA, J. M., ALFARO, P. & WALSH, N. 2001. Asymmetrical soft-sediment deformation structures triggered by rapid sedimentation in turbiditic deposits (Late Miocene, Guadix Basin, southern Spain). *Facies*, 44, 283-294.
- MORETTI, M., VAN LOON, A. T., LIU, M. & WANG, Y. 2014. Restrictions to the application of 'diagnostic' criteria for recognizing ancient seismites. *Journal of Palaeogeography*, 3, 162-173.
- MORSILLI, M. & POMAR, L. 2012. Internal waves vs. surface storm waves: a review on the origin of hummocky cross-stratification. Oxford, UK: Terra Nova.
- MULDER, T. & COCHONAT, P. 1996. Classification of offshore mass movements. *Journal of Sedimentary research*, 66, 43-57.
- MULDER, T., RAZIN, P. & FAUGERES, J.-C. 2009. Hummocky cross-stratification-like structures in deep-sea turbidites: Upper Cretaceous Basque basins (Western Pyrenees, France). *Sedimentology*, 56, 997-1015.
- MULDER, T. & SYVITSKI, J. P. 1995. Turbidity currents generated at river mouths during exceptional discharges to the world oceans. *The Journal of Geology*, 103, 285-299.
- MULDER, T., SYVITSKI, J. P., MIGEON, S., FAUGERES, J.-C. & SAVOYE, B. 2003. Marine hyperpycnal flows: initiation, behavior and related deposits. A review. *Marine Petroleum Geology*, 20, 861-882.
- MUTTI, E., DAVOLI, G., TINTERRI, R. & ZAVALA, C. 1996. The importance of ancient fluvio-deltaic systems dominated by catastrophic flooding in tectonically active basins. *Memorie di Scienze Geologiche*, 48, 233-291.
- MUTTI, E. & RICCI LUCCHI, F. 1978. Turbidites of the northern Apennines: introduction to facies analysis. *International geology review*, 20, 125-166.
- MUTTI, E., RICCI LUCCHI, F. & ROVERI, M. Revisiting turbidites of the Marnoso-arenacea Formation and their basin-margin equivalents: problems with classic models. Excursion guidebook of the turbidite workshop, Parma, Italy, 2002. 21-22.
- MUTTI, E., TINTERRI, R., BENEVELLI, G., DI BIASE, D. & CAVANNA, G. 2003. Deltaic, mixed and turbidite sedimentation of ancient foreland basins. *Marine Petroleum Geology*, 20, 733-755.
- MYROW, P. 2005. Storms and storm deposits. *Sedimentary environments*.



- MYROW, P., FISCHER, W. & GOODGE, J. W. 2002. Wave-modified turbidites: Combined-flow shoreline and shelf deposits, Cambrian, Antarctica. *Journal of sedimentary research*, 72, 641-656.
- MYROW, P., LUKENS, C., LAMB, M., HOUCK, K. & STRAUSS, J. 2008. Dynamics of a transgressive prodeltaic system: Implications for geography and climate within a Pennsylvanian intracratonic basin, Colorado, USA. *Journal of Sedimentary Research*, 78, 512-528.
- MYROW, P. M. 1992. Bypass-zone tempestite facies model and proximity trends for an ancient muddy shoreline and shelf. *Journal of Sedimentary research*, 62, 99-115.
- MYROW, P. M., LAMB, M., LUKENS, C., HOUCK, K., KLUTH, C. & PARSONS, J. 2004. Hyperpycnal wave-modified turbidites of the Pennsylvanian Minturn Formation, north-central Colorado. *Minturn Fieldtrip Material.*, Department of geology, The Colorado College.
- MYROW, P. M. & SOUTHARD, J. B. 1991. Combined-flow model for vertical stratification sequences in shallow marine storm-deposited beds. *Journal of Sedimentary Research*, 61, 202-210.
- MYROW, P. M. & SOUTHARD, J. B. 1996. Tempestite deposition. *Journal of Sedimentary Research*, 66, 875-887.
- NEEF, G. 1991. A clastic dike-sill assemblage in late Miocene (c. 6 Ma) strata, Annedale, Northern Wairarapa, New Zealand. *New Zealand Journal of Geology and Geophysics*.
- NELSON, C. H. 1982. Modern shallow-water graded sand layers from storm surges, Bering Shelf; a mimic of Bouma sequences and turbidite systems. *Journal of Sedimentary Research*, 52, 537-545.
- NEMEC, W., STEEL, R. J., GJELBERG, J., COLLINSON, J., PRESTHOLM, E. & ØXNEVAD, I. 1988. Anatomy of collapsed and re-established delta front in Lower Cretaceous of eastern Spitsbergen: gravitational sliding and sedimentation processes. *AAPG bulletin*, 72, 454-476.
- NYSTUEN, J. P., ANDRESEN, A., KUMPULAINEN, R. A. & SIEDLECKA, A. 2008. Neoproterozoic basin evolution in Fennoscandia, East Greenland and Svalbard. *Episodes*, 31, 35-43.
- NØTTVEDT, A. & KREISA, R. 1987. Model for the combined-flow origin of hummocky cross-stratification. *Geology*, 15, 357-361.
- OGATA, K., MULROONEY, M. J., BRAATHEN, A., MAHER, H., OSMUNDSEN, P. T., ANELL, I., SMYRAK-SIKORA, A. A. & BALSAMO, F. 2018. Architecture, deformation style and petrophysical properties of growth fault systems: the Late Triassic deltaic succession of southern Edgeøya (East Svalbard). *Basin Research*, 30, 1042-1073.
- OLARIU, C. & BHATTACHARYA, J. P. 2006. Terminal distributary channels and delta front architecture of river-dominated delta systems. *Journal of sedimentary research*, 76, 212-233.
- OLIVEIRA, C. M., HODGSON, D. M. & FLINT, S. S. 2009. Aseismic controls on in situ soft-sediment deformation processes and products in submarine slope deposits of the Karoo Basin, South Africa. *Sedimentology*, 56, 1201-1225.
- OLOVYANISHNIKOV, A., S. & D., R. 1997. Aspect of geology of the Timans, Russia, and linkage with Varanger Peninsula, NE Norway. *Norges geologiske undersøkelse*, 433, 28.
- OLOVYANISHNIKOV, V. G., ROBERTS, D., SIEDLECKA, A., ROLAND, N. W. & TESSENHORN, F. 1998. Tectonics and sedimentation of the Meso- to Neoproterozoic Timan-Varanger Belt along the northeastern margin of Baltica. Munster: Munster, Federal Republic of Germany: Deutsche Gesellschaft fuer Polarforschung.
- ONDERDONK, N. & MIDTKANDAL, I. 2010. Mechanisms of collapse of the Cretaceous Helvetiafjellet Formation at Kvalvågen, eastern Spitsbergen. *Marine Petroleum Geology*, 27, 2118-2140.
- OWEN, G. 1987. Deformation processes in unconsolidated sands. *Geological Society, London, Special Publications*, 29, 11-24.
- OWEN, G. 1995. Soft-sediment deformation in upper Proterozoic Torridonian sandstones (Applecross Formation) at Torridon, northwest Scotland. *Journal of Sedimentary Research*, 65, 495-504.
- OWEN, G. 1996. Experimental soft-sediment deformation: structures formed by the liquefaction of unconsolidated sands and some ancient examples. *Sedimentology*, 43, 279-293.

- OWEN, G. 2003. Load structures: gravity-driven sediment mobilization in the shallow subsurface. *Geological Society, London, Special Publications*, 216, 21-34.
- OWEN, G. & MORETTI, M. 2008. Determining the origin of soft-sediment deformation structures: a case study from Upper Carboniferous delta deposits in south-west Wales, UK. *Terra Nova*, 20, 237-245.
- OWEN, G. & MORETTI, M. 2011. Identifying triggers for liquefaction-induced soft-sediment deformation in sands. *Sedimentary Geology*, 235, 141-147.
- PATTISON, S. 2005. Storm-influenced prodelta turbidite complex in the lower Kenilworth Member at Hatch Mesa, Book Cliffs, Utah, U.S.A.: Implications for shallow marine facies models. *Journal of Sedimentary Research*, 75.
- PATTISON, S. A., BRUCE AINSWORTH, R. & HOFFMAN, T. A. 2007. Evidence of across-shelf transport of fine-grained sediments: turbidite-filled shelf channels in the Campanian Aberdeen Member, Book Cliffs, Utah, USA. *Sedimentology*, 54, 1033-1064.
- PEASE, V., DALY, J., ELMING, S.-Å., KUMPULAINEN, R., MOCZYDLOWSKA, M., PUCHKOV, V., ROBERTS, D., SAINTOT, A. & STEPHENSON, R. 2008. Baltica in the Cryogenian, 850–630 Ma. *Precambrian Research*, 160, 46-65.
- PEMBERTON, S. G., MACEACHERN, J. A., DASHTGARD, S. E., BANN, K. L., GINGRAS, M. K. & ZONNEVELD, J.-P. 2012. Shorefaces. *Developments in sedimentology*. Elsevier.
- PERKINS, R. & ENOS, P. 1968. Hurricane Betsy in the Florida-Bahama area: geologic effects and comparison with Hurricane Donna. *The Journal of Geology*, 76, 710-717.
- PETERSON, C. D., KRISTENSEN, K. & MINOR, R. 2014. Large-Scale Fluidization Features from Late Holocene Coseismic Paleoliquefaction in the Willamette River Forearc Valley, Central Cascadia Subduction Zone, Oregon, USA. *OJER*.
- PLINK-BJÖRKLUND, P. & STEEL, R. J. 2004. Initiation of turbidity currents: outcrop evidence for Eocene hyperpycnal flow turbidites. *Sedimentary Geology*, 165, 29-52.
- PLINT, A. 1988. Sharp-based shoreface sequences and "offshore bars" in the Cardium Formation of Alberta; their relationship to relative changes in sea level. *Society of Economic Paleontologists and Mineralogists (SEPM)*.
- PLUMMER, P. & GOSTIN, V. 1981. Shrinkage cracks; desiccation or synaeresis? *Journal of Sedimentary Research*, 51, 1147-1156.
- PRATT, B. R. 1998. Syneresis cracks: subaqueous shrinkage in argillaceous sediments caused by earthquake-induced dewatering. *Sedimentary Geology*, 117, 1-10.
- PRINGLE, I. 1972. Rb-Sr age determinations on shales associated with the Varanger Ice Age. *Geological Magazine*, 109, 465-472.
- PRIOR, D., SUHAYDA, J., LU, N.-Z., BORNHOLD, B., KELLER, G., WISEMAN, W., WRIGHT, L. & YANG, Z.-S. 1989. Storm wave reactivation of a submarine landslide. *Nature*, 341, 47-50.
- QUIN, J. G. 2011. Is most hummocky cross-stratification formed by large-scale ripples? *Sedimentology*, 58, 1414-1433.
- RAMBERG, I. B., SOLLI, A., NORDGULEN, Ø., BINNS, R. & GROGAN, P. 2008. *The Making of a land : geology of Norway*, Trondheim, The Norwegian Geological Association.
- RAVNÅS, R. & STEEL, R. 1998. Architecture of marine rift-basin successions. *AAPG bulletin*, 82, 110-146.
- REUSCH, H. 1891. *Skuringsmærker og morænegrus eftervist i Finmarken fra en periode meget ældre enn " istiden "*, Norges Geologiske Undersøkelse.
- RICE, A. 2014. Restoration of the external Caledonides, Finnmark, north Norway. *Geological Society, London, Special Publications*, 390, 271-299.
- ROBERTS, D. 1995. Principal features of the structural geology of Rybachi and Sredni Peninsulas, Northwest Russia, and some comparisons with Varanger Peninsula, North Norway. *Norges geologiske undersøkelse Special Publication*, 7, 247-258.

- ROBERTS, D. 1996. Caledonian and Baikalian tectonic structures on Varanger Peninsula, Finnmark, Norway, and coastal areas of Kola Peninsula, NW Russia. *Norges geologiske undersøkelse*, 431, 59-66.
- ROBERTS, D. 2003. The Scandinavian Caledonides: event chronology, palaeogeographic settings and likely modern analogues. *Tectonophysics*, 365, 283-299.
- ROBERTS, D., CHAND, S. & RISE, L. 2011. A half-graben of inferred late palaeozoic age in outer varangerfjorden, finnmark: Evidence from seismic reflection profiles and multibeam bathymetry. *Norsk Geologisk Tidsskrift*, 91, 193-202.
- ROBERTS, D. & OLOVYANISHNIKOV, V. 2004. Structural and tectonic development of the Timanide orogen. *Geological Society, London, Memoirs*, 30, 47-57.
- ROBERTS, D. & SIEDLECKA, A. 2002. Timanian orogenic deformation along the northeastern margin of Baltica, Northwest Russia and Northeast Norway, and Avalonian–Cadomian connections. *Tectonophysics*, 352, 169-184.
- ROBERTS, D. & SIEDLECKA, A. 2012. Provenance and sediment routing of Neoproterozoic formations on the Varanger, Nordkinn, Rybachi and Sredni peninsulas, North Norway and Northwest Russia: a review. *Norwegian Geological Survey Bulletin*, 452, 1-19.
- ROSS, J. A., PEAKALL, J. & KEEVIL, G. M. 2014. Facies and flow regimes of sandstone-hosted columnar intrusions: insights from the pipes of Kodachrome Basin State Park. *Sedimentology*, 61, 1764-1792.
- ROSSETTI, D. & GÓES, A. 2000. Deciphering the sedimentological imprint of paleoseismic events: an example from the Aptian Codó Formation, northern Brazil. *Sedimentary Geology*, 135, 137-156.
- ROSSETTI, D. D. F. 1999. Soft-sediment deformation structures in late Albian to Cenomanian deposits, São Luís Basin, northern Brazil: evidence for palaeoseismicity. *Sedimentology*, 46, 1065-1081.
- RØE, S. & HERMANSEN, M. 1993. Processes and products of large, Late Precambrian sandy rivers in northern Norway. *Alluvial sedimentation*. Blackwell Oxford.
- RØE, S.-L. 1987. Cross-strata and bedforms of probable transitional dune to upper-stage plane-bed origin from a Late Precambrian fluvial sandstone, northern Norway. *Sedimentology*, 34, 89-101.
- RØE, S.-L. 1995. Stacked fluviodeltaic cycles in the Upper Proterozoic Godkeila Member, Varanger Peninsula, northern Norway. *NORSK GEOLOGISK TIDSSKRIFT*, 75, 229-242.
- RØE, S.-L. 2003. Neoproterozoic peripheral-basin deposits in eastern Finnmark, N. Norway: stratigraphic revision and palaeotectonic implications. *Norwegian Journal of Geology*, 83.
- SCHOLZ, H., FRIELING, D. & OBST, K. 2009. Funnel structures and clastic dykes in Cambrian sandstones of southern Sweden—indications for tensional tectonics and seismic events in a shallow marine environment. *Neues Jahrbuch für Geologie und Paläontologie-Abhandlungen*, 251, 355-380.
- SCOTT, A., VIGORITO, M. & HURST, A. 2009. The process of sand injection: internal structures and relationships with host strata (Yellowbank Creek Injectite Complex, California, USA). *Journal of Sedimentary Research*, 79, 568-583.
- SEILACHER, A. 1969. Fault-graded beds interpreted as seismites. *sedimentology*, 13, 155-159.
- SHANMUGAM, G. 2019. *Slides, slumps, debris flows, turbidity currents, hyperpycnal flows, and bottom currents*.
- SIEDLECKA, A. & ROBERTS, D. 1992. *The bedrock geology of Varanger Peninsula, Finnmark, North Norway : an excursion guide*, Trondheim, Norges geologiske undersøkelse.
- SIEDLECKA, A., ROBERTS, D., NYSTUEN, J. & OLOVYANISHNIKOV, V. 2004. Northeastern and northwestern margins of Baltica in Neoproterozoic time: evidence from the Timanian and Caledonian Orogens. *Geological Society, London, Memoirs*, 30, 169-190.
- SIEDLECKA, A. & SIEDLECKI, S. 1967. Some new aspects of the geology of Varanger Peninsula (Northern Norway). *Norges geologiske undersøkelse*, 247, 288-306.

- SIMS, J. D. 1975. Determining earthquake recurrence intervals from deformational structures in young lacustrine sediments. *Developments in geotectonics*. Elsevier.
- SIRINGAN, F. P. & ANDERSON, J. B. 1994. Modern shoreface and inner-shelf storm deposits off the east Texas coast, Gulf of Mexico. *Journal of Sedimentary Research*, 64, 99-110.
- SNEDDEN, J. W., SWIFT, D. J., LECKIE, D. A. & KRISTINIK, L. F. 1991. Is there evidence for geostrophic currents preserved in the sedimentary record of inner-to middle-shelf deposits?; discussion and reply. *Journal of Sedimentary Research*, 61, 148-154.
- SOUTHARD, J. B., LAMBIE, J. M., FEDERICO, D. C., PILE, H. T. & WEIDMAN, C. R. 1990. Experiments on bed configurations in fine sands under bidirectional purely oscillatory flow, and the origin of hummocky cross-stratification. *Journal of Sedimentary Research*, 60, 1-17.
- STRACHAN, L. J., RARITY, F., GAWTHORPE, R. L., WILSON, P., SHARP, I. & HODGETTS, D. 2013. Submarine slope processes in rift-margin basins, Miocene Suez Rift, Egypt. *Bulletin*, 125, 109-127.
- STURT, B. A., PRINGLE, I. R. & ROBERTS, D. 1975. Caledonian Nappe Sequence of Finnmark, Northern Norway, and the Timing of Orogenic Deformation and Metamorphism. *Bulletin of the Geological Society of America*, 86, 710-718.
- SWIFT, D. J. 1985. Response of the shelf floor to flow. *Shelf Sands and Sandstone Reservoirs: SEPM*, 13, 135-241.
- SWIFT, D. J., FIGUEIREDO, A. G., FREELAND, G. & OERTEL, G. 1983. Hummocky cross-stratification and megaripples; a geological double standard? *Journal of Sedimentary Research*, 53, 1295-1317.
- SWIFT, D. J. & NIEDORODA, A. W. 1986. Fluid and sediment dynamics on continental shelves. *Canadian Society of Petroleum Geologists Memo*.
- TAŞGIN, C. K., ORHAN, H., TÜRKMEN, İ. & AKSOY, E. 2011. Soft-sediment deformation structures in the late Miocene Şelmo Formation around Adiyaman area, Southeastern Turkey. *Sedimentary Geology*, 235, 277-291.
- TORSVIK, T., SMETHURST, M., MEERT, J. G., VAN DER VOO, R., MCKERROW, W., BRASIER, M., STURT, B. & WALDERHAUG, H. 1996. Continental break-up and collision in the Neoproterozoic and Palaeozoic—a tale of Baltica and Laurentia. *Earth-Science Reviews*, 40, 229-258.
- TORSVIK, T. H. & COCKS, L. R. M. 2005. Norway in space and time: A Centennial cavalcade. *Norwegian Journal of Geology/Norsk Geologisk Forening*, 85.
- TRAYKOVSKI, P., WIBERG, P. L. & GEYER, W. R. 2007. Observations and modeling of wave-supported sediment gravity flows on the Po prodelta and comparison to prior observations from the Eel shelf. *Continental Shelf Research*, 27, 375-399.
- VAN LOON, A. & BRODZIKOWSKI, K. 1987. Problems and progress in the research on soft-sediment deformations. *Sedimentary Geology*, 50, 167-193.
- VAN WAGONER, J. C., MITCHUM, R., CAMPION, K. & RAHMANIAN, V. 1990. Siliciclastic sequence stratigraphy in well logs, cores, and outcrops: concepts for high-resolution correlation of time and facies. *American Association of Petroleum Geologists Methods in Exploration Series*.
- WALKER, R. G. & PLINT, A. G. 1992. Wave- and storm-dominated shallow marine systems. *Facies Models; Response to Sea-level Change*, 219-238.
- WHEATCROFT, R. & BORGELD, J. 2000. Oceanic flood deposits on the northern California shelf: large-scale distribution and small-scale physical properties. *Continental Shelf Research*, 20, 2163-2190.
- WHEATLEY, D. F. & CHAN, M. A. 2018. Clastic Pipes and Soft-Sediment Deformation of the Jurassic Carmel Formation, Southern Utah, USA: Implications For Pipe Formation Mechanisms and Host-Rock Controls. *Journal of Sedimentary Research*, 88, 1076-1095.
- WILLIAMS, P. F. & RUST, B. R. 1969. The sedimentology of a braided river. *Journal of Sedimentary Research*, 39.
- WILSON, R. D. & SCHIEBER, J. 2014. Muddy prodeltaic hyperpynites in the lower Genesee Group of central New York, USA: Implications for mud transport in epicontinental seas. *Journal of Sedimentary Research*, 84, 866-874.



- WRIGHT, M. E. & WALKER, R. G. 1982. Cardium Formation at Seebe, Alberta--Storm-Transported Sandstones and Conglomerates. *AAPG Bulletin*, 66, 644-645.
- XIONG, H., HUANG, G., FU, S. & QIAN, P. 2018. Progress in the Study of Coastal Storm Deposits. *Ocean Science Journal*, 53, 149-164.
- YAMAGUCHI, N. & SEKIGUCHI, H. 2010. Effects of settling and preferential deposition of sediment on ripple roundness under shoaling waves. *Journal of Sedimentary Research*, 80, 781-790.
- YOKOKAWA, M., MASUDA, F. & ENDO, N. 1995. Sand particle movement on migrating combined-flow ripples. *Journal of Sedimentary Research*, 65, 40-44.
- ZHANG, W., ROBERTS, D. & PEASE, V. 2015. Provenance characteristics and regional implications of Neoproterozoic, Timanian-margin successions and a basal Caledonian nappe in northern Norway. *Precambrian Research*, 268, 153-167.